Study of Electrooptical Properties of New Type of Polymer/Liquid Crystal Composite for Display Devices

Hiroshi Ono

1995 ***February***

OSAKA UNIVERSITY
GRADUATE SCHOOL OF ENGINEERING SCIENCE
DEPARTMENT OF MATERIAL PHYSICS
TOYONAKA OSAKA

Abstract

New type of polymer/liquid crystal (LC) composite films for minute display are proposed to improve the electrooptical properties. Effects of anchoring strength and morphology on the electrooptical properties of poly(vinyl alcohol) (PVA)/LC composite film have been investigated. In order to control the anchoring strength, a novel composite film with interface layer between the matrix polymer and liquid crystal is proposed. Variable kinds of composite films with different anchoring strength at the interface between the polymer and the LC have been able to be composed by changing the material and composition of the interface layers. It has been found that the electrooptical properties of the PVA/LC composite film are improved by reducing the anchoring strength at the interface between the polymer and LC. Several materials, i.e., benzylmethacrylate (BzMA), nonaoxyethylenediacrylate (9EG-A) and perfluorooctylethylacrylate (FA108) are used for the interface layer in this study. The author discusses the electrooptical properties of the composite films paying special attention to the anchoring strength and clarifies the relation between the physical characteristics of interface layer and the electrooptical properties.

Methacrylate copolymers of BzMA and perfluorooctylethylmethacrylate (FMA) are synthesized and applied to the polymer/LC composite films. Due to a small interaction between the LC and the copolymers, the copolymer/LC composite films show low driving voltage. However, electrooptical properties of PVA/LC composite films are superior to those of copolymer/LC composite films.

A New fabrication method for PVA/LC composite film with

deformed and disordered LC droplets is also proposed. LC droplets can be deformed by forming the PVA/LC composite film from water and methanol mixture (WM-mixture). The composite films have scattered the light strongly and have showed the high contrast. In addition, in order to control the size of LC droplet, the effects of the saponification and block character of PVA on electrooptical properties and morphology have been investigated. The LC droplet size can be varied by changing the saponification rate and block character because the surface tension of PVA aqueous solution can be controlled.

The composite film formed from the WM-mixture has scattered light intensively and has showed the following electrooptical properties: the driving voltage of 6 V_{rms}, hysteresis of less than 0.2 V_{rms}, turn-on time of 0.2 ms, and turn-off time of 11 ms. It has been elucidated from the data that the new type of PVA/LC composite film is superior to the traditional PVA/LC composite (NCAP) film which has the electrooptical properties of driving voltage of 56 V_{rms}, hysteresis of 14 V_{rms}, turn-on time of 10 ms, and turn-off time of 500 ms.

Contents

1. Introduction 1

1.1. Electrooptical Properties of Polymer/ Liquid Crystal (LC) Composite 1

1.1.1. Electrooptical measurements 3

1.1.2. Interaction at interface between polymer and LC 9

1.2. Historical and Present Scopes 13

1.3. Purpose and Present Methods 16

References 21

2. Control of Interaction at Interface between Poly(vinyl alcohol) (PVA) and LC 24

2.1. Proposal of New Type of PVA/LC Composite Films with Controlled Interface Layer. 24

2.1.1. Introduction 25

2.1.2. Experimental 25

2.1.3. Results and Discussion 28

Conclusions 41

References 42

2.2. Comparison of Electrooptical Properties of PVA/LC Composite Films with Different Kinds of Interface Layer. 43

2.2.1. Introduction 44

2.2.2. Experimental 44

2.2.3. Results and Discussion 47
Conclusions 57
References 59

3. Control of Interaction between Polymethylmethacrylate (PMMA) and LC 60

3.1. Electrooptical Properties of Polymer/LC Composite using New Optical Methacrylate Polymer with Fluorinated Side Group. 60
3.1.1. Introduction 61
3.1.2. Experimental 62
3.1.3. Results and Discussion 66
Conclusions 80
References 81

3.2. Fabrication of PMMA/LC Composite with Controlled Interface Layer by Two-Phase Separation Method 82
3.1.1. Introduction 83
3.1.2. Experimental 83
3.1.3. Results and Discussion 84
Conclusions 91
References 92

4. Control of Morphology of PVA/LC Composite 93

4.1.Control of Shape of LC Droplets by Changing Solvent 93
4.1.1. Introduction 94
4.1.2. Experimental 95
4.1.3. Results and Discussion 97
Conclusions 108
References 109

4.2. Control of Size of LC Droplets by Changing Saponification Rate of PVA 110
4.2.1. Introduction 111
4.2.2. Experimental 111
4.2.3. Results and Discussion 115
Conclusions 129
References 130
4.3. Control of Size of LC Droplets by Changing Block Character of PVA 131
4.3.1. Introduction 132
4.3.2. Experimental 133
4.3.3. Results and Discussion 134
Conclusions 143
References 143

Summary 144

Acknowledgments 145

Appendix

I. Characteristics of liquid crystal (ZLI2061) 146

II. List of abbreviations 147

III. List of publications 148

1. Introduction

Electroactive organic materials are very interesting as optical elements for integrated devices and large area displays, such as optical modulating and liquid crystal displays. Because of low cost, easy fabrication, low weight and variability of materials, polymeric materials have a great advantage compared to inorganic materials. This thesis describes a new type of polymer/low-molecular-weight liquid crystal (LC) composite films, which are of great interests from their potentials for wide varieties of applications in light shutters, flexible displays without polarizer, switchable windows, and other devices due to the possibility of electric-field-controlled light scattering.[1-25)]

1.1. Electrooptical Properties of Polymer/LC Composite

Polymer/LC composite films are usually sandwiched between substrates coated with transparent conducting electrodes, such as indium-tin-oxide (ITO), and may be switched from a scattering state to a transparent state by application of an appropriate electric field, as described in Fig. 1.1 schematically. In the absence of the electric field (OFF-state), the LC droplets are randomly aligned and the film scatters light. The light scattering results from the mismatch of the refractive indices of the LC droplets and polymer binder, and from inhomogeneous nematic director. Application of an electric field across the composite film (ON-state) makes

the director of the droplets aligned parallel to the field. If the ordinary refractive index (n_o) of the LC is matched with the refractive index of the polymer binder (n_p), the films are transparent in the ON-state for normally incident light.

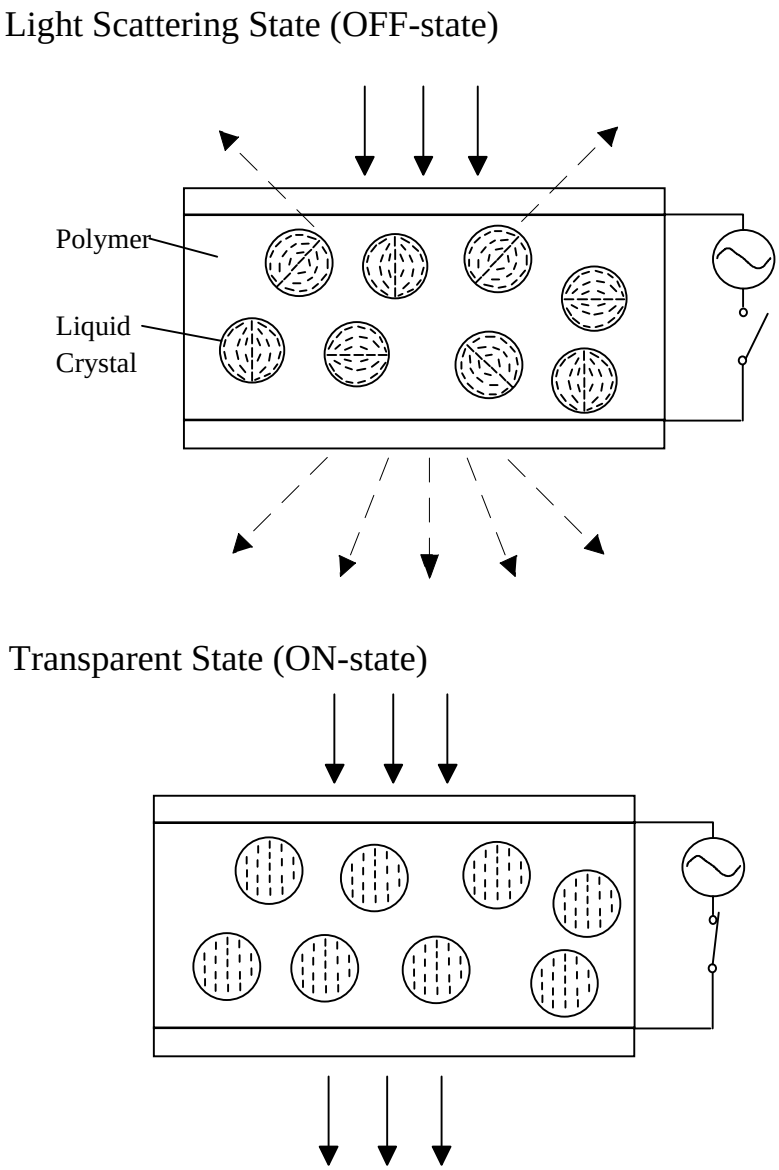

Fig. 1.1. Schematic representation of principle of operation of the polymer/LC composite film.

1.1.1. Electrooptical measurements

Electrooptical properties are measured by the following method in this thesis. Figure 1.2 draws the experimental setup for electrooptical measurements of polymer/LC composite films. A measurement system is composed of He-Ne laser light source (632.8 nm), a function generator, a high speed power amplifier, a silicon photodiode, a digitizing oscilloscope, and a personal computer. A square wave output with 1 kHz of the function generator controlled by the personal computer is amplified by the high speed power amplifier and is used to drive a sample cell. The He-Ne laser beam is passed through the sample cell perpendicular to the glass substrate (parallel to the electric field), and the transmitted light intensity is monitored with the silicon photodiode, the digitizing oscilloscope and the personal computer. In order to measure the driving voltage and hysteresis, the electric field is first increased (up-process) and then decreased (down-process) at a fixed rate of 0.89 V_{rms}/s. In order to measure the response time, the electric field is turned on and off, and the transmitted light intensity is monitored by the digitizing oscilloscope. In this thesis, root mean square voltage (V_{rms}), defined as a half value of peak-to-peak voltage of the square wave output, is used.

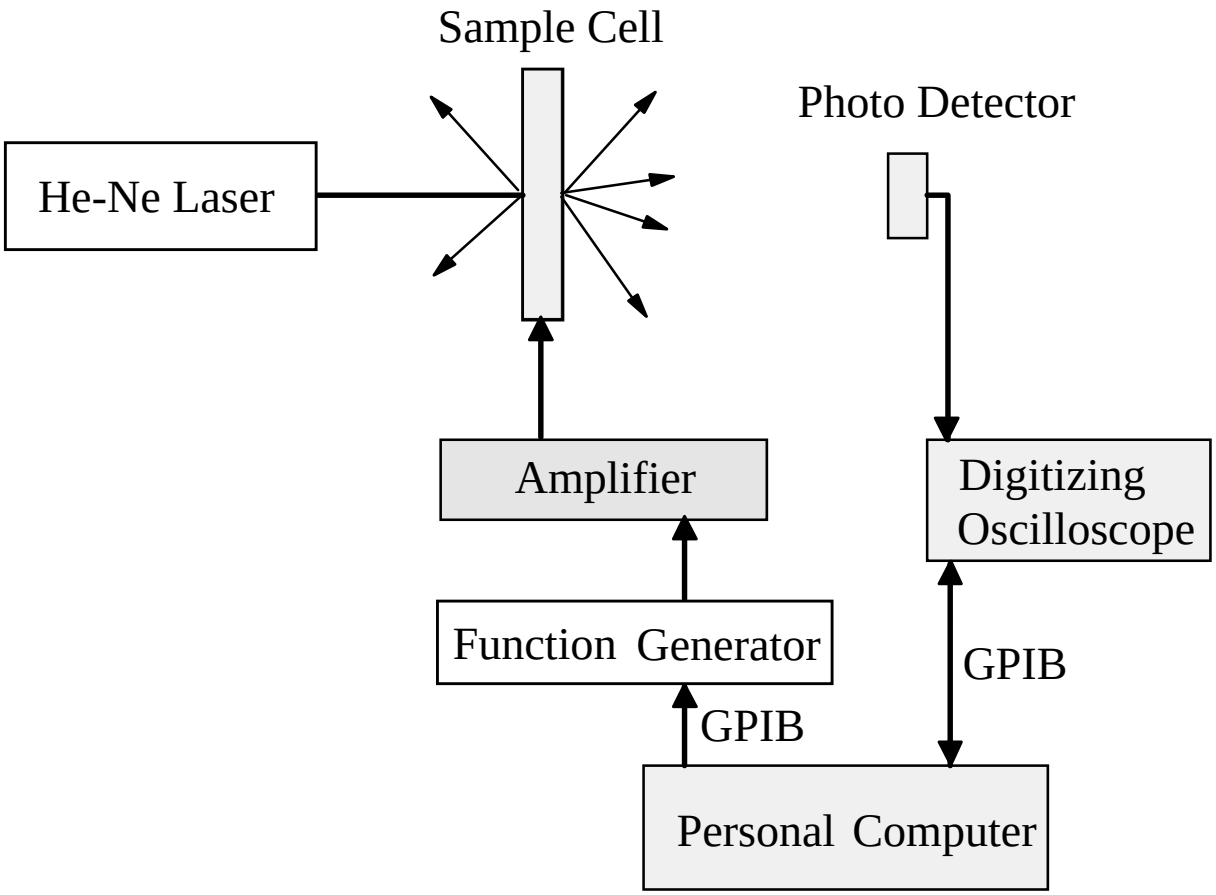

Fig. 1.2. Schematic drawing of experimental setup for electrooptical measurements of polymer/LC composite films.

The typical electrooptical properties of polymer/LC composite films are shown in the Figs. 1.3(a) and 1.3(b). Figure 1.3(a) shows the applied voltage dependence of transmittance of the sample cells (V-T curve). T_S is defined as transmittance in the ON-state and T_{min} defined as transmittance in the OFF-state. The driving voltage (V_{90}) is defined as the voltage reached to 90 % transmittance of $T_S - T_{min}$ in the voltage up-process, the hysteresis (ΔV) defined as the voltage difference between the up- and down-processes at the half value of $T_S - T_{min}$. Figure 1.3(b) shows the typical electric characteristic of the composite film. t_{on} is defined as the time taken from the OFF-state reaching to 90 % transmittance of $T_S - T_{min}$ by applying the voltage, and t_{off} defined as time taken from the ON-state decreasing to 10 % transmittance of $T_S - T_{min}$ by removing the voltage.

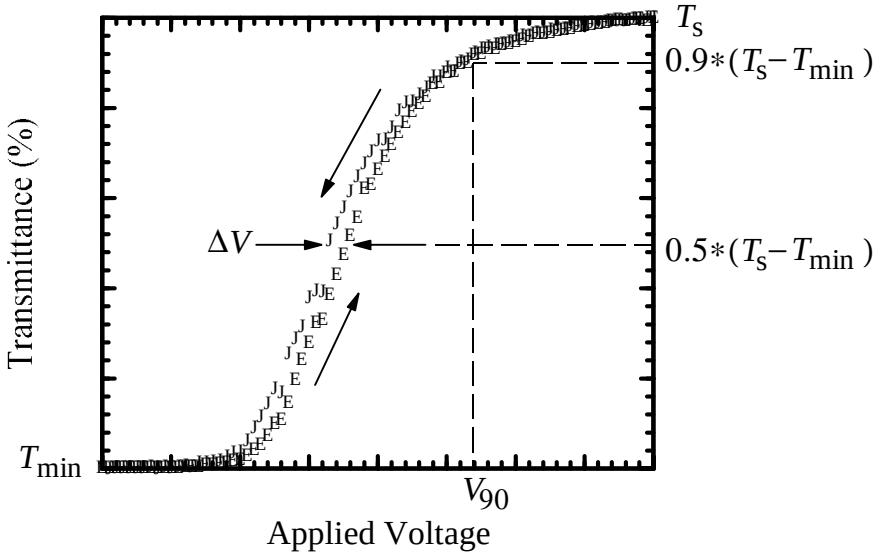

Fig. 1.3(a). Typical data of the applied voltage dependence of transmittance of the composite film.

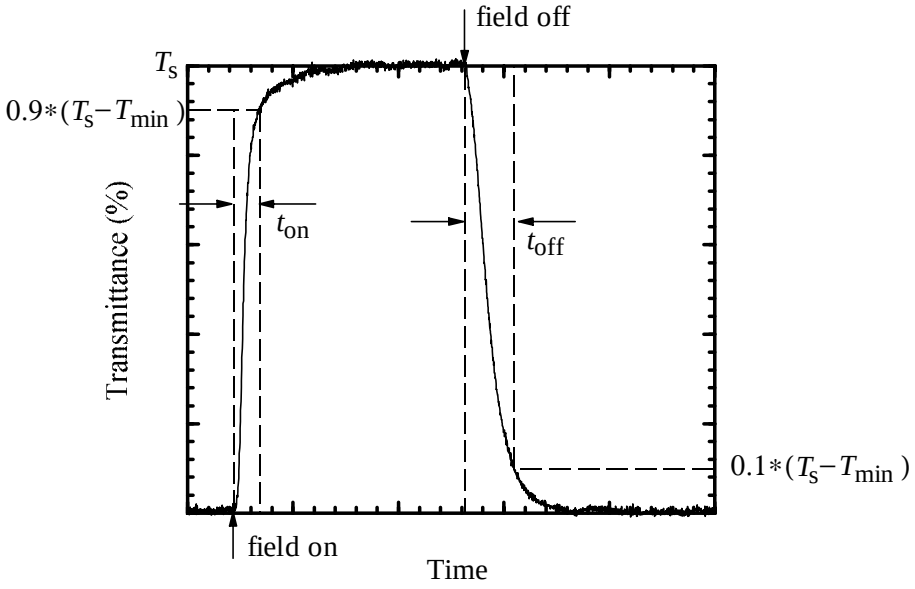

Fig. 1.3(b). Typical electric-switching characteristic of the composite film.

The electrooptical properties of polymer/LC composite films are affected by the following.

1. Dielectric constants of the polymer and LC.
2. Morphology of the composite film (the size and shape of LC droplets, thickness of the composite film).
3. The interaction at the interface between the matrix polymer and the LC (anchoring strength).
4. Thermal dynamics at the interface between the polymer and the LC.

Wu and coworkers formulated the relation between the electrooptical properties and the shape and size of the droplet.[20] They elucidated that the driving voltage (E_{th}) was high and the response time (t_{off}) was short in the case of the small size of LC droplet as follows,

$$E_{th} = \frac{1}{a}\left|\frac{K(l^2-1)}{\Delta\varepsilon}\right|^{1/2}, \quad (1)$$

$$t_{off} = \frac{\gamma a^2}{K(l^2-1)}, \quad (2)$$

where a and b are the lengths of the semi-major and semi-miner axes of the LC droplet, respectively, $l=a/b$, K an elastic constant, γ a viscous constant, and $\Delta\varepsilon$ a dielectric anisotropy. Fuh *et al*. measured the distribution of size and spacing of LC droplets of the composite films cured with various tungsten-halogen light intensities.[23] They concluded that the droplet size was small in the composite films cured with a high curing light intensity because of the high rate of polymerization and the composite films with

large LC droplets had the low driving voltage.

Koval and coworkers investigated the response time for two types of polymer dispersed LCs with normally and tangentially (fabricated by adding a small amount of lecithin) anchored drops.[6] They observed different response time due to different anchored LC drops. West *et al*. studied the electrooptical properties as a function of temperature of a polymer dispersed LC film composed of E7 (nematic mixture) dispersed in a polyvinylformal (PVFM) matrix.[24] They postulated that changes of the polymer/LC interface at the glass transition of the polymer meight be responsible for the observed electrooptic behavior. However, preliminary measurements of the anchoring strength as a function of temperature could not show any abrupt change at the glass temperature of matrix polymer. Li *et al*. reported the switching of a polymer dispersed LC film by a magnetic-field and considered the origin of the hysteresis by comparing with the electric field response.[25] They suggested that the hysteresis resulted from an inherent bistability in the director configuration in the LC droplets.

1.1.2. Interaction at interface between polymer and LC

The electrooptical properties of composite films are also affected by the interaction at the interface between the matrix polymer and the LC. At a nematic interface, there appears, in general, a surface torque field which couples with the orientational degrees of freedom of nematic molecules and aligns them in a preferred direction. Macroscopically, the effect of this surface torque can be described in terms of the interfacial free energy, $\gamma(\theta)$, which depends on the angle of the director at the interface, θ, equals the angle of the preferred direction θ_e. Though there are still arguments as to the functional form of $\gamma(\theta)$, it is generally possible, if $|\theta - \theta_e| << 1$, to expand it about θ_e to give

$$\gamma(\theta) = \gamma(\theta_e) + \frac{1}{2} E_a (\theta - \theta_e)^2. \qquad (3)$$

Here, E_a is a materiel parameter called the anchoring strength coefficient, or the anchoring energy for short. As it stands, the anchoring energy gives a measure of the amount of work which should be performed to rotate the interface director from its preferred direction, θ_e, and dose reflect, in some integrated manner, the strength of the surface torque field. The extrapolation length (d_e) is also conveniently used for the amount of the material parameter for the interaction at the interface between the polymer and LC. The d_e is given from E_a and elastic constant (K),

$$d_e = K / E_a, \qquad (4)$$

and is described as shown in Fig. 1.4, schematically.

(a)

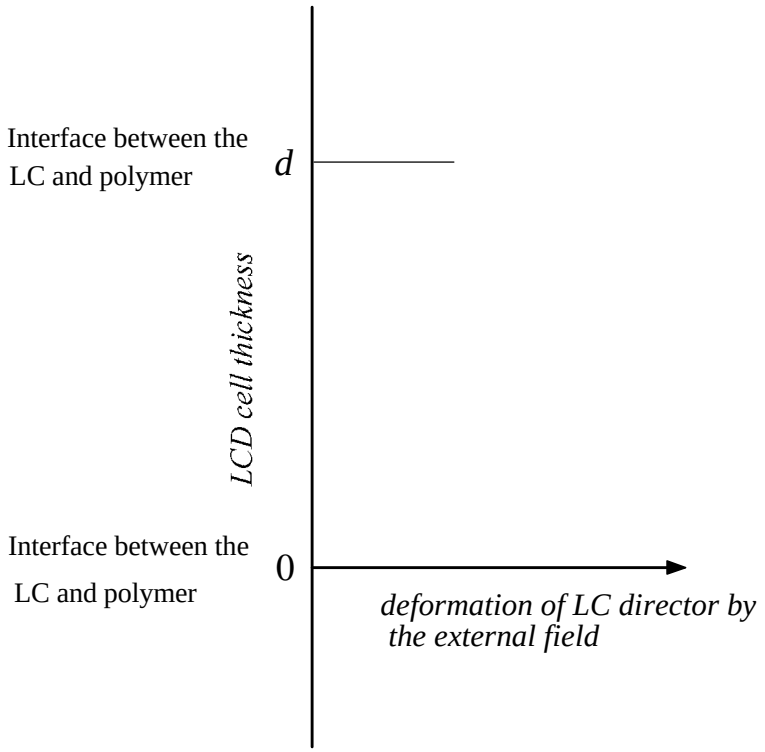

(b)

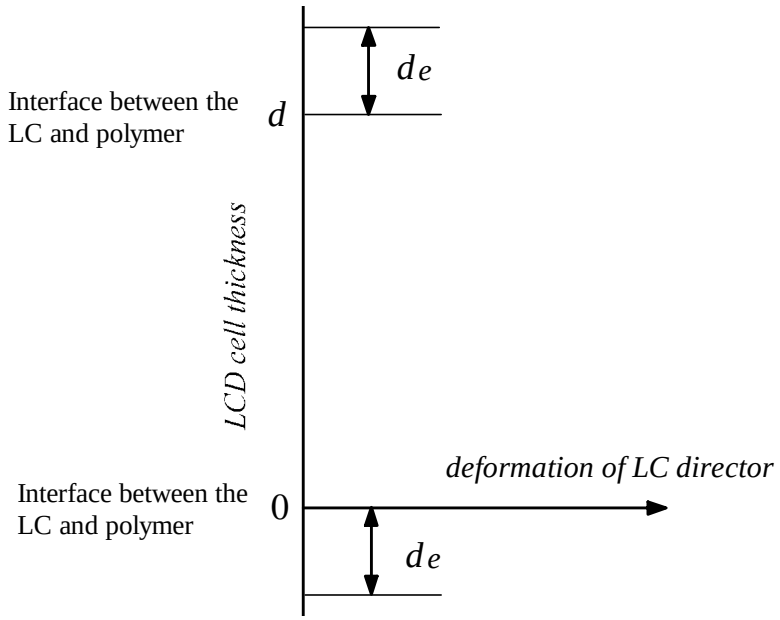

Fig. 1.4. The definition of the extrapolation length (d_e). (a) strong anchoring and (b) weak anchoring.

The extrapolation length at the interface between the SiO_2 surface and the nematic LC was measured by Yokoyama and van Sprang for the first time[26] and the extrapolation lengths at the interface between several kinds of polymers and the LC are determined by the method in the present thesis. A Freedericksz cell consisting of glass substrates coated with ITO and the polymer is used as a model for the composition of the polymer matrix in the polymer/LC composite film. The measurement system of optical retardation is composed of a 3 mW He-Ne laser (632.8 nm) light source, two λ/4 plates, a polarizing prism, an analyzing prism, a polarization modulator, a lock-in amplifier, a photodetector, and a rotation system of the analyzing prism. They are arranged in accordance with an automatic ellipsometric configuration. The capacitance of the LC cell is directly determined by measuring the ratio of the applied voltage and the out-of-phase component of the current across the sample cell. A sinusoidal wave output with 7 kHz of the function generator controlled by the personal computer is amplified with the high speed power amplifier and is used to drive the sample cell. The voltage is applied step by step from 0 V_{rms} to 80 V_{rms} (sufficiently high compared with the threshold voltage), and the retardation and the capacitance are simultaneously measured. Finally, the extrapolation length is calculated by using the following equation of Yokoyama and van Sprang,

$$\frac{R}{R_0} = \frac{I_0}{CV} - \frac{2d_e}{d} \qquad (5)$$

where C, V, R_0, and d are the capacitance of the cell, the applied voltage, the optical retardation (R) at V=0, the cell thickness, respectively, and I_0 is

a constant which depends only on the material parameters of LC.

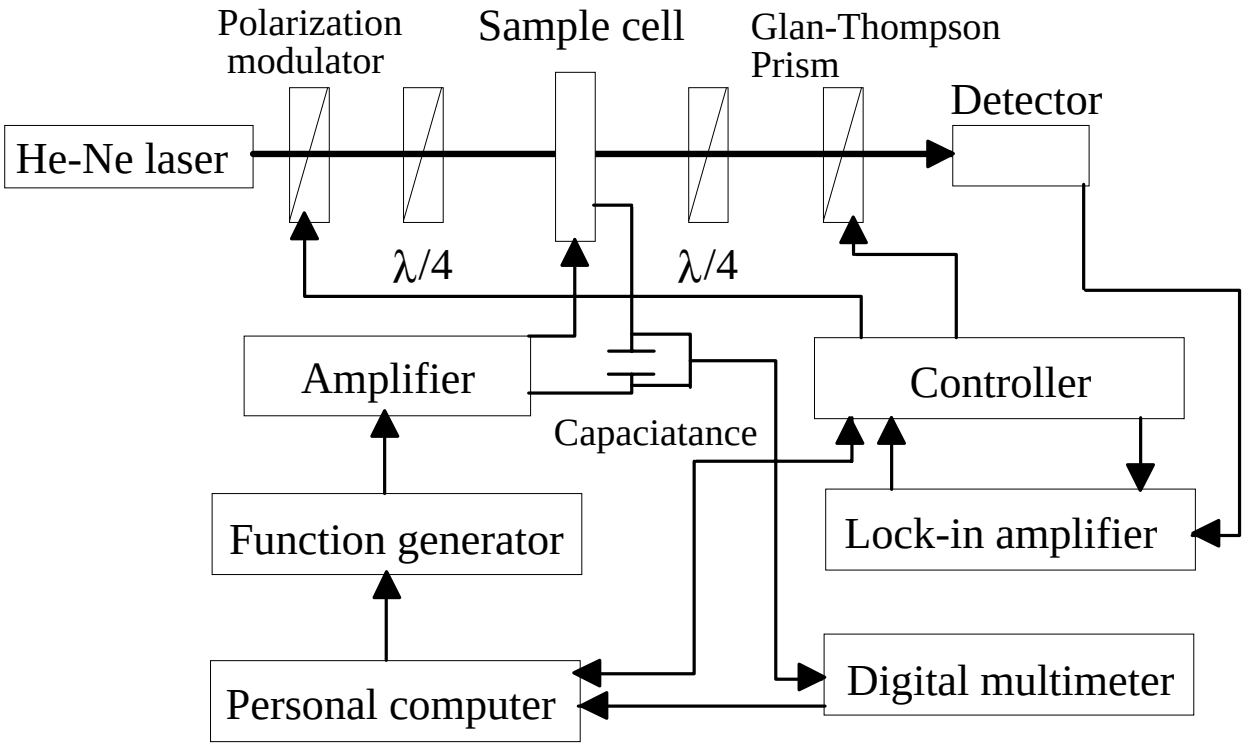

Fig. 1.5. Schematic drawing of experimental setup for extrapolation length at the interface between the polymer and the LC.

1.2. Historical and Present Scopes

Several methods to disperse the LC droplets in the polymer matrix were reported with regard to methods of a solvent-induced phase separation (SIPS),[7,11,14,16-19] a photopolymerization-induced phase separation (PPIPS),[4,15,21,22] and an LC emulsion in aqueous polymer solution.[2,3,9,13,20] Schematic representation of these fabrication methods of polymer/LC composite films are described in Fig. 1.6.

At 1982, Crighead *et al.* reported on a new display consisting of an optically nonabsorbing matrix with micrometer size pores filled with a liquid crystal.[1] They obtained the optical response of the cell which showed a decay of the transmission with time, typically within 30-100 ms. In addition, T_{max} was only 10-30 %. At 1986, Doane and coworkers presented a new material consisting of microdroplets of nematic LCs which are spontaneously formed in a solid polymer at the time of its polymerization.[2] The droplets were formed spontaneously upon curing a homogeneous mixture of a resin formed from epichlorohydrin and bisphenol A, the LC compound and a polyamine curing agent. The cell required a driving voltage of about 30 V_{rms}. At 1986, Drzaic *et al*. gave a description of the macroscopic properties of a composite film formed from the LC emulsion in aqueous polymer, such as poly(vinyl alcohol) (PVA) solution (namely "NCAP").[3] The driving voltage of a typical NCAP film was about 40-100 V_{rms}. At 1987, Smith *et al*. formed a polymer/LC composite films by ultraviolet (UV) initiated polymerization of monomer/LC solutions (PPIPS).[4] Nomura and coworkers reported thin films composed of nematic LCs in polymer matrices are promising materials at 1990.[5] They produced several diameters of microspheres, and

made films using them. They determined the light scattering characteristics of these films by the refractive indices of the LC and polymers and the microsphere size. The saturation voltage was 40-80 V_{rms} and decreased monotonously with increasing mean diameter. Kajiyama *et al*. proposed the composite film consisting of PMMA/LC formed by solvent-induced phase separation (SIPS) and obtained the driving voltage of 40-120 V_{rms} at 1992.[7)]

Among them, NCAP film is practically used for architectural applications because of its feasibility for mass production and for treating large areas. However NCAP films for minute displays can not been used because those have a high driving voltage (40-100 V_{rms}), a large hysteresis and a slow response time.

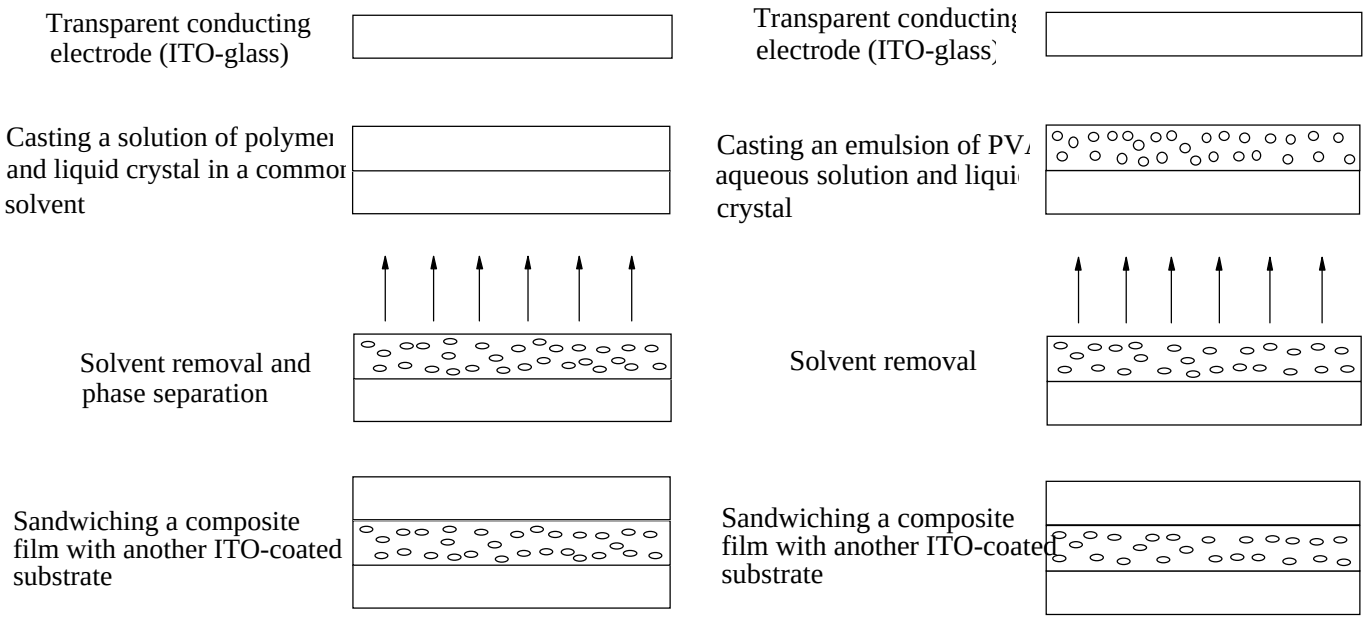

(a) Solvent-induced phase separation (SIPS) (b) Emulsification

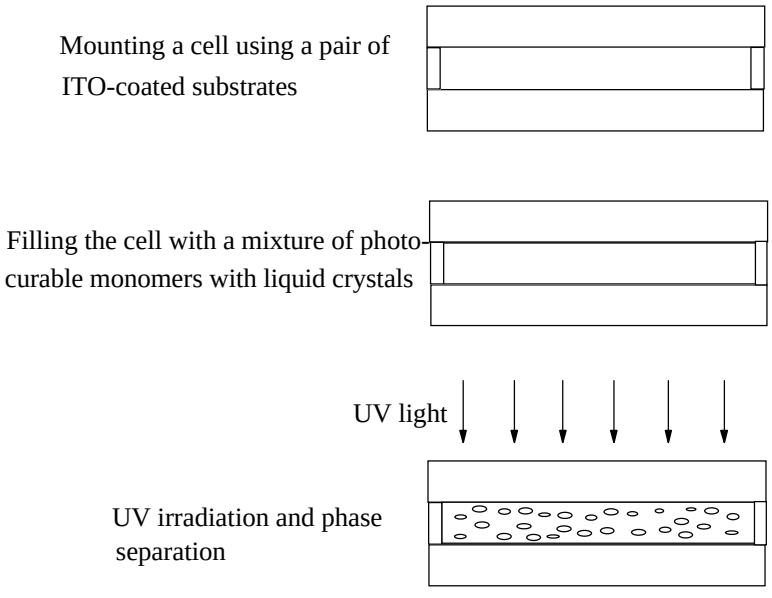

(c) Photopolymerization-induced phase separation (PPIPS)

Fig. 1.6. Schematic representation of three typical fabrication methods of

polymer/LC composite films.

1.3. Purpose and Present Methods

The purpose of the present thesis is to improve the electrooptical properties of PVA/LC composite films and to clarify the mechanism of the improvement of the electrooptical properties. In addition, new fabrication methods for PVA/LC composite films with controlled droplet size are proposed. The following conditions are required in order to utilize polymer/LC composite films for minute displays using the TFT devices.

1. The driving voltage is about or less than 5 V_{rms}.
2. Low hysteresis.
3. Fast response time.
4. High contrast.

The present thesis consists of the following three sections.

2. Control of Interaction at Interface between PVA and LC.
3. Control of Interaction at Interface between PMMA and LC.
4. Control of Morphology of PVA/LC Composite.

In order to improve the electrooptical properties of PVA/LC composite, in section 2, a new type polymer/LC composite film which is prepared by casting the PVA/LC emulsion with added photocurable monomers followed by photocuring and the elctrooptical properties are studied paying special attention to the anchoring energy at the interface between the polymer and the LC. The new fabrication method is described

in Fig. 1.7 schematically.

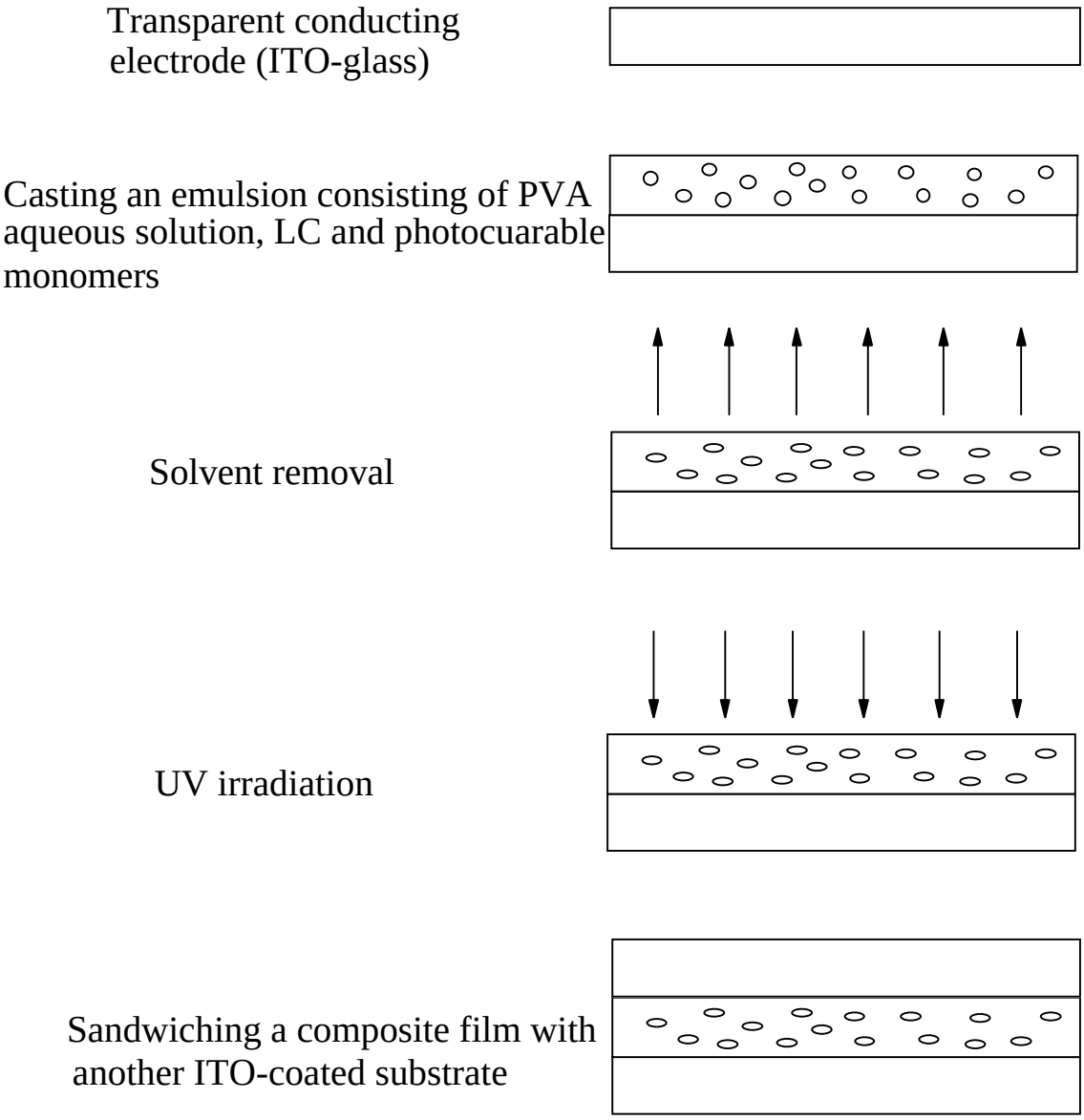

Fig. 1.7. Schematic representation of a new fabrication method of PVA/LC composite films. This method is called emulsification and

photopolymerization-induced phase separation method (PPIPS).

The schematic structure of the composite film formed by this method is described in Fig. 1.8(b). The interaction at the interfaces between the polymer and the LC can be controlled by this new fabrication method by changing the material and composition of the interface layer. The photocured polymers make of the interface layers between the LC droplets and the PVA matrix, and reduce the anchoring force between the LC and the polymer layer appreciably. The new type of PVA/LC composite film has showed the electrooptical properties as follows: the driving voltage is 19 V_{rms}, hysteresis of 5 V_{rms}, turn-on time of 0.2 ms, and turn-off time of 11 ms. It is clear from the data that the new type of PVA/LC composite film is superior to the traditional PVA/LC composite film possessing the electrooptical properties of the driving voltage of 56 V_{rms}, hysteresis of 14 V_{rms}, turn-on time of 10 ms, and turn-off time of 500 ms.[3,9)]

The electrooptical properties are studied on three kinds of composite films with added three combinations of photocurable mixtures of benzylacrylate (BzA) and perfluorooctylethylacrylate (FA108), benzylmethacrylate (BzMA) and FA108, and nonaoxyethylenediacrylate (9EG-A) and FA108, paying attention to the LC droplet size and the anchoring energy at the interface between the polymer and the LC, and the effects of photocurable monomers on morphology and electrooptical properties of PVA/LC composite films with added photocured polymers. It has been clarified that the improvement of the electrooptical properties caused by adding a suitable amount of fluorinated acrylate can be explained by the low anchoring energy of copolymers comprising the perfluorooctyl and benzyl side groups. In addition, it is suggested that the electrooptical properties are influenced by the thermal motion at the

(a) Traditional PVA/LC composite (T-cell)

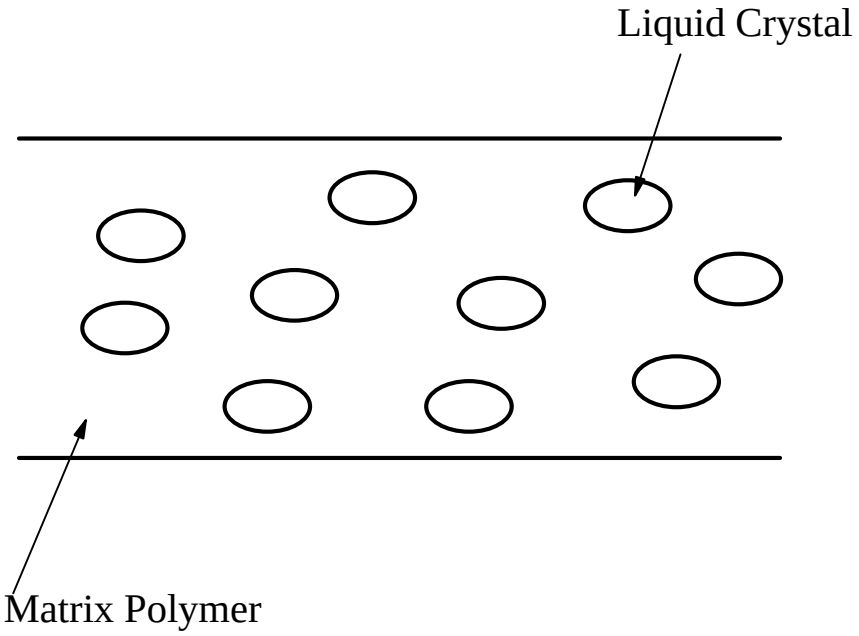

interface between the polymer and the LC in the ON-state.

(b) PVA/LC/photocured polymer composite (PLP-cell)

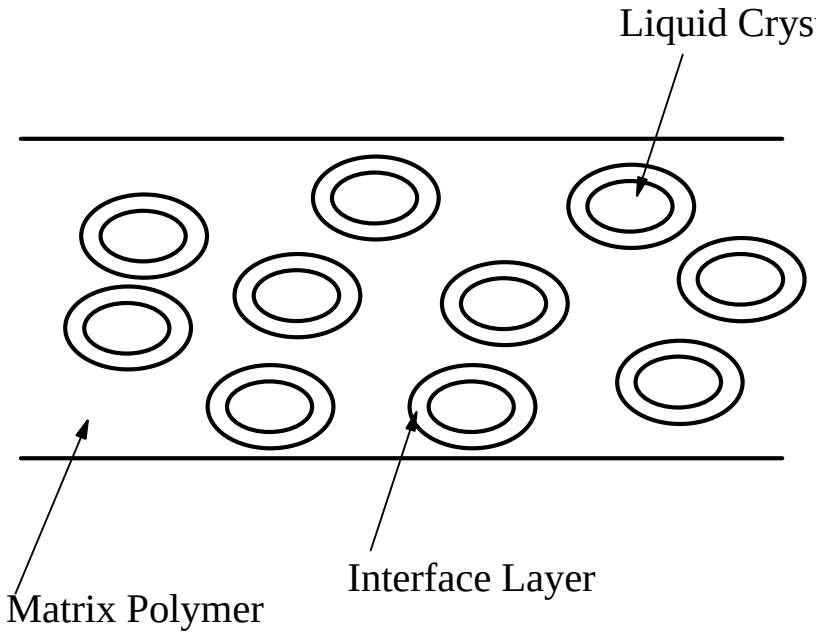

Fig. 1.8. Schematic structure of the new type of the composite film proposed in the present thesis.

The PVA/LC composite films with added photocrosslinkable monomers (the mixture of 9EG-A with FA108) show a driving voltage of 15 V_{rms} and hysteresis of less than 1 V_{rms}.

In section 3, a new optical polymer, poly-(benzylmethacrylate-co-perfluoroocthylmethacrylate) (poly-BzMA-co-FMA), is synthesized by a radical solution polymerization and is applied to the polymer/LC composite films by the SIPS method. Contact angle of the copolymers with various liquids is increased with increasing the FMA composition in the copolymer as a result of decrease in the interaction between the LC and the copolymer with increasing the FMA composition. Due to a small interaction between the LC and the copolymers, the copolymer/LC composite films show the low driving voltage corresponding to about 1/3 value of the PMMA/LC composite film. This section describes fabrication of composite films with a thin photocured polymer layer between the PMMA matrix and LC droplet by two-phase separation method, composed of SIPS followed by PPIPS. The author can fabricate the PMMA/LC composite with thin layer between the PMMA and LC by controlling the solubility of materials.

Section 4 describes that the relationship between the physical characteristics of PVA and the morphology is clarified, and that the PVA/LC composite film has a low driving voltage of less than 6 V_{rms} and a low hysteresis of less than 0.2 V_{rms}. This superior data has been achieved by using the composite film under the condition that the LC droplets surrounded by a thin layer of the photocured polymer, are deformed as well as disordered to enhance light scattering. The composite film is formed from the emulsion composed of a mixture of water with

methanol (WM-mixture), PVA, LC, and a photocrosslinkable mixture. LC droplet size in the PVA/LC composite film can be controlled by changing the saponification rate or blend ratio of PVA with different saponification rate because the surface tension of PVA aqueous solution is increased with increasing the saponification rate of PVA. It is also clarified that the anchoring strength is decreased with decreasing the saponification rate. A new fabrication method for the PVA/LC composite films with controlled size LC droplets is also presented. It is clarified that the LC droplet size is changed by changing the dispersion state of hydrosis in PVA (Block character) because the surface tension of PVA is changed.

References

1) H. G. Craighead, Julian Cheng and S. Hackwood: *Appl. Phys. Lett.* **40** (1982) 22.
2) J. W. Doane, N. A. Vaz, B. G. Wu and S. Zumer: *Appl. Phys. Lett*. **48** (1986) 269.
3) P. S. Drzaic: *J. Appl. Phys.,* **60** (1986) 2142.
4) Vaz, N. A. Smith, G. W. and Montgomery, G. P., Jr.: *Mol. Cryst. Liq. Cryst.* **146** (1987) 1.
5) H. Nomura, S. Suzuki and Y. Atarashi: *J. Appl. Phys*. **68** (1990) 2922.
6) A. V. Koval, M. V. Kurik, O. D. Lavrentovich, and V. V. Sergan: *Mol. Cryst. Liq. Cryst.* **193** (1990) 217.
7) T. Kajiyama, H. Kikuchi and A. Takahara: *Proc. SPIE* **1665** (1992) 20.

8) K. Kato, K. Tanaka, S. Tsuru and S. Sakai: *Jpn. J. Appl. Phys.* **32** (1993) 4594.

9) P. S. Drzaic and A. M. Gonzales: *Mol. Cryst. Liq. Cryst.* **222** (1992) 11.

10) L. C. Chien: *Proc. SPIE* **1815** (1992) 220.

11) T. Kajiyama, A. Miyamoto, H. Kikuchi and Y. Morimura: *Chem. Lett*. (1989) 813.

12) F. G. Yamagishi, L. J. Miller and C. I van Ast: *Proc. SPIE* **1080** (1989) 24.

13) J. W. Doane, N. A. Vaz, B. G. Wu and S Zumer: *Appl. Phys. Lett.* **48** (1986) 269.

14) K. Takizawa, H. Kikuchi, H. Fujikura, Y. Namikawa and K. Tada: *Jpn. J. Appl. Phys.* **33** (1994) 1346.

15) G. M. Zhang, Z. H. Zhou, Z. Changxing, B. Wu and J. W. Lin: *Proc. SPIE* **1815** (1992) 233.

16) A. Miyamoto, H. Kikuchi and T. Kajiyama: *Polym. Prepr. Jpn.* **40** (1991) 1022.

17) S. Kobayashi, A. Miyamoto, H. Kikuchi and T. Kajiyama: *Polym. Prepr. Jpn.* **40** (1991) 1023.

18) F. Usui, H. Kikuchi and T. Kajiyama: *Polym. Prepr. Jpn.* **41** (1992) 3710.

19) K. Park, H. Kikuchi and T. Kajiyama: *Polym. Prepr. Jpn.* **42** (1993) 660.

20) B. G. Wu, J. H. Erdmann and J. W. Doane: *Liq. Cryst.* **5** (1989) 1453.

21) S. Ducharme, J. C. Scott, R. J. Twieg and W. E. Moerner: *Phys. Rev. Lett.* **66** (1991) 1846.

22) H. L. Hampsh, J. Yang, G. K. Wong and J. M. Torkelson: *Macromolecules* **21** (1988) 526.

23) A. Y. Fuh and T. C. Ko: *Proc. SPIE* **1815** (1992).

24) J. L. West, J. R. Kelly, K. Jewell, and Y. Ji: *Appl. Phys. Lett.* **60** (1992) 3238.

25) Z. Li, J. R. Kelly, P. Palffy-Muhoray and C. Rosenblatt: *Appl. Phys. Lett.* **60** (1992) 3132.

26) H. Yokoyama and H. A. van Sprang: *J. Appl. Phys*. **57** (1985) 4520.

2. Control of Interaction at Interface between PVA and LC

2.1. Proposal of New Type of PVA/LC composite Films with Controlled Interface Layer

Electrooptical properties are studied on a new type of polymer/liquid crystal (LC) composite film composed of a poly(vinyl alcohol) (PVA), LC, and a photocured polymer. The composite films are prepared by casting the PVA/LC emulsion with a mixture of benzylmethacrylate (BzMA) with perfluorooctylethylacrylate (FA108) followed by photocuring, resulting in a low driving voltage of 19 V_{rms}, a rapid turn-on time of 0.2 ms, and a rapid turn-off time of 11 ms. The results can not be entirely explained by the change in droplet shape and size. It is suggested that photocurable monomers polymerize at the interface which causes change in the boundary condition between PVA and the LC.

2.1.1. Introduction

The electrooptic properties of polymer/LC composite films are influenced by such parameters as film thickness, droplet shape, size and density, the electric properties of polymer and LC, and surface interaction between the polymer wall and LC molecule. In particular, electrooptical response time and the driving voltage strongly depend on the interaction between the LC droplet and the polymer matrix.[1,2)]

The purpose of the present section is to realize a new type of PVA/LC composite film with a lower driving voltage and a faster response time compared with traditional NCAP film. The composite film was formed by dissolving a small amount of photocurable monomers in PVA/LC emulsions. The photocurable monomers were added to the emulsion of a nematic LC in an aqueous solution of PVA to change the boundary condition at the interface between the LC droplet and the PVA matrix. The electrooptical properties were compared with PVA/LC composite films with added photocured polymers and traditional PVA/LC composite films without the photocured polymers. The morphology of the composite films varied with the composition of photocured polymers. It was suggested that the extremely thin layer of the photocured polymers caused change in the boundary condition at the interface between the LC and the PVA matrix.

2.1.2. Experimental

Materials

PVA (trade name PVA205, having the degree of polymerization of 500 and the saponification rate of 88 mol%) was supplied by Kuraray Co., Ltd. Nematic LC mixture with positive dielectric anisotropy (ZLI2061) was obtained from Merck Japan Ltd., perfluorooctylethylacrylate (FA108) from Kyoeisha Chemical Company, and dimethoxyphenylacetophenone (DMPA), a photoinitiator, from Tokyo Kasei Industries. Benzylmethacrylate (BzMA) was supplied by Wako Chemicals and purified by column chromatography to remove inhibitors. The glass substrate with an ITO electrode was obtained from Matsunami Glass Company. Transmittance of the ITO-coated glass substrate was 86 % at 632.8 nm and the DC resistance of the ITO electrode was 150 Ωcm.

Sample preparation

PVA205 was dissolved into distilled water at 23 ℃ to prepare a 15 wt% aqueous solution of PVA205. The solution was heated to 100 ℃ to dissolve PVA205 completely. After the solution was cooled to be at room temperature, a mixture of photocurable monomers (mixture of BzMA and FA108, and 5 wt% of DMPA) and ZLI2061 was dispersed in the solution and stirred at 5000 rpm for 5 min on and off every 15 s with a small propeller blade to prepare a LC emulsion (water-in-oil-type emulsion). This procedure produced a creamy white emulsion containing air, which was allowed to rest for 20-24 h to degas. The concentration of ZLI2061 was controlled at 60 wt% in the composite film. The emulsion was then spin-coated onto an ITO-coated glass substrate at 1500 rpm and then cured for 40 min by using a mask aligner (Mikasa model MA-10) with a lamp intensity of 11-13 mW/cm^2 at 365 nm. The film was then laminated

under pressure to another piece of ITO-coated glass substrate to form the finished cell. BzMA and FA108 were mixed at weight ratios of 0:100, 20:80, 40:60, 60:40, 80:20, and 100:0. Weight ratios of photocurable monomers and PVA205 were controlled at 5:95, 10:90, 25:75, and 50:50. Traditional PVA/LC cells (T-cells) were also constructed by the same emulsification method for comparison with the PVA/LC/photocured polymer cells (PLP-cells).

Morphology observations

Morphology of composite films was observed by scanning electron microscopy (SEM). The LC and photocured polymers of the composite films were extracted with methylene chloride at 23 ℃ for 30 s to observe the morphology. The samples were sputter-coated with a thin layer of gold and palladium alloy for operation in the SEM mode. The droplet shape and size of polymer/LC composite films were observed in a vertical view.

Measurements of surface tensions

Surface tensions of ZLI2061, PVA aqueous solutions, and photocurable monomers were determined from the contact angles (θ). The contact angle measurements were carried out on a Teflon-sheet surface at 23 ℃ with a Kyowa contact angle meter. The values of $\cos\theta$ against surface tensions (Zisman plots) of a Teflon sheet were plotted by measuring the contact angles of *n*-heptane, *n*-hexane, water, ethyleneglycol, and diethyleneglycol. The surface tension of the liquid was well established by previous work as 20.3, 18.4, 36.3, 47.7, and 44.4 dyn/cm, respectively.[3] The surface tension of a test liquid could be determined from Zisman plots by measuring the contact angle of the liquid on the

Teflon-sheet surface. If the surface tension of the test liquid is lower than that of the Teflon sheet, it is impossible to determine the contact angle. The critical surface tension of a Teflon sheet was sufficiently low (～ 19 dyn/cm) to determine the contact angle of most liquids.

2.1.3. Results and Discussion

Morphology of composite films

It is well known that the droplet size of oil in emulsion rapidly increases during the first few hours of storage, agglomerating to form large droplets. In the present work, the droplet size in the emulsion may grow in the course of degassing. BzMA and FA108 could be dissolved together, and showed different solubilities from ZLI2061. BzMA and ZLI2061 could be dissolved together, while FA108 and ZLI2061 could not. When the droplet size grew, the order of LC, BzMA and FA108 were re-arranged according to the differences in the solubilities and surface tensions of BzMA and FA108.

Structural characteristics of LC droplets in the polymer/LC composite film were controlled by the surface energy of the LC mixture and PVA aqueous solution. It is desirable that the LC droplet in the emulsion (water continuous) be a perfect sphere in order to minimize the surface energy. As shown in Figs. 2.1(a)-2.1(c), the domain shapes were oblate with minor axes aligned perpendicular to the film plane. The LC droplets in these films adopt a bipolar configuration, minimizing their elastic deformation energy when the bipolar symmetry axis is aligned along a major axis of the spheroid. Figure 2.1(a) shows that the domain

size of the T-cell was 2-3 μm. On the other hand, as shown in Figs. 2.1(b) and 2.1(c), the sizes of the holes for the PLP-cells were larger than that of the T-cell but their shapes were similar. If the photocured polymers themselves formed droplets, the holes formed by extracting the photocured polymers could be observed in addition to the LC droplets, since both the LC and photocured polymers were extracted by the methylene chloride. Our result suggests that photocured polymers themselves did not form the droplets and were present in the same droplets as ZLI2061.

The sizes of LC droplets in the composite films were estimated from the absorbance spectrum according to Rayleigh-Gans-Debye theory (Debye plot) before LC and photocured polymers were extracted by methylene chloride. It is known that a large slope of the Debye plot indicates small droplet size.[4] All measurements of absorbance spectra were performed for sufficiently thin films (∼4 μm) in order to remove the effects of high-order scattering. Debye plots of three T-cells, which were constructed from PVA aqueous solutions with different concentrations, and two PLP-cells are shown in Fig. 2.2. The sizes of LC droplets were nominally changed by the addition of the photocured polymers since the slope for a T-cell (line (c) in Fig. 2.2) was almost equivalent to the slopes for two PLP cells (lines (d) and (e) in Fig. 2.2).

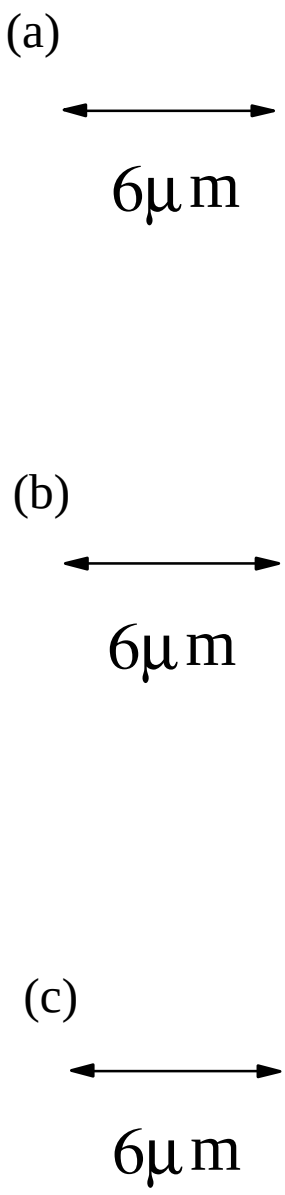

Fig. 2.1. Morphology of PVA/LC composite films with various concentrations of photocured polymers. Weight ratio of BzMA and FA108 was fixed at 60:40. All composite films were constructed with 15 wt% of PVA aqueous solutions. (a) 0 wt% (T-cell), (b) 10 wt% (PLP-cell) and (c)

25 wt% (PLP-cell).

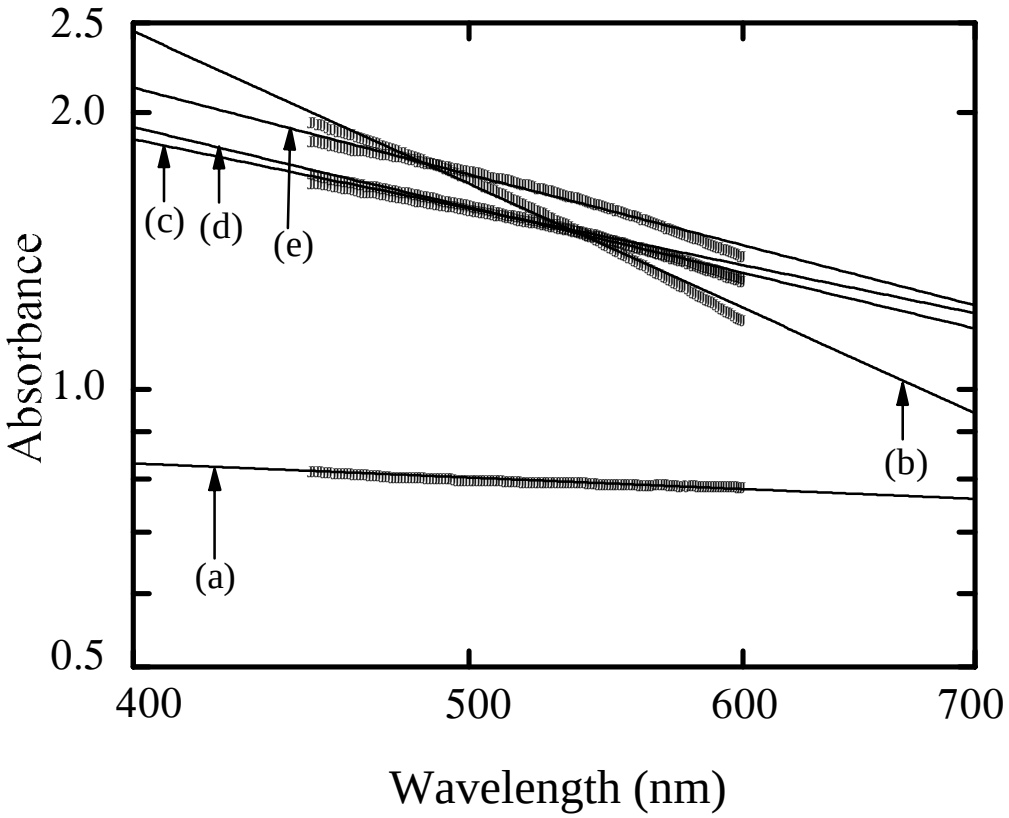

Fig. 2.2. Debye plots of composite films. Concentration of ZLI2061 in the three T-cells was controlled at 60 wt%. Weight ratio of BzMA and FA108 was fixed at 60:40. (a) T-cell constructed with 13 wt% of PVA aqueous solution, (b) T-cell constructed with 18 wt% of PVA aqueous solution, (c) T-cell constructed with 15 wt% of PVA aqueous solution, (d) PLP-cell with 10 wt% of photocured polymers constructed with 15 wt% of aqueous solution, (e) PLP-cell with 25 wt% of photocured polymers constructed with 15 wt% of aqueous solution. In this figure, dots indicate experimental data and lines indicate fitted lines.

Comparisons of electrooptical properties of PLP-cell with T-cell

Three T-cells were fabricated from PVA aqueous solutions with different concentrations to change the surface tensions of PVA aqueous solutions and the droplet sizes of the composite films, in order to examine the influence of the droplet size because the electrooptical properties are affected by the droplet size. Concentrations of PVA aqueous solutions were 13 wt%, 15 wt% and 18 wt%. The surface tensions of the PVA solutions were 52, 47 and 43 dyn/cm, respectively. The sizes of LC droplets in these NCAP films were determined from the absorbance spectrum, as shown in Fig. 2.2 (lines (a), (b) and (c)). The sizes of LC droplets in the T-cells were < 1 μm with 18 wt% of solution, 2-3 μm with 15 wt% of solution, 4-5 μm with 13 wt% of solution. V_{90} of the T-cells were larger than 40 V_{rms} and t_{off} were longer than 100 ms as summarized in Table 2.1.

Table 2.1. Electrooptical properties of T-cells constructed with PVA aqueous solutions with different concentrations.

	Size (μm)	ΔV (Vrms)	V_{90} (Vrms)	t_{on} (ms)	t_{off} (ms)
18 wt%	<1	20	>80	>200	>500
15 wt%	2–3	14	56	10	>500
13 wt%	4–5	12	42	5	120

In comparison, Fig. 2.3 shows V-T curves of a T-cell and a typical PLP-cell with application of a 1 kHz square-wave field. The voltage required to drive the T-cell was 56 V_{rms}, whereas the PLP-cell was driven above 19 V_{rms}. ΔV of the PLP-cell was lower than that of the T-cell and t_{off} of the PLP-cell was 11 ms. The improvements of the electrooptical properties of the PLP-cells cannot be entirely explained by the change in the droplet shape or size. Moreover, the dielectric constant of matrix polymer was not changed by the addition of photocured polymers. These results suggest that the electrooptical properties of the PLP-cell were improved by the change of the boundary condition at the interface between the LC droplet and the polymer matrix due to the addition of photocured polymers. The anchoring force of the polymer surface may be decreased by the photocured polymers as a consequence of the change in the boundary condition.

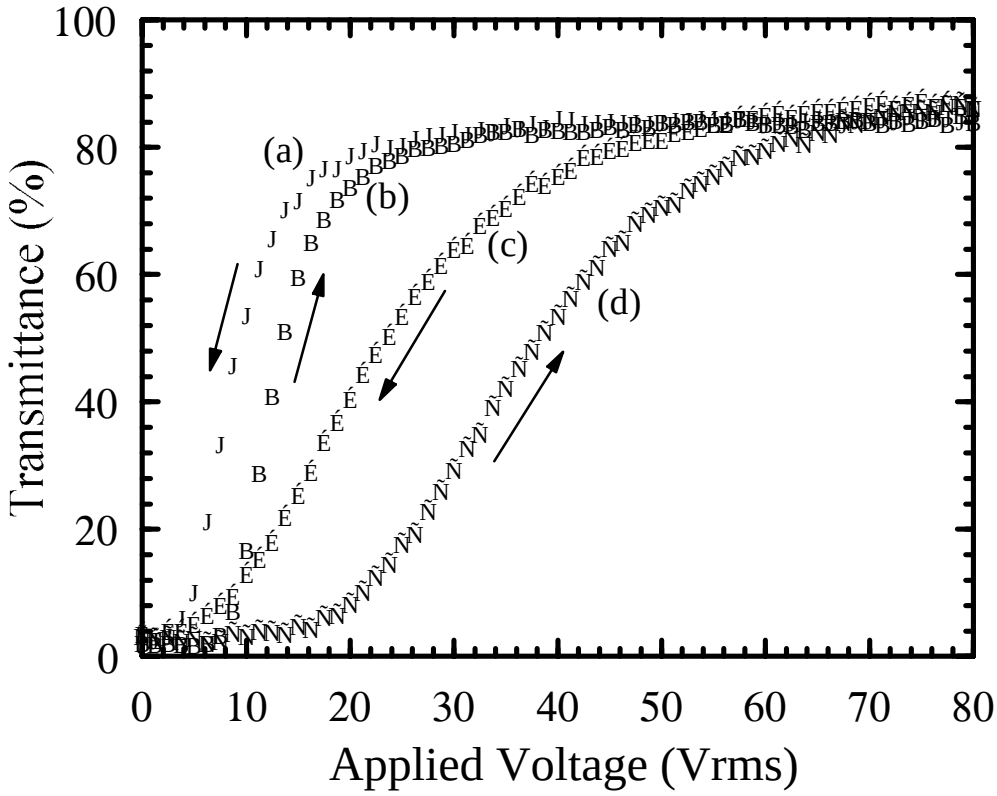

Fig. 2.3. Comparison of V-T curves of a T-cell and a PLP-cell. The T- cell consists of 40 wt% of PVA205 and 60 wt% of ZLI2061. The PLP-cell consists of 60 wt% of ZLI2061, 30 wt% of PVA205, and 6 wt% of BzMA and 4 wt% of FA108. (a) Voltage down-process of a PLP-cell, (b) Voltage up-process of a PLP-cell, (c) Voltage down-process of a T-cell, (d) Voltage up-process of a T-cell.

The hysteresis in the electric-field response is phenomenologically well known, but its mechanism is poorly understood. As the origin of the hysteresis, Li *et al*. proposed four hypotheses:[5] (1) accumulation of space charge in the film, (2) electric polarization effects of the polymer binder, (3) slow component in a relaxation process after removing voltage, and (4) inherent bistability in the director configuration in the droplets. They concluded that (1) and (2) were not dominant because the response to the magnetic field was similar to that to electric-field. Since t_{off} of the PLP-cell was considerably different from that of the T-cell, as shown in Figs. 2.4(a) and 2.4(b), the slow component of the T-cell should influence the hysteresis. It is well known that t_{on} and t_{off} depend on the viscosity of LC and the anchoring force of the polymer surface. The viscosity of LC in the PLP-cell should be similar to that of the T-cell when the LC and the polymers (PVA and photocured polymers) are completely separated from each other. The increase of the anchoring force requires t_{on} and t_{off} to be slow. t_{on} and t_{off} of the T-cell were 10 ms and over 500 ms, respectively, whereas, t_{on} and t_{off} of the PLP-cell were 0.2 ms and 11 ms, respectively. The hysteresis might be caused by different anchoring forces of LC molecules between the center and the wall of LC droplets. The PLP-cell might be lower in the inherent bistablilty than the T-cell since the anchoring force was reduced. In addition, the thermal motion at the interface between the polymer and the LC in the ON-state could influence the hysteresis and response time. The slow component of t_{off} of the T-cell might result from the thermal motion of the PVA.

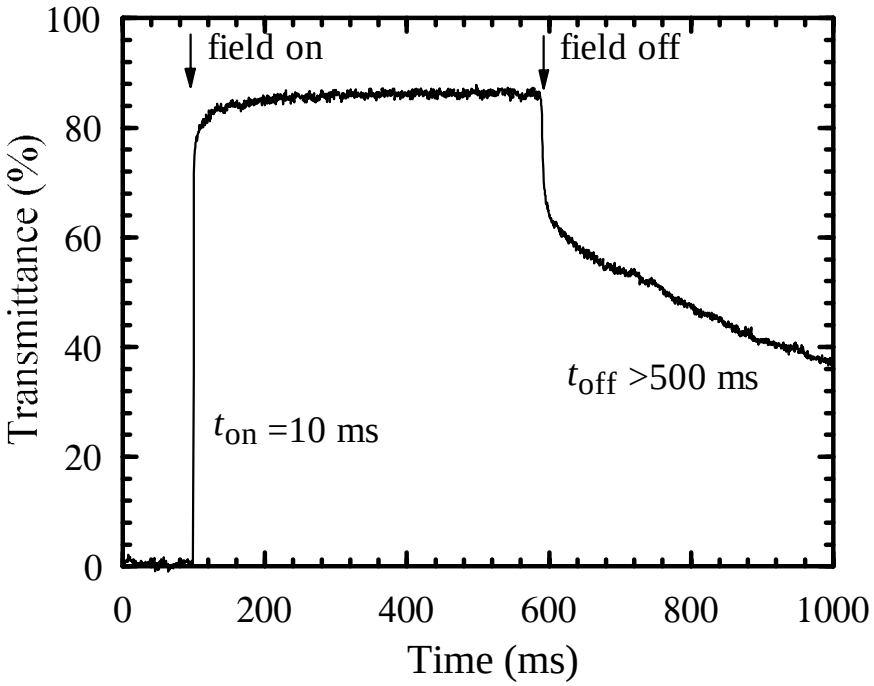

Fig 2.4(a). Electric-switching characteristic of a T-cell, consisting of 40 wt% of PVA205 and 60 wt% of ZLI2061.

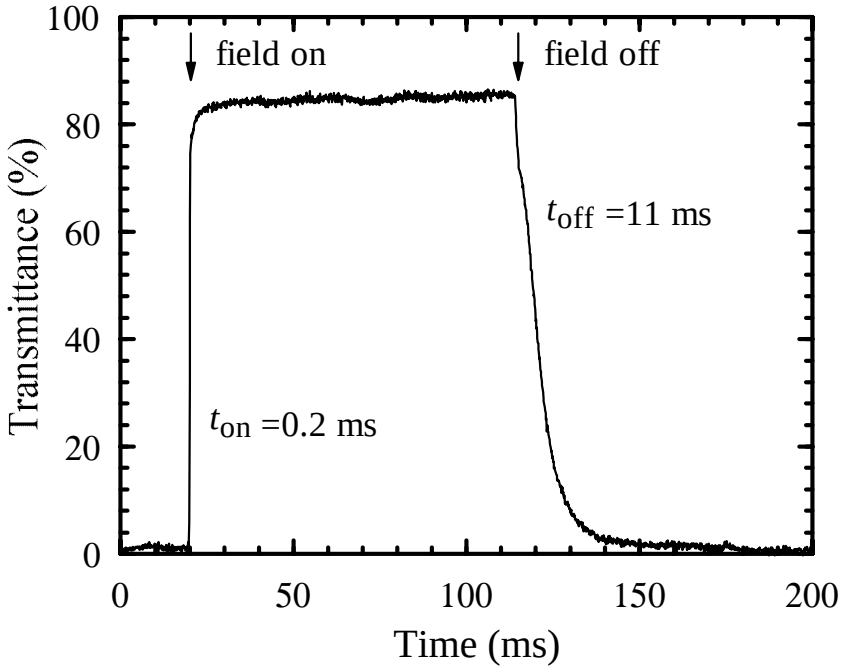

Fig. 2.4(a). Electric-switching characteristic of a PLP-cell, consisting of 60 wt% of ZLI2061, 30 wt% of PVA205, 6 wt% of BzMA and 4 wt% of FA108.

T_S of the T-cell was 84 %, which was close to the transmittance (86 %) of a glass substrate coated with ITO. The refractive index of PVA spin-coated film onto the quartz glass was measured by the prism coupling method at 632.8 nm, and the refractive index of PVA205 was 1.51. The ordinary refractive index of ZLI2061 is 1.496, nearly equal to the refractive index of PVA-205. T_{min} of the T-cell was nearly equal to zero. The optical anisotropy ($\Delta n = n_e - n_o$) of ZLI2061 is 0.18, large enough to cause light scattering in the OFF-state. T_S of the PLP-cell was slightly lower than that of the T-cell. The refractive index of copolymers of BzMA and FA108, which depends on the concentration, is expected to be between 1.56 and 1.34. The lower T_S of the PLP-cell as compared with that of the T-cell resulted from the refractive index mismatch between photocured polymers and ZLI2061 in the ordinary state.

Dependence on concentration of photocured polymers

Figure 2.5 shows the effect of the ratio of photocured polymers on the electrooptical properties. Both BzMA and FA108 are required to achieve low V_{90} and high T_S. In the absence of BzMA, polymerized FA108 might form droplets in the composite films since FA108 cannot be dissolved in ZLI2061. Because of the refractive index mismatch between the polymerized FA108 and PVA, T_S was low in the absence of BzMA. Consequently, the driving voltage was not reduced as a result of no change in the boundary condition between LC and PVA205. In the presence of BzMA, BzMA might transport FA108 into the interface between PVA205 and ZLI2061 because FA108 is soluble in BzMA and BzMA is soluble in ZLI2061. The lowest V_{90}, ΔV and the highest T_S could be obtained in the range of 40-60 wt% of BzMA, as shown in Fig. 2.5.

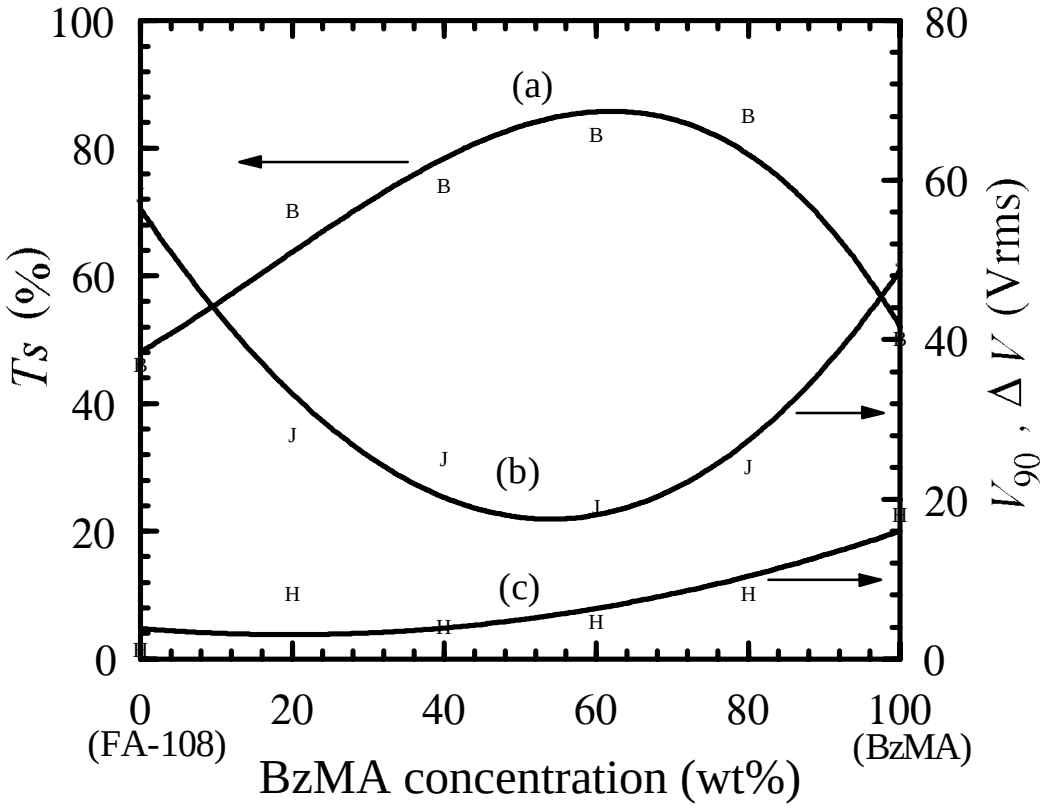

Fig. 2.5. BzMA concentration effect on electrooptical properties of PLP-cells. PLP-cells consists of 60 wt% of ZLI2061, 30 wt% of PVA205 and 10 wt% of BzMA and FA108. The weight ratios of BzMA and FA108 were 0:100, 20:80, 40:60, 60:40, 80:20, and 100:0. (a) Saturated transmittance (T_S), (b) Driving voltage (V_{90}) and (c) Hysteresis (ΔV).

These results indicate that both BzMA and FA108 are needed to form the interface layer (consisting of BzMA and FA108 copolymer) between LC and PVA205.

The effect of the concentration of photocured polymers in the polymer matrix is shown in Fig. 2.6. The lowest V_{90} and ΔV were obtained when 10-25 wt% of photocured polymers were added to the matrix polymer. The highest T_S was obtained with less than 25 wt% of photocured polymers, whereas large amount of photocured polymers lowered T_S. This phenomenon should be caused by light scattering between LC, photocured polymers, and PVA205 because of the thick photocured polymer layers. In order to prevent light scattering, the amount of photocurable monomers added should be less than 25 wt%. V_{90} and ΔV drastically decreased upon adding 10 wt% of photocurable monomers. These results suggest that the boundary condition at the interface between the LC droplet and the PVA matrix is changed due to extremely thin layers of photocured polymers. The calculated thickness of the interface layer consisting of photocured polymers surrounding a 3 μm LC droplet is less than 30 nm when 10 wt% of photocurable monomers is added.

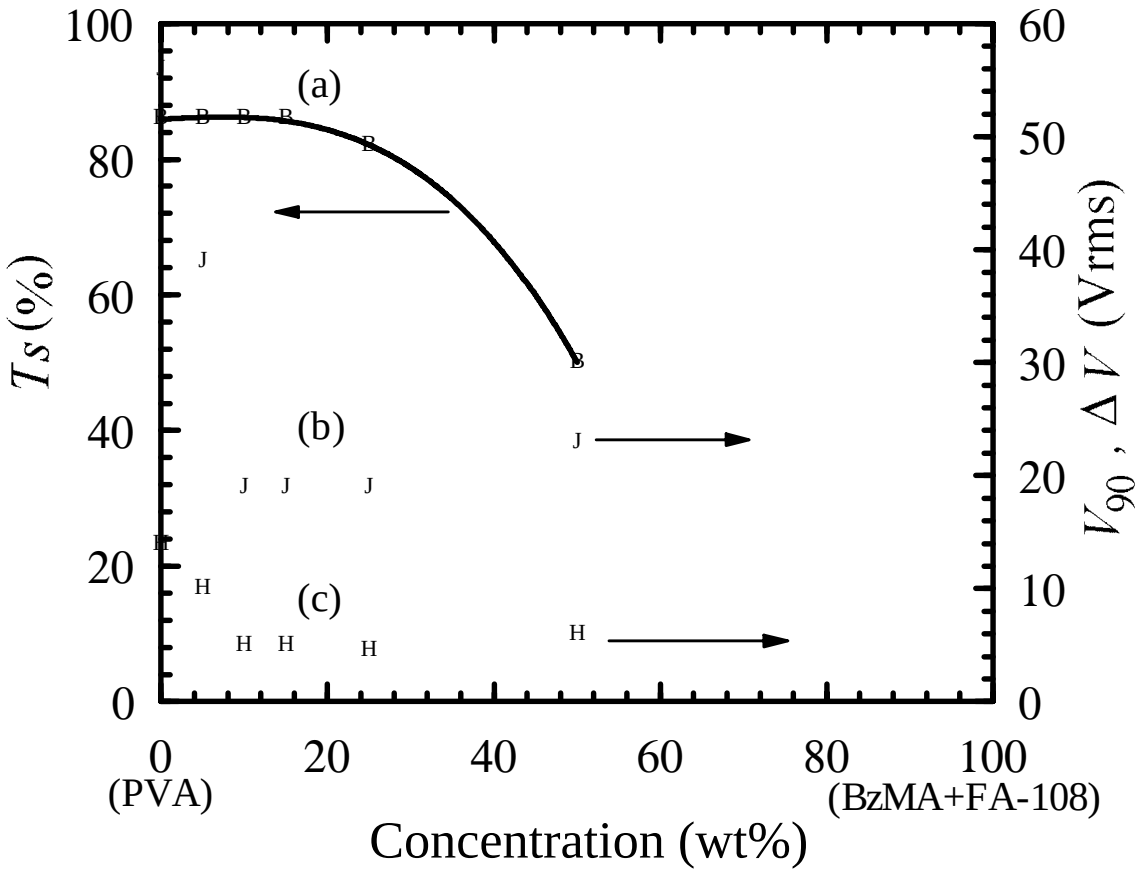

Fig. 2.6. Influence of the concentration of photocured polymers on electrooptic properties of PLP-cells. PLP-cells consist of 60 wt% of ZLI2061 and 40 wt% of PVA205, BzMA, and FA108. The weight ratio of BzMA and FA108 was fixed at 60:40. The weight ratios of PVA205 and photocurable monomers were 5:95, 10:90, 25:75, and 50:50. (a) Saturated transmittance (T_S), (b) Driving voltage (V_{90}) and (c) Hysteresis (ΔV).

Conclusions

A new type of PVA/LC composite film was formed with the addition of the photocured polymers, changing the composition and the concentration of photocured polymers. A PLP-cell composed of the composite film showed the following electrooptical properties: the driving voltage of 19 V_{rms}, hysteresis of 5 V_{rms}, turn-on time of 0.2 ms, and turn-off time of 11 ms. It is clear from the data that the PLP-cell is superior to the traditional PVA/LC cells which have the electrooptical properties of driving voltage of 56 V_{rms}, hysteresis of 14 V_{rms}, turn-on time of 10 ms, and turn-off time of 500 ms. The lowest driving voltage, hysteresis, and the highest saturated voltage were attained when the addition ratio of BzMA and FA108 was set at 60:40. Both BzMA and FA108 were necessary as photocurable monomers in order to improve the electrooptical properties. In the presence of both BzMA and FA108, BzMA may transport FA108 into the interface between PVA205 and ZLI2061 forming a copolymer of BzMA and FA108 extracted from ZLI2061. The morphology of the composite film varied with the surface tensions and solubilities of ZLI2061, BzMA, and FA108. These results suggest that the photocured polymers form interface layers between the LC droplet and the PVA matrix, and reduce the anchoring force between the LC and the polymer layer.

The driving voltage and hysteresis decreased drastically upon adding 10 wt% of photocurable monomers. The boundary condition at the interface between the LC droplet and the PVA matrix was changed due to the extremely thin layers of photocured polymers. The saturated transmittance was nearly equal to the transmittance of the ITO-coated glass substrate when the addition amount of photocurable monomers added was

less than 25 wt%. Light was not scattered, indicating that the interface layers between the LC and PVA were sufficiently thin.

References

1) A. V. Koval, M. V. Kurik, O. D. Lavrentovich, and V. V. Sergan: *Mol. Cryst. Liq. Cryst.* **193** (1990) 217.
2) O. Yonekura, H. Kikuchi and T. Kajiyama: *Polym. Prepr. J.* **42** (1993) 659.
3) J. H. Scofield: *J. Electron Spectrosc.* **8** (1976) 129.
4) A. B. Loebe: *Off. Dig.* **31** (1959) 200.
5) Z. Li, J. R. Kelly, P. Palffy-Muhoray and C. Rosenblatt: *Appl. Phys. Lett.* **60** (1992) 3132.

2.2. Comparison of Electrooptical Properties of PVA/LC Composite Films with Different Kinds of Interface Layer

The electrooptical properties of three kinds of poly(vinyl alcohol) (PVA)/liquid crystal (LC) composite films with three combinations of added photocurable mixtures of benzylacrylate (BzA) and perfluorooctylethylacrylate (FA108), benzylmethacrylate (BzMA) and FA108, and nonaoxyethylenediacrylate (9EG-A) and FA108 are studied, paying special attention to the LC droplet size and the anchoring energy at the interface between the polymer and the LC, and effects of photocurable monomers on morphology and electrooptical properties of PVA/LC composite films with added photocured polymers. The PVA/LC composite films with added photocrosslinkable monomers have showed a low driving voltage of 15 V_{rms} and a low hysteresis of less than 1 V_{rms}, suggesting the improvement of electrooptical properties caused by reduction of the anchoring energy and the thermal motion of polymers.

2.2.1. Introduction

The purpose of the present section is to clarify the relation between the electrooptical properties and physical characteristics of photocured polymers by using three combinations of photocurable mixtures of benzylacrylate (BzA) and perfluorooctylethylacrylate (FA108), benzylmethacrylate (BzMA) and FA108, and nonaoxyethylenediacrylate (9EG-A) and FA108. PVA/LC composite films with added these mixtures were prepared by the emulsification and photopolymerization-induced phase separation methods (PPIPS), as explained in Fig. 1.7. The electrooptical properties of the composite films with differently sized LC droplets and different anchoring energies at the interface between the LC and the polymers were measured.

2.2.2. Experimental

Materials

PVA (trade name PVA205, having the degree of polymerization of 500 and the saponification rate of 88 mol%) was supplied by Kuraray Co., Ltd. The nematic LC mixture consisting of cyanobiphenyl derivatives with positive dielectric anisotropy (ZLI2061) was obtained from Merck Japan Ltd. The four kinds of photocurable monomers shown in Fig. 2.7 were used. Benzylmethacrylate (BzMA) was obtained from Wako Pure Chemicals and benzylacrylate (BzA) from Osaka Yuki Chemicals.

(a) BzA

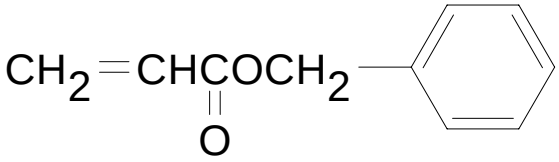

(b) BzMA

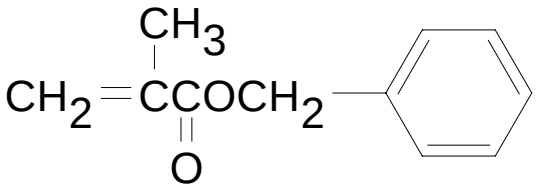

(c) 9EG-A

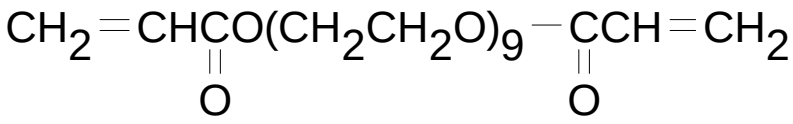

(d) FA108

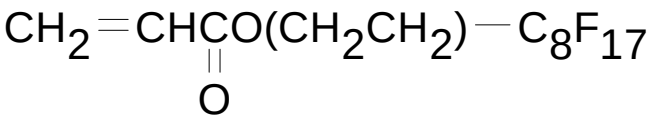

Fig. 2.7. Chemical formula of photocurable monomers. (a) Benzylacrylate (BzA), (b) Benzylmethacrylate (BzMA), (c) Nonaoxyethylenediacrylate (9EG-A), and (d) Perfluorooctylethylacrylate (FA108)

BzMA and BzA were purified by column chromatography to remove the polymerization inhibitor. Nonaoxyethylenediacrylate (9EG-A) and perfluorooctylethylacrylate (FA108) were supplied by Kyoeisya Chemical Company, and dimethoxyphenylacetophenone (DMPA), a photoinitiator, from Tokyo Kasei Industries. The glass substrate coated with an indium-tin-oxide (ITO) electrode was obtained from Matsunami Glass Company.

Sample preparation and droplet size measurements

PVA205/ZLI2061 composite films with added photocured polymers were formed by the emulsification and photopolymerization induced phase separation method,[1)] using the following three combinations of photocurable monomers: BzMA and FA108 (BMF), BzA and FA108 (BAF), and 9EG-A and FA108 (EGF). The concentrations of ZLI2061 and photocured polymers in a composite film were adjusted to 60 wt% and 10 wt%, respectively. The weight ratio of BzMA and FA108 was 60:40 (BMF64), weight ratio of BzA and FA108 or 9EG-A and FA108 was adjusted to 20:80, 40:60, 60:40 (BAF64, EGF64), and 80:20, and pure BzA was used to investigate the effects of the composition. The composite films were formed from PVA aqueous solutions with different concentrations, controlled at 13, 15 and 18 wt%. The size of the LC droplets varied with the PVA concentration, and identified by scanning electron microscopy (SEM) and Debye plots. Film thickness was controlled at 12 ± 1 μm by changing the revolution speed of spin-coating.

2.2.3. Results and Discussion

Effects of LC droplet size on T_S

The ordinary refractive index of ZLI2061 (1.496) is nearly equal to the refractive index of PVA205 (1.51), so that the T_S of the PVA205/ZLI2061 composite films (without photocured polymer) was 84 % close to the transmittance (86 %) of a glass substrate coated with ITO, as shown in Table 2.2.

Table 2.2. Electrooptical properties of PVA/ZLI2061 composite films formed from PVA aqueous solutions with different concentrations.
Weight ratio of PVA and ZLI2061 is 40:60.

	Size (μm)	*Ts* (%)	ΔV (Vrms)	V_{90} (Vrms)	t_{on} (ms)	t_{off} (ms)
18 wt%	<1	84[a)]	>20	>80	>200	>500
15 wt%	2–3	84	14	56	10	>500
13 wt%	4–5	84	12	42	5	120

a) Determined using 100 Vrms sinusoidal voltage.

It is clear from Figs. 2.8 and 2.9 that T_S of the composite film with added photocured polymer took the highest value when BAF64 or EGF64 was used. The result was similar to the case of the composite films with added BMF, explaining refractive index mismatch between the photocured polymer and ZLI2061 in the ordinary state in the previous report.[1)]

Table 2.3. Electrooptical properties of PVA/BzA/FA-108/ZLI-2061 composite films formed from PVA aqueous solutions with different concentrations. Weight ratio of PVA, BzA, FA-108, and ZLI-2061 is 30:6:4:60.

	Size (μm)	*Ts* (%)	ΔV (Vrms)	V_{90} (Vrms)	t_{on} (ms)	t_{off} (ms)
18 wt%	<1	70	15	70	0.1	8.0
15 wt%	1–2	78	9	38	0.4	8.0
13 wt%	2–3	80	5	24	0.6	18.0

Table 2.4. Electrooptical properties of PVA/BzMA/FA-108/ZLI-2061 composite films formed from PVA aqueous solutions with different concentrations. Weight ratio of PVA, BzMA, FA-108, and ZLI-2061 is 30:6:4:60.

	Size (μm)	*Ts* (%)	ΔV (Vrms)	V_{90} (Vrms)	t_{on} (ms)	t_{off} (ms)
18 wt%	<1	80	10	30	0.2	10.0
15 wt%	2–3	82	5	19	0.2	11.0
13 wt%	4–5	83	4	18	0.8	25.0

Table 2.5. Electrooptical properties of PVA/9EG-A/FA-108/ZLI-2061 composite films formed from PVA aqueous solutions with different concentrations. Weight ratio of PVA, 9EG-A, FA-108, and ZLI-2061 is 30:6:4:60.

	Size (μm)	*Ts* (%)	ΔV (Vrms)	V_{90} (Vrms)	t_{on} (ms)	t_{off} (ms)
18 wt%	<1	80	2.5	38	0.2	8.0
15 wt%	2–3	83	1.8	24	0.2	9.0
13 wt%	4–5	84	<1	15	0.2	13.0

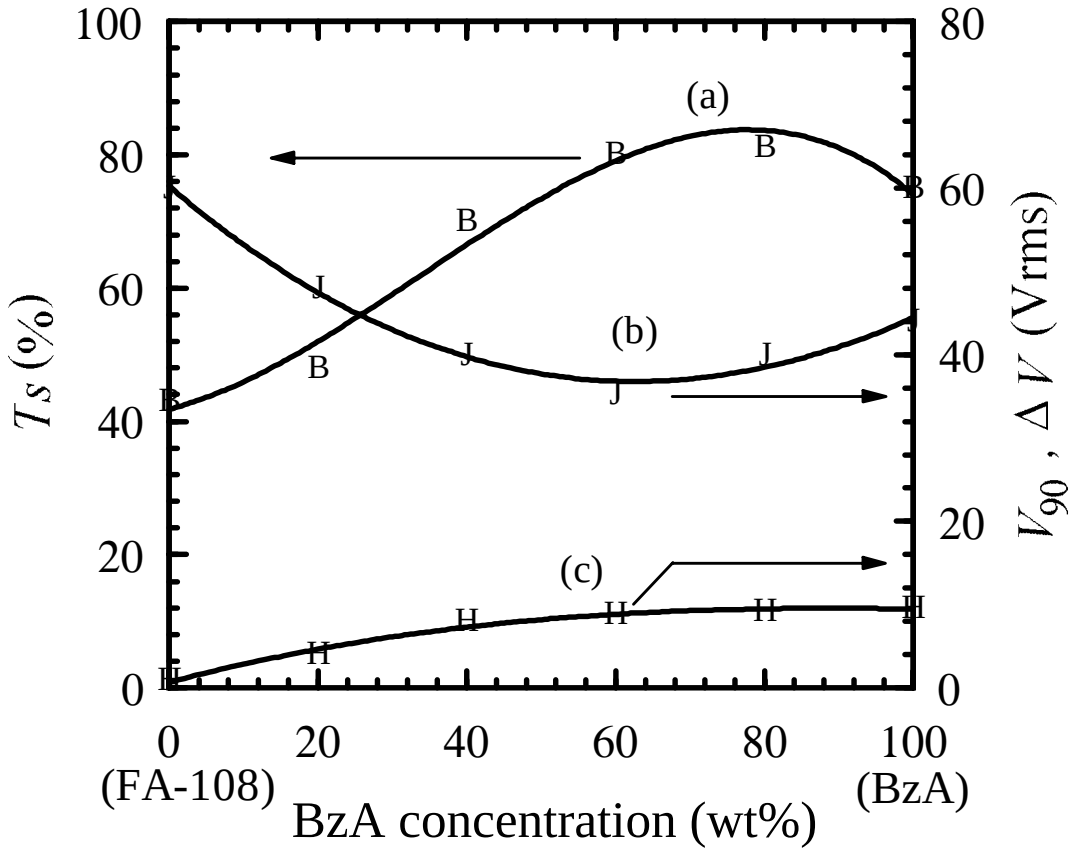

Fig. 2.8. BzA concentration effect on electrooptical properties of the composite films with added BAF. The composite films consist of 60 wt% of ZLI2061, 30 wt% of PVA205, and 10 wt% of BAF. The weight ratio of BzA and FA108 was adjusted to 0:100, 20:80, 40:60, 60:40, 80:20, and 100:0. Composite films were formed from the 15 wt% aqueous solution of PVA205. (a) Saturated transmittance (T_S), (b) Driving voltage (V_{90}) and (c) Hysteresis (ΔV).

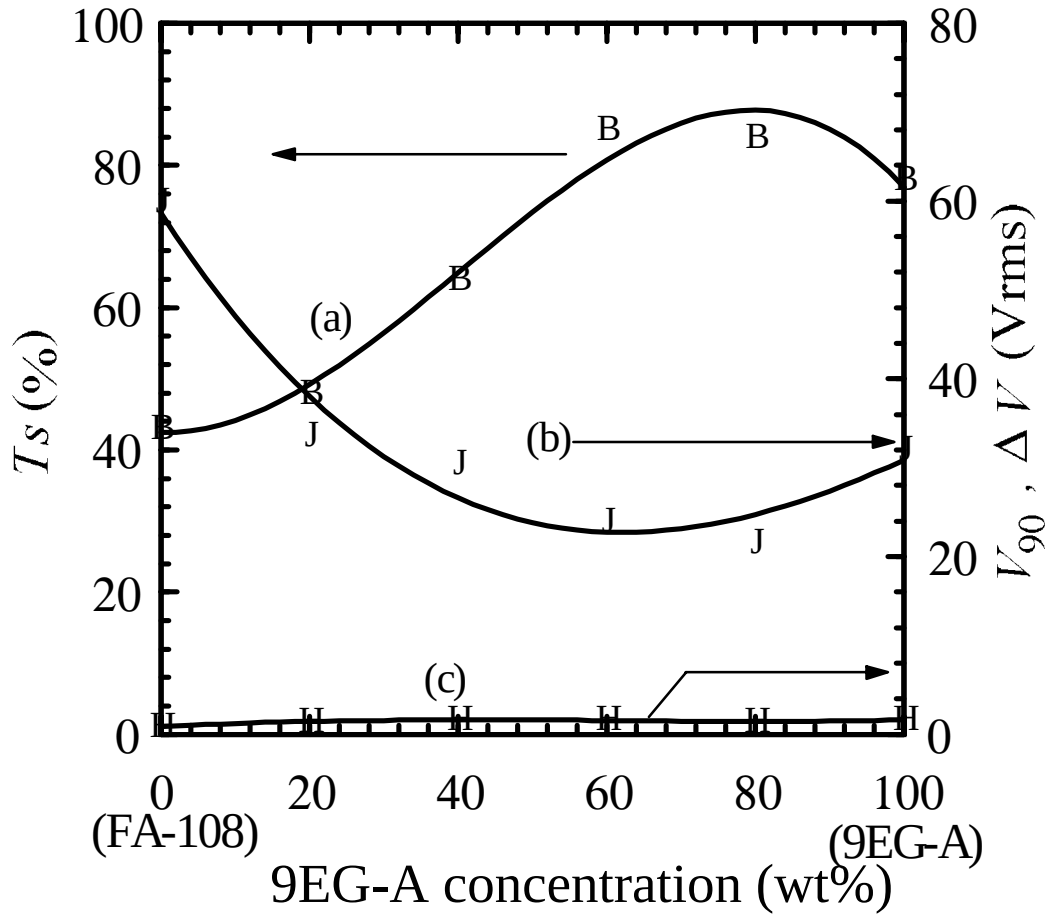

Fig. 2.9. 9EG-A concentration effect on electrooptical properties of the composite films with added EGF. The composite films consist of 60 wt% of ZLI2061, 30 wt% of PVA-205 and 10 wt% of EGF. The weight ratio of 9EG-A and FA108 was adjusted to 0:100, 20:80, 40:60, 60:40, 80:20, and 100:0. Composite films were formed from the 15 wt% aqueous solution of PVA205. (a) Saturated transmittance (T_S), (b) Driving voltage (V_{90}) and (c) Hysteresis (ΔV).

T_S of the composite films with photocured polymers formed from PVA aqueous solutions with high concentration was relatively low, as shown in Tables 2.3-2.5, whereas that of the PVA205/ZLI2061 composite films (without photocured polymers) did not vary with the LC droplet size, as shown in Table 2.2. The results suggest that the photocured polymers formed interface layers between the LC droplet and the PVA matrix, and the layer of photocured polymers was sufficiently thin compared with wavelength of the light in the large-sized LC droplet. The thin layer could not scatter light in spite of the refractive index mismatch between the photocured polymer and ZLI2061 in the ordinary state. However, the interface layer of photocured polymers in the small-sized LC droplets could scatter light as a result of the relatively thick layer.

The composite films with BAF had lower T_S values than the films with BMF because of the smaller droplets in the thicker layer, as shown in Tables 2.3 and 2.4. Fuh *et al*. measured the distribution of size and spacing of LC droplets of the composite films cured with various tungsten-halogen light intensities.[2)] They concluded that the droplet size was small in the composite films cured with a high curing light intensity because of the high rate of polymerization. The droplet size was smaller in the composite films with added BAF than those with added BMF because the rate of polymerization of acrylate monomers was faster than that of methacrylate monomers.

Effects of the LC droplet size on V_{90}, ΔV, t_{on}, and t_{off}

Wu *et al*. formulated the relation between the electrooptical property and the shape and size of the droplet, elucidating that the driving voltage was high and the response time was short in the small-sized LC

droplet.[3] The composite films formed from a PVA aqueous solution with low concentration were low in V_{90} and ΔV, and long in t_{on} and t_{off} as shown in Tables 2.2-2.5 in consequence of the large sizes of droplets, qualitatively consistent with the relations of Wu *et al*.

As summarized in Tables 2.3 and 2.4, V_{90} and ΔV of the composite films with added BAF were higher than those of the films with added BMF, and t_{on} and t_{off} of the composite films with BMF were shorter than those of the films with BAF. The extrapolation length at the interface between poly-BzA and ZLI2061 was nearly equal to that between poly-BzMA and ZLI2061, as summarized in Table 2.6. The difference in the electrooptical property between the composite films with added BAF and those with added BMF can be explained in terms of the smaller droplet size in the former films according to the theory of Wu *et al*.

Table 2.6. Extrapolation length (nm) at thePVA/ZLI2061, poly-BzMA/ZLI2061, poly-BzA/ZLI2061, and poly-9EG-A/ZLI2061 interfaces.

PVA205	poly-BzA	poly-BzMA	poly-9EG-A
86.0	312.5	298.5	325.3

Improvement of electrooptical properties by the addition of photocured polymers

As shown in Tables 2.2-2.5 and Figs. 2.10(a)-2.10(d), V_{90} and ΔV of the composite films with added photocured polymers were lower than those of traditional PVA/ZLI2061 composite films without the photocured polymers.

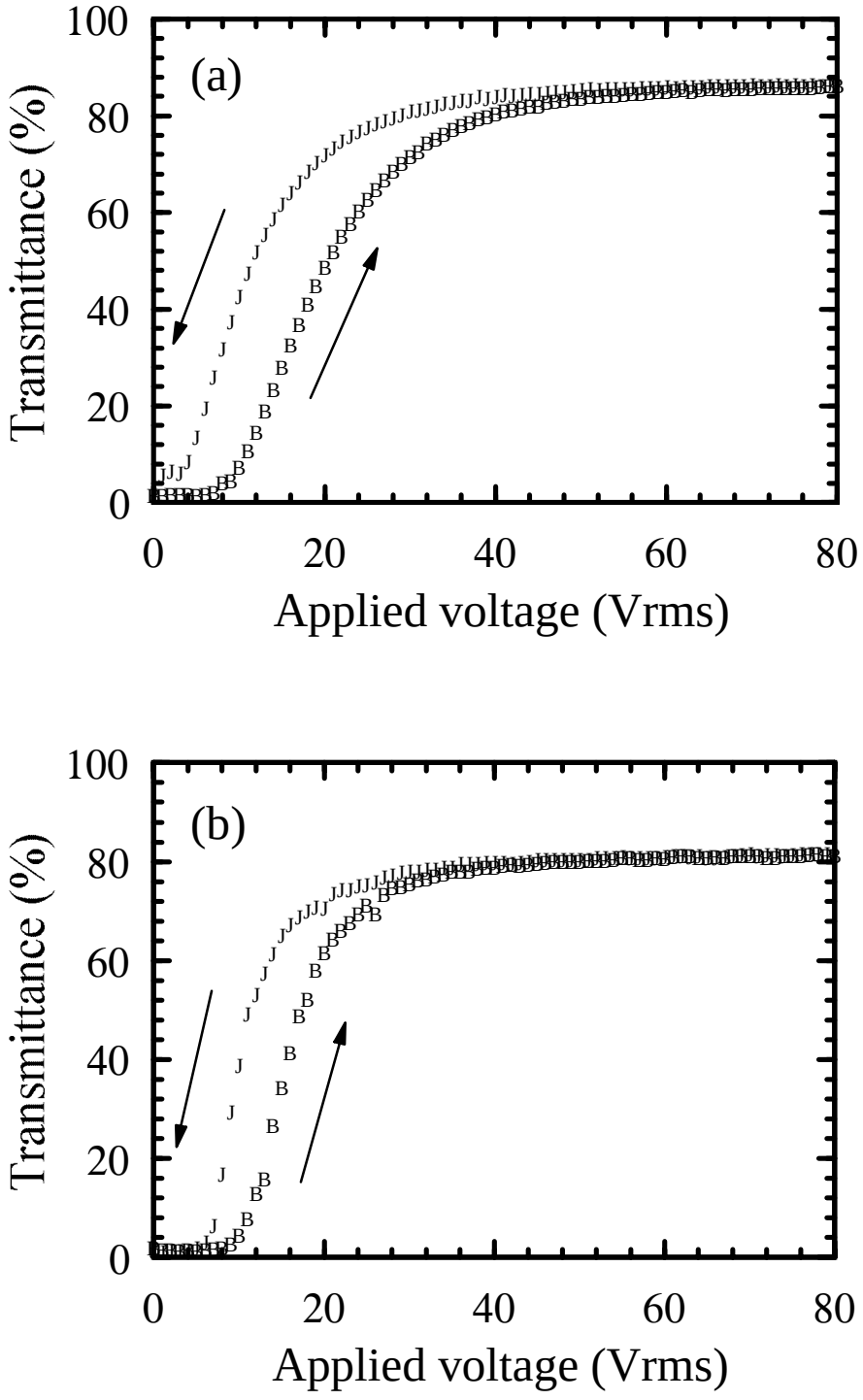

Fig. 2.10. V-T curves of the composite films. (a) Traditional composite film without photocured polymer. PVA205/ZLI2061=40/60. (b) Composite film with added BAF64. PVA205/BzA/FA108/ZLI2061=30/6/4/60.

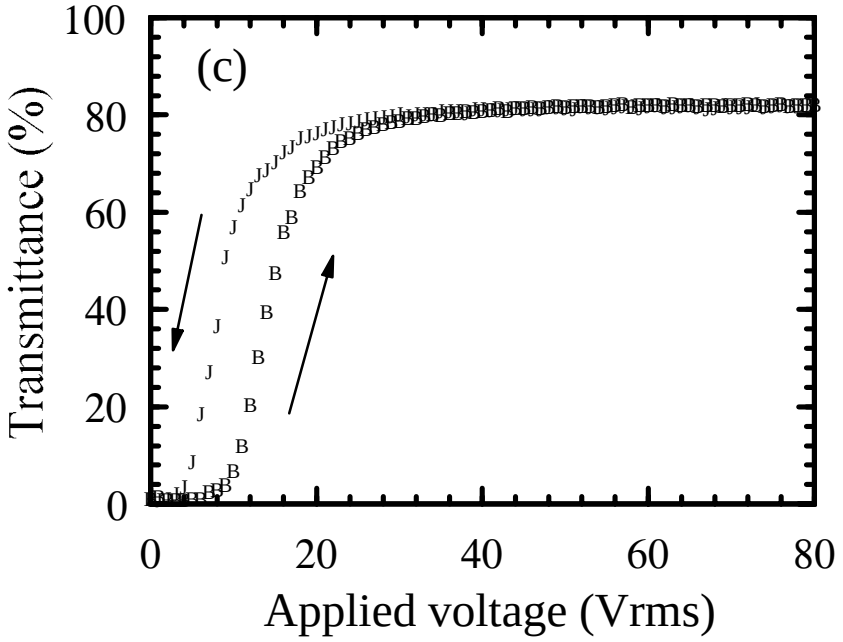

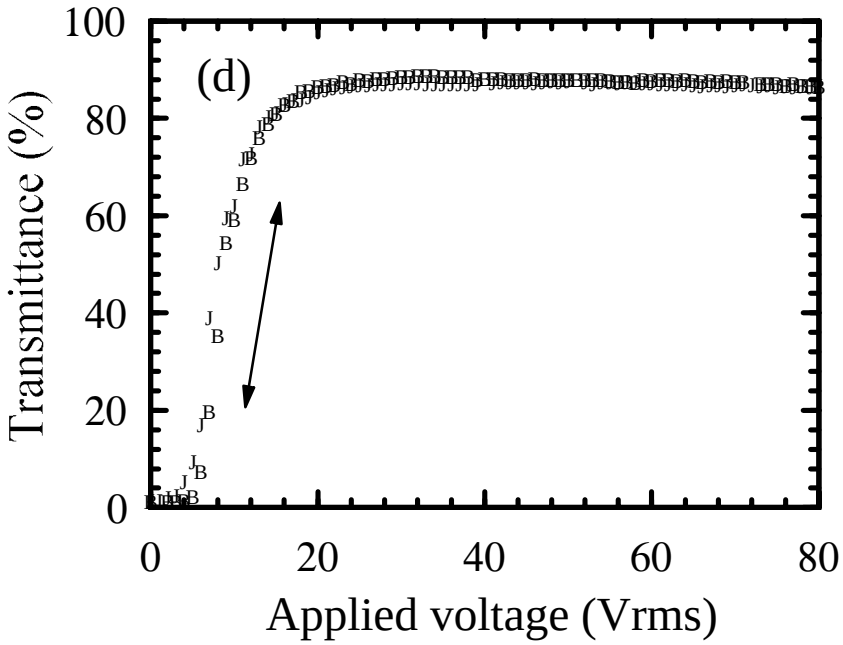

Fig. 2.10. V-T curves of the composite films. (c) Composite film with added BMF64. PVA205/BzMA/FA108/ZLI2061=30/6/4/60. (d) Composite film with added EGF64. PVA205/9EG-A/FA108/ZLI2061=30/6/4/60.

In addition, t_{on} and t_{off} of the composite films with added photocured polymers were shorter than those of traditional PVA/ZLI2061 composite films. These improvements of electrooptical properties cannot be entirely explained by the change in the droplet size since the droplet size of these composite films formed from the PVA aqueous solutions with the constant concentration was scarcely changed without the composite films with BMF or EGF. As shown in Table 2.6, the extrapolation length at the interface between the photocured polymer and ZLI2061 was 3-4 times as long as that at the interface between PVA205 and ZLI2061. These results suggest that the photocurable monomers were polymerized at the interface between LC and PVA, reducing the anchoring energy to improve the electrooptical properties as a result of releasing the LC molecules from the interaction with the polymers.

Effect of the addition of fluorinated acrylate

As shown in Figs. 2.8 and 2.9, V_{90} and ΔV were reduced by adding a suitable amount of FA108. The droplet size scarcely changed with the addition of fluorinated acrylate. To clarify the effect of the composition of photocured polymer, methacrylate copolymers comprising perfluoroocthyl side groups and benzyl side groups were synthesized by radical polymerization.[4)] The extrapolation length was long, and the contact angle was large at the interface between the copolymer and ZLI2061 according to the increase in the content of fluorinated side group as shown in Fig. 2.11. The extrapolation length at the interface between ZLI2061 and the copolymers with 10 wt% of fluorinated side group was 10 times as long as that of PVA205.

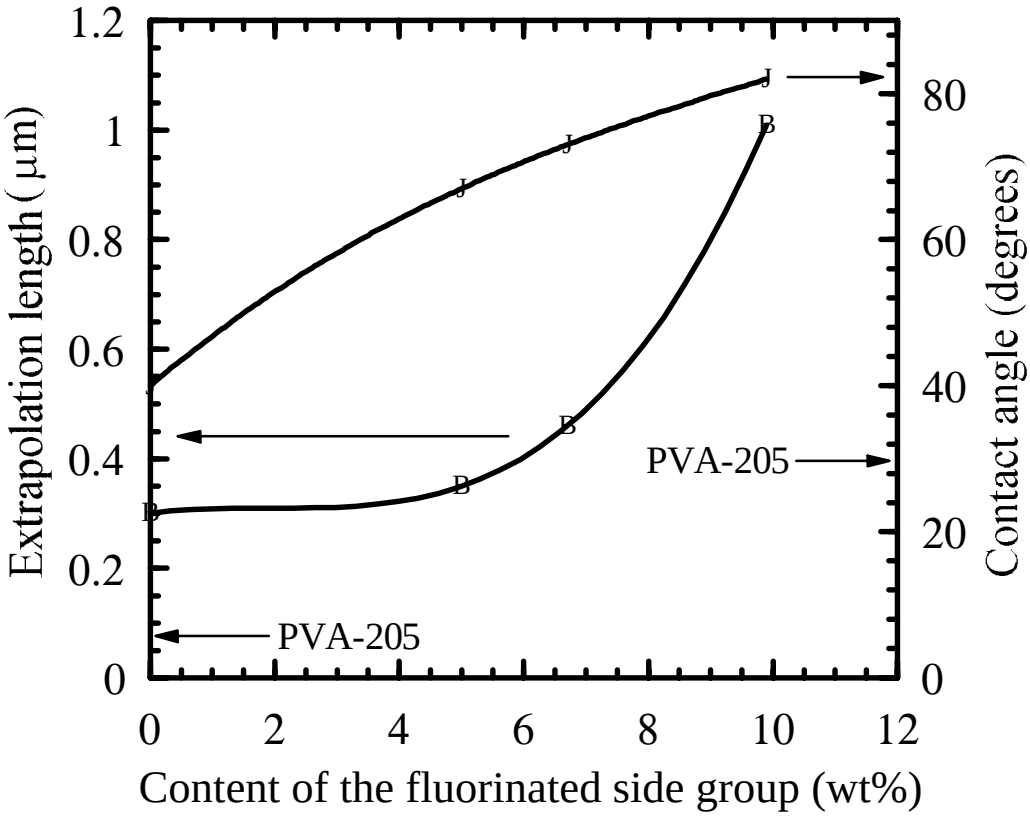

Fig. 2.11. Effect of content of the fluorinated side group on the extrapolation length and the contact angle.

The phenomena suggest that V_{90} and ΔV were reduced since the anchoring force at the interface between the polymers and ZLI2061 were reduced by adding the fluorinated acrylate, and the bistable director configuration of the LC collapsed with the reduction of the interaction between the polymer having fluorinated side group and LC.

Composite films with added photocrosslinked polymers

As shown in Fig. 2.10(d), ΔV was reduced by adding the photocrosslinkable monomers, i.e., EGF. Since both the droplet size and the extrapolation length of the composite films with added EGF were nearly equal to those with added BMF as shown in Tables 2.2-2.4, the reduction of ΔV could not be explained in terms of the morphology or the anchoring energy. Kajiyama *et al*. indicated that the electrooptical property was influenced by the thermal motion of matrix polymer.[5)] The ΔV of the composite films with added photocrosslinked polymer was reduced because the photocrosslinked polymer could suppress the thermal motion at the interface between the polymer and the LC in the ON-state.

Conclusions

The electrooptical properties of the PVA/LC composite films with added photocured polymers were studied paying special attention to the extrapolation length at the interface between the polymers and the LC. The extrapolation length was 86 nm in PVA-205, 312.5 nm in poly-BzA, 298.5 nm in poly-BzMA, and 325.3 nm in poly-9EG-A. The saturated

transmittance of the composite films with added photocured polymers forming the small size of the LC droplet was lower than that of the PVA205/ZLI2061 composite films without the photocured polymer. The photocured polymer formed the interface layer between the LC droplet and the PVA matrix, and the layer of the photocured polymer was sufficiently thin compared with the light wavelength in the large size of the LC droplet. The electrooptical properties were improved because the interaction between the polymer matrix and the LC was reduced by the interface layer of the photocured polymer between PVA205 and ZLI2061. The improvement of the electrooptical properties caused by adding a suitable amount of fluorinated acrylate can be explained by the low anchoring energy of copolymers comprising the perfluorooctyl and benzyl side groups.

The composite films with added photocrosslinkable monomers (EGF) showed the following electrooptical properties: the driving voltage was 15 V_{rms}, hysteresis less than 1 V_{rms}, turn-on time 0.2 ms, and turn-off time 13 ms. It is clear from the data that the composite film with photocrosslinkable monomers (EGF) is superior to the composite films added with photopolymerizable (without photocrosslinking) monomers (BMF) having the electrooptical properties of the driving voltage 18 V_{rms}, hysteresis 5 V_{rms}, turn-on time 0.8 ms, and turn-off time 25 ms. It is suggested that the electrooptical properties were influenced by the thermal motion at the interface between the polymer and the LC in the ON-state.

References

1) H. Ono and N. Kawatsuki: *Jpn. J. Appl. Phys.* **33** (1994) 6268.
2) A. Y. Fuh, C. Y. Hung, B. W. Tzen, C. R. Sheu, Y. N. Chyr, G. L. Lin and T. C. Ko: *Jpn. J. Appl. Phys.* **33** (1994) 1088.
3) B. G. Wu, J. H. Erdmann and J. W. Doane: *Liquid Cryst.* **5** (1989) 1453.
4) N. Kawatsuki and H. Ono: *J. Appl. Polym. Sci.* **55** (1995) 911.
5) S. Kobayashi, A. Miyamoto, H. Kikuchi, and T. Kajiyama: *Polym. Prepr. Jpn.* **40** (1991) 1023.

3. Control of Interaction between PMMA and LC

3.1. Electrooptical Properties of Polymer/LC Composite using New Optical Methacrylate Polymer with Fluorinated Side Group

Methacrylate copolymers of benzylmethacrylate (BzMA) and perfluorooctylethylmethacrylate (FMA) are synthesized to apply to the polymer/liquid crystal (LC) composite films. The copolymers are prepared by a radical solution polymerization. High composition of FMA has resulted in a precipitation during the polymerization. Contact angle of the LC on the copolymer films have decreased with increasing the FMA composition. Due to a small interaction between the LC and the copolymers, the copolymer/LC composite films have showed low driving voltage in the range of 18-25 V_{rms} corresponding to about 1/3 value of the PMMA/LC composite film.

3.1.1. Introduction

The polymer/liquid crystal (LC) composite and/or polymer dispersed liquid crystal (PDLC) have been intensively studied because of great potential for applications of large scale, low cost, flexible devices and improved brightness owing to the absence of polarizers.[1-6] They can be electrically switched between an opaque scattering state and a transparent state. Several methods to disperse the LC droplets in the polymer matrix were reported with regard to methods of solvent-induced phase separation (SIPS)[2,3], a photopolymerization-induced phase separation (PPIPS)[4] and an LC emulsion in aqueous polymer solution.[5]

These polymer/LC composite films have been developed on the basis of the same and simple operating principle. The composite film is opaque in the absence of an electric field because of the refractive index mismatching between the polymer and the randomly aligned LC. When the electric field is applied to the film, the nematic director of the LC should be aligned along the electric field to make the film transparent as a result of the index matching aligning the droplet directors parallel to the applied field.

One of the problems of the polymer/LC composite film is that the driving voltage is relatively higher than that of the conventional LC display which contains no polymer matrix. It has been known that an interaction at the interface between the polymer matrix and the LC plays an important role for the alignment of LC molecules. In general, the lower the boundary interaction between the polymer and the LC is, the more easily the LC molecules tend to align under the electric field. Therefore the characteristics of the polymer matrix is an important factor as well as the

LC and the shape of LC domain.[7)]

This section describes synthesis and characterization of methacrylate copolymers of perfluorooctylethylmethacrylate (FMA) and benzylmethacrylate (BzMA) (poly-BzMA-co-FMA) with various copolymerization ratio, and electrooptical properties of the polymer/LC composite films fabricated by the SIPS method. Solvents were selected by measuring solubilities of the copolymers and the LC and the contact angle on the copolymer films. The dependence of the copolymer composition and molecular weight on the electrooptical properties of the copolymer/LC composite film was also investigated. The fluorinated polymer is expected to reduce the anchoring strength at the interface between the polymer and LC. In addition, Since refractive index of poly-BzMA is higher than that of PMMA, it is expected that the refractive index of poly-BzMA-co-FMA can be controlled in the wider range than that of PMMA-co-FMA.

3.1.2. Experimental

Materials

FMA (Hoechst Japan Co., Ltd.) and BzMA (Wako Pure Chemical Co.) were purified by column chromatography to remove an inhibitor before polymerization. 2, 2'-Azobis-(2-methylpropionitrile) (AIBN) (Tokyo Kasei Co.) was recrystallized from the ethanol solution and stored at 0 ℃. PMMA is commercially available (Aldrich, Mn=5,920, Mw=12,300) and used as received. This work adopted a mixture of nematic liquid crystal consisting of 4-alkyl (or alkyloxy)-4'-cyanobiphenyl and 4-alkyl-4'-cyanotriphenyl named E7 (BDH-Merck Japan, n_o=1.521,

n_e=1.746, T_{NI}=61 ℃). All other solvents and chemicals were used as received.

Polymer synthesis

The copolymers were synthesized by a free radical solution polymerization in toluene with AIBN as the initiator. The concentration of monomers was about 9.1 % (w/w). The monomer feed ratio and the synthesized copolymer composition are summarized in Table 3.1. As an example for the general copolymerization procedure the synthesis of copolymer **1f** is described as follows:

Table 3.1. Monomer feed ratio and copolymer composition.

Polymer	Feed ratio BzMA : FMA wt : wt	Feed ratio BzMA : FMA mol : mol	[monomer] / [AIBN]	Composition [a] BzMA : FMA wt : wt	Composition [a] BzMA : FMA mol : mol
1a	100 : 0	100 : 0	31.1	100 : 0	100 : 0
1b	90 : 10	96.5 : 3.5	31.8	92.3 : 7.7	97.3 : 2.7
1c	80 : 20	92.4 : 7.6	30.2	84.1 : 15.9	94.1 : 5.9
1d	70 : 30	87.6 : 12.4	24.9	75.9 : 25.1	90.1 : 9.9
1e	70 : 30	87.6 : 12.4	1.7	72.8 : 27.2	89.0 : 11.0
1f	50 : 50	75.1 : 24.9	20.7	52.6 : 47.4	77.0 : 23.0
1g	20 : 80	43.0 : 57.0	14.5	38.5 : 61.5	65.4 : 34.6 [b]

a) Determined by NMR

b) Determined by FT-IR

Copolymer **1f**: 2.5 g (4.7 mmol) of FMA, 2.5 g (14.2 mmol) of BMA and 150 mg of AIBN were dissolved in 50 ml of toluene. The reaction mixture was treated with a gentle stream of nitrogen. After sealing, the mixture was heated to 60 ℃ for 6 h. The resulting homogeneous viscous solution was cooled and added dropwise into 500 ml of methanol to precipitate the polymer. After two additional precipitations from dichloromethane solution into methanol, the copolymer was dried at 30 ℃ in vacuum for 48 h.

Yield: 2.5 g (50 wt%). ^{1}H-NMR ($CDCl_3$): δ (ppm)=0.75 (brs), 0.92 (brs), 1.2 ～ 1.4 (m), 1.6 ～ 1.9 (m), 2.35 (brs, $OCH_3CH_2C_8F_{17}$), 4.15 (brs, $OCH_2CH_2C_8F_{17}$), 4.90 (brs, OCH_2Ph), 7.29 (s, $OCH_2C_6H_5$).

IR (film on NaCl): 1730 (C=O), 1587 (Ph), 1454, 698 (Ph), 656 (C-F) cm^{-1}

Copolymer **1g** was found to be insoluble in the reaction medium and precipitated during the reaction. This copolymer was purified by washing with methanol and extraction with hot methanol for a few days. The yields of the isolated polymers were found to be in the following range: **1a** (34 %), **1b** (49 %), **1c** (53 %), **1c** (53 %), **1d** (47 %), **1e** (51 %), **1f** (50 %), and **1g** (40 %).

Characterization

Differential scanning calorometry data were obtained with a Metler TA-4000 heating at a rate of 10 ℃/min. The molecular weight and molecular weight distributions were measured in the THF fluent with a Waters 150C GPC system equipped with a UV detector. The columns (Shodex) were calibrated with polystyrene standards of known molecular weight. FT-IR spectra were recorded with a JEOL JIR-5500. ^{1}H NMR

spectra were measured with a JEOL JXR nmr instrument operating 270 MHz. Copolymer composition was determined by ^{1}H NMR or IR spectroscopy using separated signals of each monomer. Refractive indices were measured by an Abbe's refractometor using casted copolymer films. Solubility tests of copolymers were conducted with a copolymer concentration of 10 % (w/w). The solubility behavior of copolymer/LC mixture in chloroform with the concentration of 35, 40 and 45 % (w/w) were examined with regard to the LC concentration range between 50-80 % in the mixture at 23 ℃ with a Kyowa CA-DT contact angle meter. Film thickness of the copolymer/LC composite films was measured by a Rank-Tayler Hobson Talystep on the basis of a stylus contact method. A polarization microscope was used to observe the LC droplets of the polymer/LC composite film. Transmittance change of the composite film was measured with a Hitachi U-4000 UV-VIS spectrometer.

Preparation of the polymer/LC composite film

A polymer/LC composite film in this study was prepared by the SIPS method using a chloroform solution at a ratio of the copolymer and the LC 40:60.[2,3] Concentration of the copolymer/LC mixture was adjusted to 30-50 wt% to get a composite film with similar thickness. The solution was first filtered through a 0.5 μm Teflon filter and spin-coated on an indium-tin-oxide (ITO) coated glass substrate at 500-1000 rpm for 10 s and then 1500 rpm for 70 s at 23 ℃ forming a 17 ± 1 μm-thick film. For the measurements of electrooptical properties, the resultant film sample was sandwiched with an another ITO glass substrate. Transmittance of the composite films fabricated from the copolymer **1a** and **1b** changed after repeating the voltage impression several times, so

that the electrooptical properties were measured on the composite films fabricated from copolymers **1c**-**1f**. Morphology of the composite films showed a slight change over a period of measurements.

3.1.3. Results and Discussion

Polymer synthesis

The copolymers were synthesized by a free radical polymerization using AIBN as an initiator. The results of GPC and DSC measurements and refractive index of copolymers **1a**-**1g** are summarized in Table 3.2. In the case of the synthesis of **1f** and **1g**, FMA tended to separate from the

Table 3.2. Results of GPC, DSC and refractive index investigation.

Polymer	Molecular weight [a]			Tg (°C) [b]	Refractive index [c]
	Mn	Mw	Mw/Mn		
1a	22,600	45,100	2.00	66.8	1.568
1b	17,370	40,370	2.32	62.6	1.554
1c	17,500	40,100	2.29	62.4	1.536
1d	19,100	36,800	1.93	61.4	1.515
1e	55,900	170,000	3.00	62.0	1.510
1f	18,100	34,200	1.89	56.5	1.449
1g	10,720	20,900	1.95	55.0	1.403

a) Determined by GPC, polystylene standards, UV detection.

b) Determined by DSC, heating rate 10 K/min, first heating.

c) n_D

d) Soluble portion in THF.

solution at room temperature but was soluble in the solvent above 40 ℃. Copolymer **1g** was found to be insoluble in the reaction medium and precipitated as a viscous swelled polymer during the reaction. This means that the copolymer with high composition of FMA is insoluble in toluene. Copolymers **1a-1f** were completely soluble. The results of GPC measurement showed that all copolymers distributed mono-modally. The number average molecular weight was in the order of 10,700-22,600 g/mol and the weight average molecular weight in the order of 20,900-45,100 g/mol except **1e**. Molecular weight of **1e** was higher than other copolymers because of low concentration of AIBN. Because **1g** was precipitated during the polymerization, molecular weight of the soluble portion of **1g** was low compared to that of **1a-1d** and **1f**. All polymers were amorphous. The glass transition temperatures (Tg) and the refractive index of the copolymers varied with the copolymer composition. Both the Tg and the refractive index decreased with increasing the composition of FMA.

Solubility

The solubility behavior of the copolymers was influenced by the FMA composition. Table 3.3 summarizes the results of solubility tests at 23 ℃ fixing the concentration at 10 wt%. Copolymers **1a-1e** could be dissolved in all solvents tested while copolymers **1f** and **1g** showed low solubilities. Copolymer **1f** was insoluble in DMF, and **1g** insoluble in both DMF and toluene but partially soluble in chloroform and THF suggesting low solubility of FMA in the solvents tested.

Table 3.3. Solubility of copolymers.

Polymer	Solubility [a]			
	$CHCl_3$	Toluene	THF	DMF
1a	+	+	+	+
1b	+	+	+	+
1c	+	+	+	+
1d	+	+	+	+
1e	+	+	+	+
1f	+	+	+	±
1g	± [b]	-	± [b]	-

a) Determined for a 10 % (w/v) solution.

b) Pertially soluble, swelled.

The solubility behavior of the copolymer/LC mixtures in chloroform was affected by not only the composition of FMA in the copolymer but also the concentration of copolymer/LC mixtures. Table 3.4 lists the results for copolymers **1d** and **1f** at 23 ℃. The mixture of **1d** and the LC was dissolved at all conditions tested. Copolymers **1a**-**1c** and **1e** showed the same results as **1d**. On the other hand, solubility of the mixture of **1f** and the LC was affected by the LC content in the polymer/LC mixture as well as the concentration of the mixture in the solution. A phase separation between the LC and the copolymer solution occurred when the LC content in the mixture was high and both the LC and the copolymer precipitated at the mixture concentration 45 wt% as shown in Table 3.4. However both the copolymer **1f** and the LC in a pure state were soluble

more than 50 wt% in chloroform, respectively. It can be seen from these results that solubility of the LC in the copolymer solution decreases with increasing the composition of FMA because of low interaction between **1f** and the LC.

Table 3.4. Solubility behavior of copolymer/LC mixtures.

Polymer	cont. [a]	LC concentration (wt%) [b]			
		50	60	70	80
1d	35	+	+	+	+
	40	+	+	+	+
	45	+	+	+	+
1f	35	+	+	+	- [c]
	40	+	+	- [c]	- [d]
	45	- [d]	- [d]	- [d]	- [d]

a) Mixture concentration in $CHCl_3$ solution, wt%.

b) wt% in LC/copolymer mixture.

c) LC was separated from the solution.

d) Both LC and copolymer separated from the solution.

Contact angle

The boundary interaction between a copolymer and the LC can be estimated from a contact angle of the polymer film with the LC. A transparent polymer film without the LC was prepared by a casting method from methylene chloride or THF solutions. Figure 3.1 shows the variation

of contact angle of the copolymer films with the LC, H_2O, ethylene glycol (EG) and hexane. Contact angle became larger with increasing the composition of FMA in the copolymer. The contact angle values 82-117 degrees for H_2O on the copolymers and 37-83 degrees for the LC were higher than the value 62 degree for PMMA. However, the contact angle of PMMA film. These results also show that the interaction between the copolymer and the LC decreased with increasing the composition of FMA and was lower than that between PMMA and the LC.

Morphology of the copolymer/LC composite film

Morphology of the composite film is usually observed by a scanning electron microscope (SEM) after extracting the LC by methanol did not effective to the present composite films despite methanol could not dissolve the copolymers and PMMA. The extracted LC domains in the composite films were destroyed to become transparent except in the case of the PMMA/LC composite film. A polarization microscope was useful for observing the film morphology. Figure 3.2 shows the photographs of **1c**-**1e** and PMMA with 60 wt% of the LC composite film without extracting the LC. It can be seen from the photographs that the **1d**/LC, **1e**/LC and PMMA/LC composite films were similar in morphology to one another and the **1c**/LC was slightly larger in the LC domain size than others.

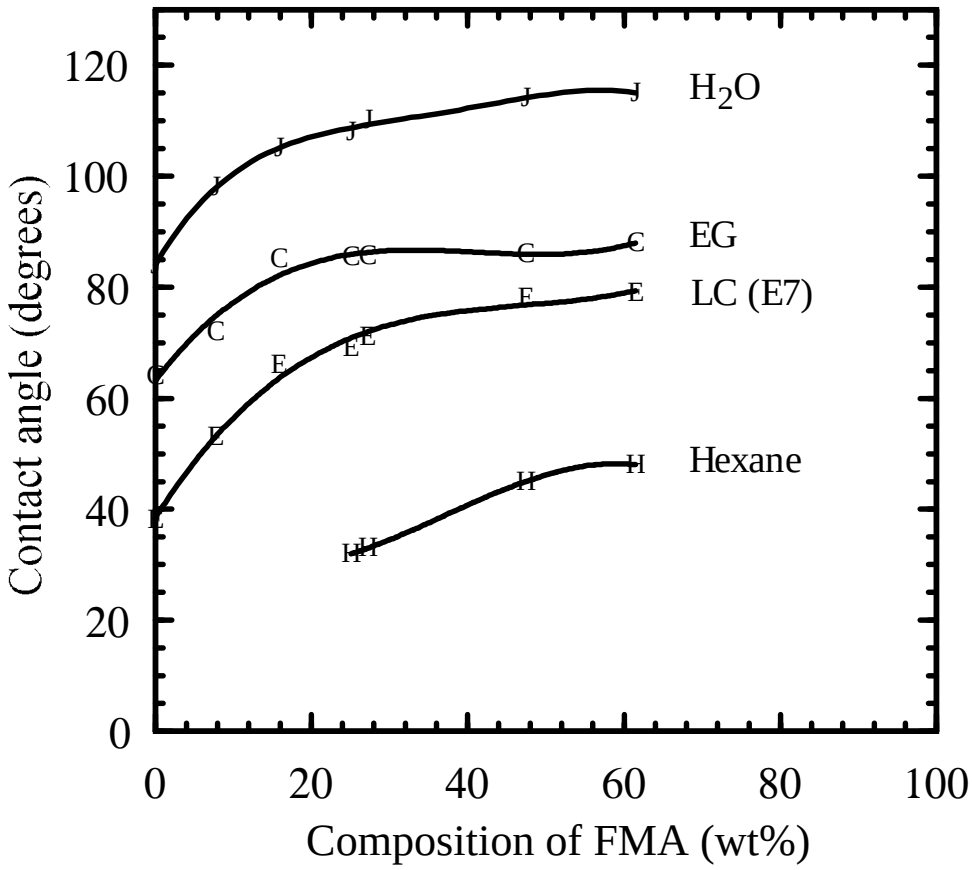

Fig. 3.1. Contact angle dependence on composition of FMA.

(a) (b)

(c) (d)

Figure 3.2. Cross-nicoled polarized microscope observation of the composite films. a: **1c** (5.9 mol% of FMA)/LC, b: **1d** (9.9 mol% of FMA)/LC, c: **1e** (11.0 mol% of FMA)/LC, and d: PMMA/LC composite

films. white: LC, black: polymer.

SEM observation for the PMMA/LC composite films showed that the size of the LC droplet was between 3-10 μm.

The **1a**/LC and **1b**/LC composite films slowly increased in transmittance even when they were stored at 23 ℃ and became transparent after storing for one month suggesting that the LC domain became large. This tendency was also observed for the other copolymers but the growing speed was much slower than **1a** and **1b**. Figure 3.3 shows change in Transmittance of light of the wavelength 500 nm for the composite films stored at 23 ℃. The PMMA/LC composite films showed no change in Transmittance. High composition of BMA might cause a fast change of the Transmittance, and higher molecular weight of the polymer could contribute to maintain the morphology because the **1e**/LC composite film was stabler in transmittance than the **1d**/LC composite film, as shown in Fig. 3.3.

Electrooptical properties

Measurement of the electrooptical properties of each copolymer/LC composite film was carried out on the film sandwiched between the ITO glasses just after the sample preparation, so that the LC droplet in each sample kept similar size. The light transmittance was measured on the composite films prepared from **1c**-**1f** and PMMA except those from **1a** and **1b** since the latter one changed in the transmittance with repeating the electric field impression. Table 3.5 lists the results of maximum transmittance (T_{max}), threshold voltage (V_{90}: a voltage at which the transmittance reached 90 % of T_{max}), hysteresis [voltage difference between up- and down-processes reached to the half of T_{max} to T_{min}

(minimum transmittance)], and response time.

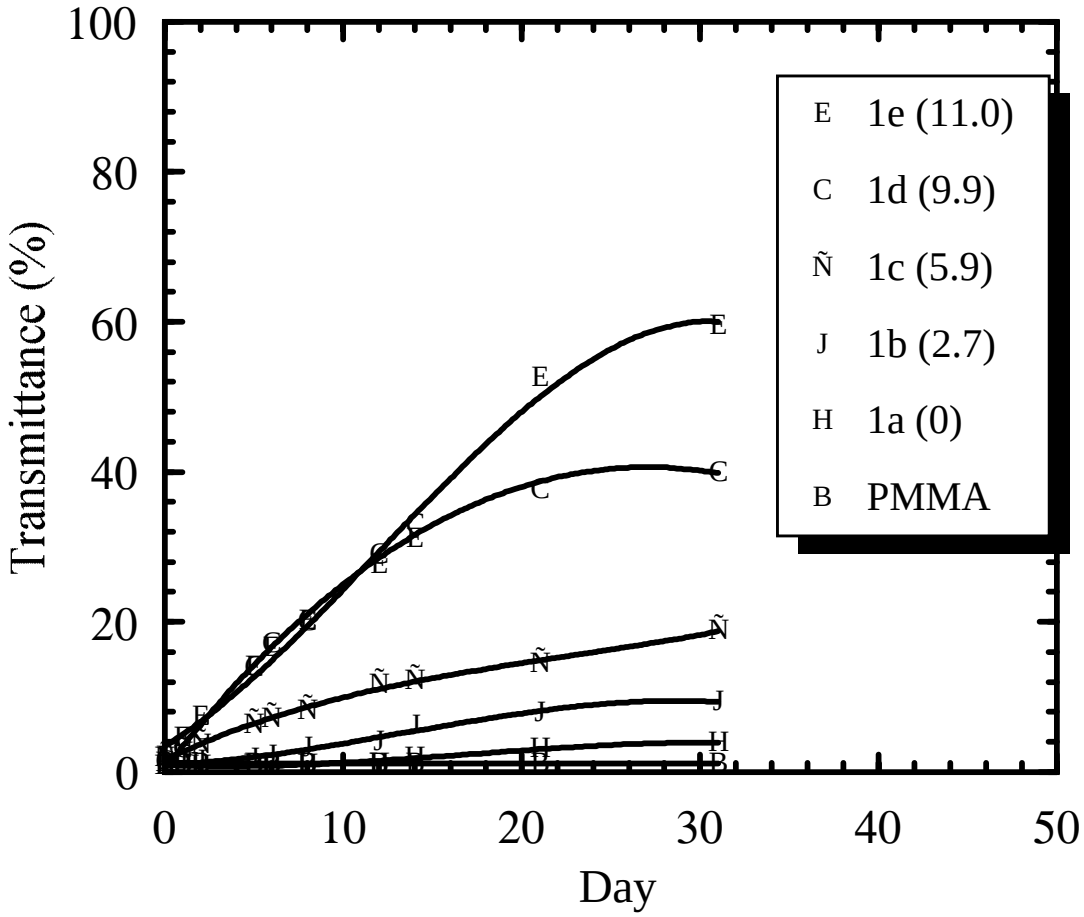

Fig. 3.3. Change of Transmittance of the copolymer/LC composite films with time. Film was stored at 23 ℃ and measured at 500 nm. The values in ( ) show the content of the fluorinated side group (mol%).

Table 3.5. Electrooptical properties of the copolymer/LC composite films.

	Polymer				
	1c	**1d**	**1e**	**1f**	PMMA
T_{max} (%) [a]	77	83	81	72	82
V_{90} (V_{rms}) [b]	18	24	25	21	57
Hys.(V_{rms}) [c]	5.0	5.5	2.5	7.5	24
t_{on} (ms) [d]	<1	2	2.5	1.5	9
t_{off} (ms) [e]	>100	>100	14	30	>100

a) Maximum transmittance.

b) Voltage at which the transmittance reached 90 % of T_{max}.

c) Hysteresis.

d) Time for a transmittance change from minimum to 90 % of T_{max}.

e) Time for a transmittance change from T_{max} to 10 % of T_{max}.

Driving voltage of the composite film

Fig. 3.4 shows the transmittance as a function of applied voltage at 1 kHz with a sweep rate 0.89 V_{rms}/s for the composite films prepared from **1d**, **1f** and PMMA. It can be seen that V_{90} and T_{max} varied with the copolymer composition. As shown in Table 3.5 and Fig. 3.4, V_{90} of the **1c**-**1f**/LC composite films was much lower than that of the PMMA/LC, resulting from a small interaction between the copolymers and the LC compared to the interaction between PMMA and LC. The **1f**/LC composite film was slightly lower in V_{90} than the **1d**- and **1e**/LC composite films

because of higher content of FMA, namely, high content of fluorinated side group.

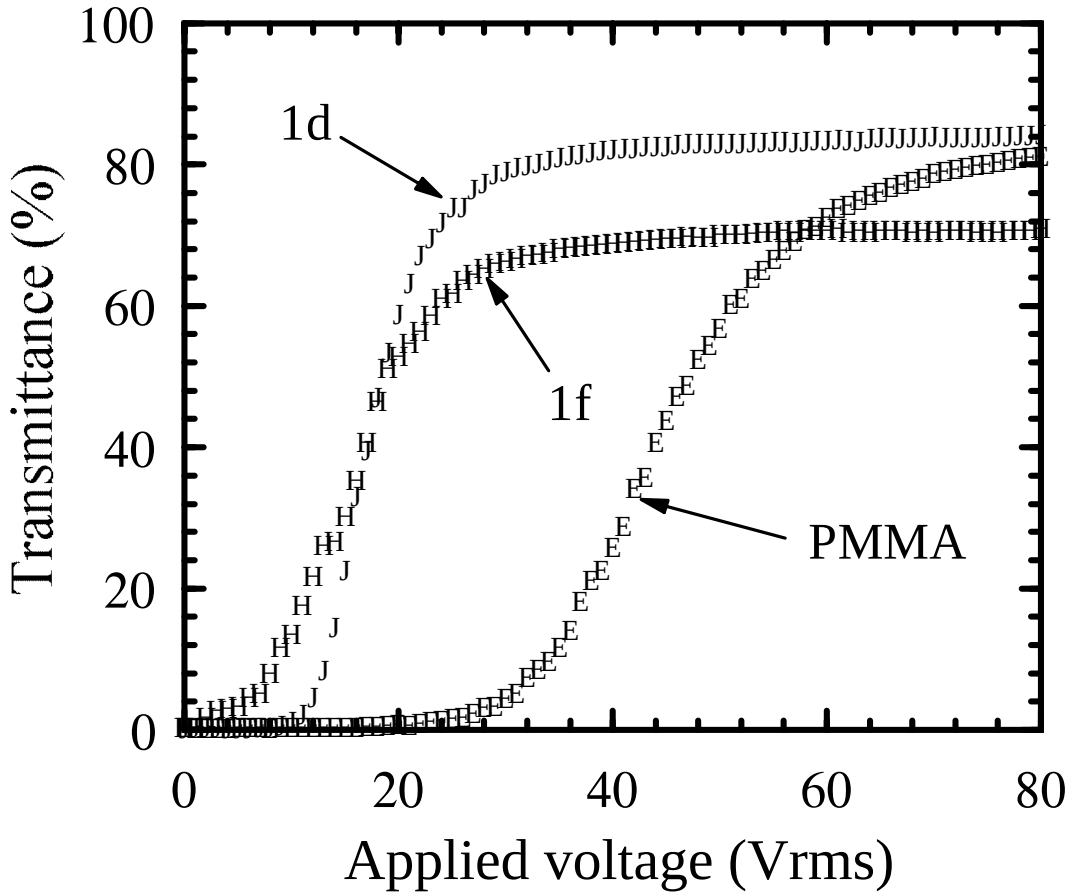

Fig. 3.4. Transmittance vs applied voltage curves for a copolymer/LC composite film. **1d** (9.9 mol% of FMA)/LC and **1f** (23.0 mol% of FMA)/LC.

In addition, lower V_{90} of the **1c**/LC composite film than other films might be caused by a large droplet size compared to others as shown in Fig. 3.2.

***Maximum transmittance* (T_{max})**

T_{max} was affected by the refractive index of the copolymer. Because of the large index mismatching between the LC (n_o=1.523) and the copolymer **1f** (n=1.449), the maximum transmittance of the **1f**/LC composite film was lower than that of the films prepared from **1c** (n=1.536), **1d** (n=1.515), **1e** (n=1.510) and PMMA (n=1.490).

Hysteresis

Hysteresis of each film was between 2.5-24 V_{rms}, depending on the molecular structure of the copolymers. The composite films prepared from the copolymers **1c**-**1f** were lower in hysteresis than the composite film prepared from PMMA. It is known that fluorine containing monomer could decrease the hysteresis.[8] It is interesting that the hysteresis of **1e**/LC was 2.5 V_{rms}, whereas **1d**/LC showed a higher hysteresis value of 5.5 V_{rms}. The morphology of the LC domain of each film was almost invariable concerning the microscope observation as shown in Fig. 3.2. Molecular weight of the copolymer could play an important role in this phenomenon and the hysteresis might have a relation to the switching behavior as described below.

Switching behavior

Experimental values of response time of the composite films are also listed in Table 3.5, where t_{on} is defined as the time for a transmittance change from T_{min} to 90 % of the (T_{max}−T_{min}) upon turning the electricity on, and t_{off} is measured as the time for a transmittance change from T_{max} to 10 % of the (T_{max}−T_{min}) upon turning the electricity off. t_{on} value was around a few milliseconds except in the case of PMMA/LC composite film, where t_{on} was 9 ms. The **1c**/LC composite film was faster in t_{on} than other composite films because of the large droplet size.[2)] On the other hand the composite films were very slow in t_{off} except the composite films prepared from **1e** and **1f**. Figure 3.4 shows switching behavior of composite films of **1d**/LC and **1e**/LC upon the applied voltage on and off. These copolymers had a similar copolymer composition and the morphology of the composite films were almost invariable, as shown in Fig. 3.2. These composite films agreed in t_{on} with each other but their t_{off} was completely different. In the case of the **1d**/LC composite film, both fast and slow decays were present, taking more than 100 ms to return the original scattering state, whereas t_{off} of the **1e**/LC composite film was 14 ms. The slow decay was also observed in the **1c**/LC and PMMA/LC composite films. t_{off} of the **1f**/LC composite film was about 30 ms and longer than that of the **1e**/LC. It can be assumed that the slow decay was caused by a local molecular motion of the matrix polymer upon the electricity off. If the molecular weight of the matrix copolymer was high, the local molecular motion was suppressed as a result of the absence of slow decay, which could cause the lower hysteresis of the **1e**/LC composite film too.

Fig. 3.5. Switching behavior of the composite films. Applied voltage was 80 V_{rms} of 1 kHz square wave. **1d** (9.9 mol% of FMA)/LC and **1e** (11.0 mol% of FMA)/LC.

Conclusions

Methacrylate copolymers comprising the perfluorooctylethyl side group and the benzyl side group were synthesized. The copolymer was precipitated during the polymerization if the content of FMA was high. Solubility of the copolymers in organic solvents with various liquids increased with increasing the FMA composition in the copolymer as a result of decrease in the interaction between the LC and the copolymer with increasing the FMA composition.

The copolymer/LC composite films were prepared by the SIPS method from a chloroform solution. Because of the low interaction between the copolymer and the LC, threshold voltage of the copolymer/LC composite films was in a range 18-25 V_{rms} much lower than that of the PMMA/LC composite film. The former were also smaller in hysteresis than the latter. t_{off} varied with the molecular weight of the copolymers. t_{off} of the composite film with the low molecular weight polymer matrix behaved in two decay ways according to the local molecular motion of the matrix polymer upon the electricity off.

Reference

1) L. C. Chien: *Proc. SPIE* **1815** (1992) 220.
2) T. Kajiyama, H. Kikuchi and A. Takahara: *Proc. SPIE* **1665** (1992) 20.
3) T. Kajiyama, A. Miyamoto, H. Kikuchi, and Y. Morimura: *Chem. Lett*. (1989) 813.
4) F. G. Yamagishi, L. J. Miller, and C. I van Ast: *Proc. SPIE* **1080** (1989) 24.
5) P. Drzaic: *J. Appl. Phys.* **60** (1986) 2142.
6) J. W. Doane, N. A. Vaz, B. G. Wu, and S Zumer: *Appl. Phys. Lett.* **48** (1986) 269.
7) B. K. Kim and Y. S. Ok: *J. Appl. Polym. Sci*. **49** (1993) 1769.
8) N. Yamada, T. Hirai, N. Ohnishi, S. Kouzaki, F. Funada, and K. Awane: *12th Int. Display Res. Conf*. (1992) 699.

3.2. Fabrication of PMMA/LC Composite with Controlled Interface Layer by Two-Step Phase Separation Method

A polymer/liquid crystal (LC) composite film is fabricated by a combination of a solvent-induced phase separation (SIPS) and a photopolymerization-induced phase separation (PPIPS) method, using polymethylmethacrylate (PMMA), LC and photocurable monomers. Electrooptical properties for the composite films have showed a low driving voltage of 18 V_{rms}, a rapid turn-on time of 0.8 ms, a rapid turn-off time of 10 ms and a small hysteresis of less than 1 V_{rms}.

3.1.1. Introduction

The purpose of the present section is to clarify the electrooptical properties of PMMA/LC composite films with interface layer at the interface between PMMA and LC. The author describes fabrication of composite films with a thin photocured polymer layer between the PMMA matrix and the LC droplet by two-step phase separation method, composed of the solvent-induced phase separation (SIPS) followed by a photopolymerization-induced phase separation (PPIPS), as indicated in Fig. 1.7.

3.1.2 Experimental

A polymer/LC composite film was prepared from a chloroform solution of PMMA (30 wt%), photocurable monomers (9.5 wt% of benzylmethacrylate (BzMA) and perfluorooctylethylacrylate (FA108) mixture), dimethoxyphenylacetophenone (DMPA, for a photo-initiator, 0.5 wt%) and the nematic LC (Merck-E7, 60 wt%). Weight ratio of the BzMA and the FA108 was controlled at 100:0, 80:20, 65:35, 50:50, 20:80 and 0:100. The solution was spin-coated glass substrate, resulting a 16-19 μm thick phase separated film. Then the film was exposed for 60 min by using an UV lamp (11-13 mW/cm^2 at 365 nm) followed by lamination with another ITO coated glass substrate. Conventional PMMA/LC composite film (P-film) was also fabricated by a SIPS method from a chloroform solution. Electrooptical measurements were performed in the same procedure, as described previously.[1)]

3.1.3 Results and Discussion

To form the thin photocured polymer layer between the polymer and the LC, solubilities and compatibility of the materials should be important factors for the two-step phase separation method. The BzMA showed a good solubility in PMMA and FA108, and the film casted from a chloroform solution was transparent. On the other hand, the casted films from PMMA/FA108 and PMMA/BzMA/FA108 (60/32/8-60/0/40, wt%) were opaque, showing the incompatibility of FA108 in PMMA matrix. When the LC was added in the BzMA/FA108 mixture, the LC became separated. Therefore the photocurable monomers might be dispersed around or in the LC droplet in the case of the casted film from the PMMA/BzMA/FA108/LC solution before the UV exposure. For example, Figs. 3.6(a) and 3.6(b) shows the morphology of the PMMA/BzMA/LC composite film extracted with methanol before and after the UV irradiation. Both the LC and the BzMA were extracted before the UV irradiation and only LC was extracted after the irradiation because both the BzMA monomer and the LC could dissolve in methanol. The size of the hole after irradiation was 2-8 μm, as shown in Fig. 3.6(b), while the extracted hole before the irradiation was larger than that of after the irradiation. This may be the consequence that the BzMA dissolved in the LC droplet rather than PMMA matrix before UV irradiation and poly-BzMA was separated from the LC after irradiation. Because same results were obtained for the PMMA/BzMA/FA108/LC composite film (M-film), photocurable monomers (BzMA and FA108) were dispersed in the LC droplet not in the PMMA matrix before the UV irradiation.

Fig. 3.6. Scanning electron micrographs for PMMA/BzMA/LC (30/10/60 wt/wt/wt) composite film. (a) before UV irradiation and (b) after irradiation. Both film was extracted by methanol.

The relation of applied voltage and transmittance is shown in Fig. 3.7. The maximum transmittance (T_{max}) was the same value of 82 % as the P-film in all cases of the M-films. The M-films were lower in the driving voltage (V_{90}: a voltage at which the transmittance reached 90 % of T_{max}) than the P-film and the value was between 18 and 24 V_{rms}. The minimum V_{90} achieved when the ratio of BzMA/FA108 was 50:50. These values were about 1/3 of that of the P-film and the similar range as the composite film composed of the copolymer of benzylmethacrylate-co-perfluorooctylethymethacrylate (poly-BzMA-co-FMA) with the same LC.[2)] Improved V_{90} could be explained by the change of the boundary condition at the interface between the LC droplet and PMMA due to the addition of the photocured polymers same as described in the composite film fabricated from the PVA. The extremely thin layer of the photocured polymer should be formed at the interface between the PMMA and the LC. The calculated thickness of the interface layer consisting of photocured polymers surrounding a 3 μm LC droplet is less than 30 nm when 10 wt% of photocurable monomers is added. In addition, V_{90} of a composite film using a mixture of the PMMA and the poly-BzMA-co-FMA (3/1, wt/wt) as a polymer matrix (PB-film) was slightly smaller than that of the P-film, as shown in Fig. 3.7, but the hysteresis and response time were not improved. In this case, poly-BzMA-co-FMA was dispersed in the PMMA matrix and could not formed a thin layer around the LC droplet. In contrast T_{max} of the PMMA/FA108/LC composite film was less than 40 %.

Fig. 3.7. Influence of the BzMA concentration and the polymer matrix on V-T properties. The weight ratios of BzMA and FA108 were between 100:0-0:100. M-films consist of PMMA, BzMA, FA108, and LC (Contents of BzMA in the photocurable mixture are shown in figure.) PB film consists of poly-BzMA-co-FA108 and LC. P-film shows a conventional PMMA/LC composite film.

Because the FA108 monomer was insoluble both in the PMMA and the LC, the photocured FA108 might form its own droplet in the PMMA matrix and could not form a thin layer at the interface between the PMMA and the LC, resulting a light scattering due to the refractive index mismatching between the PMMA and the poly-FA108.

The M-film was lower in the hysteresis and faster in the response time than the P- and PB-films as listed in Table 3.6. The lowest hysteresis was less than 1 V_{rms} and it was achieved when the ratio of the BzMA and FA108 was 50/50 and 65/35 wt/wt%. The fluorine containing polymer matrix is known to reduced the hysteresis of the composite film.[3] Rise time (t_{on}: the time for a transmittance change from T_{min} (minimum

Table 3.6. Electrooptical properties of the composite film.

BzMA content (wt%)	Hysteresis [a] (V_{rms})	t_{on} (ms)	t_{off} (ms)
100	3	0.9	21.6
80	3	0.8	19.7
65	<1	0.8	11.7
50	<1	0.9	10.4
20	1	0.4	10.0
P-film [b]	24	9	>100
PB-film	20	10	>100

a) defined as the voltage difference between up- and down-processes reached to half of T_{max}-T_{min} .

b) reference 3

transmittance) to 90 % of the T_{max} upon turning the electricity on) of the M-film was less than 1 ms, while t_{off} (the time for a transmittance change from T_{max} to 10 % of the T_{max} upon turning the electricity off) because faster with increasing the FA108 content within the range of 10-22 ms. For example, switching behaviors of the M- and PB-films are shown in Fig. 3.8. The M-film had a faster response than the PB-film which had fast and slow decay because of the local molecular motion, as described previously.[2] It is known that t_{on} because faster and t_{off} slower with increasing the LC droplet size.[4]

Fig. 3.8. Electric-switching characteristics of M- and PB-films. M-film consists of 60 wt% of LC, 30 wt% of PMMA, 14.75 wt% of BzMA, 14.75 wt% of FA108 and 0.5 wt% of DMPA. PB-film consists of 60 wt% of LC, 30 wt% of PMMA and 10 wt% of poly-BzMA-co-FMA. All films were performed by using an 80 V_{rms} output with 1 kHz square wave.

In the case of the composite films in this section, the size of the droplet was almost the same as long as the SEM observation. The improvements of the electrooptical properties of the M-films can be explained by the photocured copolymer at the interface between the PMMA and the LC. If the copolymer of the BzMA and FA108 was formed at the interface between the PMMA and the LC, the M-film might be lower in an anchoring force than the P-film, reducing inherent bistability in the droplets. Because t_{off} depend on the molecular weight of the polymer matrix, the fast response might be the consequence of the suppressed local molecular motion of the matrix polymer due to the thin layer of photocured copolymer at the interface between the PMMA and the LC for the M-films.

Conclusions

Improved electrooptical properties for the polymer/LC composite film fabricated from two-step phase separation method using PMMA as the polymer matrix was obtained by the addition of small amount of the photocurable monomers. These results were the consequence of the change of the boundary condition at the interface between the LC and the PMMA. Thin layer of the poly-BzMA-co-FA108 might be formed between the PMMA and the LC and it could reduce the interaction between them.

References

1) H. Ono and N. Kawatsuki: *Jpn. J. Appl. Phys*. **33** (1994) 6268.

2) N. Kawatsuki and H. Ono: *J. Appl. Polym. Sci*. **55** (1995) 911.

3) N. Yamada, T. Hirai, N. Ohnishi, S. Kouzaaki, F. Funada, and K. Awane: *12th Int. Display Res. Conf*. (1992) 699.

4) T. Kajiyama, H.Kikuchi and A. Takahara: *Proc. SPIE* **20** (1992) 1665.

4. Control of the Morphology of PVA/LC Composite

4.1. Control of Shape of LC Droplets by Changing Solvent

A poly(vinyl alcohol) (PVA)/liquid crystal (LC) composite film with a low driving voltage of 6 V_{rms}, a low hysteresis of less than 0.2 V_{rms}, and a fast response time of 11 ms at the operating voltage of 6 V_{rms} is formed from the emulsion composed of a mixture of water with methanol (WM-mixture), PVA, LC, and a photocrosslinkable mixture of nonaoxyethylenediacrylate (9EG-A) with perfluorooctylethylacrylate (FA108). It is found in the composite film that the LC droplets, surrounded by a thin layer of the photocured polymer, are deformed as well as disordered, which enhance light scattering.

4.1.1. Introduction

Low driving voltage and high contrast can be obtained by forming a thin composite film when the composite film greatly scatters light. On the basis of light scattering from a small nematic droplet in the Rayleigh-Gans approximation, Zumer and Doane found that the scattering behavior was remarkably dependent on the nematic director structure.[1)] Incorporating different nematic mixtures into the PVA/LC composite films, Drzaic and Gonzales showed that the scattering cross section of nematic droplets depended not only on the refractive index of the polymer interface, but also on the structure of the film beyond the interface.[2)] From the transmittance and microscopic structure of the stretched PVA/LC composite films, Aphonin *et al.* showed that the polaizability of the stretched composite film was expressed as a function of the droplet shape.[3)] On the other hand, the electrooptical and light scattering properties of the PVA/LC composite film having deformed and disordered droplets have not been studied since the droplet shape could not be controlled by the traditional emulsification method.

A novel PVA/LC composite film with deformed and disordered nematic droplets is presented here. The composite film was formed from an emulsion of water mixed with methanol (WM-mixture) to investigate morphology, light scattering properties, and electrooptical properties. It is expected that the morphology is affected by the solvent, since PVA can be dissolved in both water and methanol, while LC can be dissolved in methanol and can not in water.

4.1.2. Experimental

PVA (trade name PVA205 with the degree of polymerization of 500 and the saponification rate of 88 mol% supplied of Kuraray Co., Ltd.) was dissolved in the mixture of the distilled water with methanol (WM-mixture) at 23 ℃ at a weight ratio of 50:50 to prepare a 15 wt% solution of PVA205. The solution was heated to 80 ℃ to dissolve PVA205 completely, and then left at room temperature. The composite film was formed by emulsification and photopolymerization of the following methacrylates, which induced a spontaneous phase separation method.[4] The composite film formed from the WM-mixture was composed of 30 wt% of PVA205, 6 wt% of nonaoxyethylenediacrylate (9EG-A, Kyoeisya Chemical Company), 4 wt% of perfluorooctylethylacrylate (FA108, Kyoeisya Chemical Company) and 60 wt% of nematic LC mixture (ZLI2061, Merck Japan Ltd.). Three kinds of composite films with different thicknesses were prepared by changing the revolution speed of the spin-coating process, and the thicknesses, measured by the Rank-Tayler Hobson Talystep on the basis of a stylus contact method were 5, 8 and 11 μm. The film composition remained unaltered upon changing the WM-mixture to water emulsion. Composite films without the photocured polymer, consisting of 40 wt% of PVA205 and 60 wt% of ZLI2061, were also prepared from the WM-mixture, adjusting the film thicknesses to 5, 8 and 11 μm.

In order to compare the morphology of the composite films, two kinds of composite films without photocured polymer, consisting of 40 wt% of PVA205 and 60 wt% of ZLI2061, were formed from the water emulsion as well as the WM-mixture. ZLI2061 was extracted with

methylene chloride at 23 ℃ for 30 s, and the morphology of the film was observed by scanning electron microscopy (SEM) to detect the droplet shape from a vertical view.

Light scattering properties of the composite films were measured using a He-Ne light source (632.8 nm, 6.3 mW), an optical fiber, a photomultiplier, an AD converter, a rotational stage, and a personal computer. The laser beam impinging perpendicularly on the cell surface was scattered by the composite film. In order to obtain the light scattering profiles of the laser beam as a function of the detection angle, the optical fiber head was rotated around the sample cell axis to monitor the scattered light intensity by means of the photomultiplier, the AD converter, and the personal computer.

The light scattering pattern from the nematic droplets was observed with an optical polarizing microscope equipped with a He-Ne laser light source. The polarized incident laser light impinged on the surface of the composite film, and the scattered light passed through the analyzing polarizing film. The scattering pattern was projected on a white paper and images were taken photographs on a photosensitive film (Polaroid Type 612). The scattering pattern was observed when the polarization plane of the analyzer was perpendicular (Hv-scattering) and parallel (Vv-scatteriing) to that of the incident light.

4.1.3. Results and Discussion

The composite film formed from the water emulsion showed oblate droplets with minor axes aligned perpendicular to the film plane, as shown in Fig. 4.1(a), whereas the shape of the nematic droplets in the composite film formed from the WM-mixture was deformed and disordered, as shown in Fig. 4.1(b). The droplets in the composite film formed from the WM-mixture suggested the formation of a continuous phase, in contrast with the isolated droplets in the composite film formed from the water emulsion.

The droplet shape varied with the solubility of PVA and ZLI2061 as follows. Solubility of PVA205 was lower in methanol than that in water, whereas ZLI2061 was soluble in methanol but insoluble in water. Therefore, the nematic droplet was expected to form a perfect sphere in the water emulsion without methanol to minimize the surface energy since ZLI2061 can not be dissolved in a PVA205 aqueous solution. The nematic droplet in the WM-mixture was deformed by dissolution of ZLI2061 in methanol.

(a)

(b)

Fig. 4.1. Morphology of the composite films consisting of 40 wt% of PVA205 and 60 wt% of ZLI2061. (a) PVA205/ZLI2061 composite film formed from the water emulsion. (b) PVA205/ZLI2061 composite film formed from the WM-mixture.

Fig. 4.2 shows the light scattering property through the composite film formed from the water emulsion (Fig. 4.2(i)) and that from the WM-mixture (Fig. 4.2(ii)). The maximum transmission intensity, occurred from the direct laser beam without scattering, was obtained at the detection angle of zero degree. The scattered light was diffused at wider angles in the composite film formed from the WM-mixture than in the composite film formed from the water emulsion.

Figures 4.3(a) and 4.3(b) show the Hv- and Vv-scattering patterns in the composite film formed from the water emulsion, respectively. Samuels determined, experimentally and theoretically, Hv- and Vv-scattering from optically anisotropic spheres and disks in the polymer film.[5] The Hv- and Vv-scattering patterns in the composite film formed from the water emulsion were similar to those in the isotactic polypropylene spherulite and theoretical results. The results suggest that the nematic droplets with uniaxial spheres were dispersed in the composite films formed from the water emulsion, in analogy with the result of SEM observation. In contrast, the Hv- and Vv-scattering patterns in the composite film formed from the WM-mixture were similar to those in the deformed and disordered spherulites studied by Stein *et al.* as shown in Figs. 4.3(c) and 4.3(d).[6] The result suggests that the nematic droplets were deformed and disordered in the composite film formed from the WM-mixture emulsion. It is desirable in the display panels that the light be intensively scattered by the nematic director in the deformed nematic droplets randomly oriented in the composite films formed by the photopolymerization-induced phase separation.

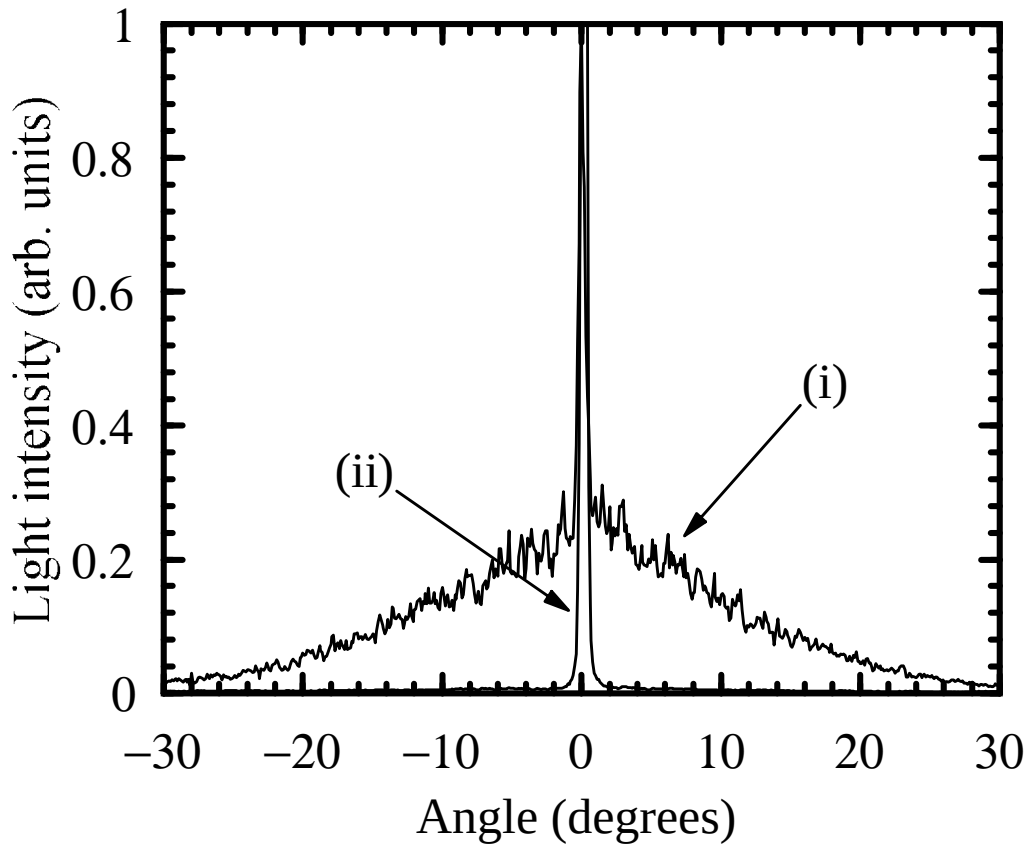

Fig. 4.2. Light scattering properties of the composite films consisting of 30 wt% of PVA205, 6 wt% of 9EG-A, 4 wt% of FA108, and 60 wt% of ZLI2061. Light intensity is normalized at zero degree. (i) The composite film formed from the WM-mixture. (ii) The composite film formed from the water emulsion.

(a) (b)

(c) (d)

Figure 4.3. Hv- and Vv-scattering patterns of the composite films consisting of 30 wt% of PVA205, 6 wt% of 9EG-A, 4 wt% of FA108, and 60 wt% of ZLI2061.

(a) Hv-scattering in the composite film formed from the water emulsion.

(b) Vv-scattering in the composite film formed from the water emulsion.

(c) Hv-scattering in the composite film formed from the WM-mixture.

(d) Vv-scattering in the composite film formed from the WM-mixture.

Similar results were obtained from the same measurements of the light scattering properties on the composite films consisting of 60 wt% of ZLI2061 and 40 wt% of PVA205 (without photocured polymer). It was suggested, therefore, that deformation of the nematic droplets was caused by dissolution in the emulsion medium regardless of the addition of photocurable monomers, and that light scattering in the composite film formed from the WM-mixture was enhanced not only by the refractive index mismatch but also by the inhomogeneous nematic director in the deformed and disordered droplet.

Electrooptical properties of composite films were measured at 23 ℃ using the same measurement system, as described previously,[1)] determining the driving voltage, the hysteresis and the response time. The V-T curves of the composite films with thicknesses 5, 8 and 11 μm are shown in Fig. 4.4. As shown in Fig. 4.4(a), the contrast in the composite films formed from the water emulsion decreased with decreasing film thickness. In contrast, the composite films formed from the WM-mixture presented high contrast although the film was thin as shown in Figs. 4.4(b) and 4.4(c). The high contrast in the composite films formed from the WM-mixture was attributed to the strong light scattering from the deformed droplets, whereas the low contrast in the composite films formed from the water emulsion was due to insufficient light scattering and direct beam irradiation without scattering. The driving voltages in the composite films formed from the WM-mixture were 6, 12 and 18 V_{rms} at the film thicknesses of 5, 8 and 11 μm, respectively.

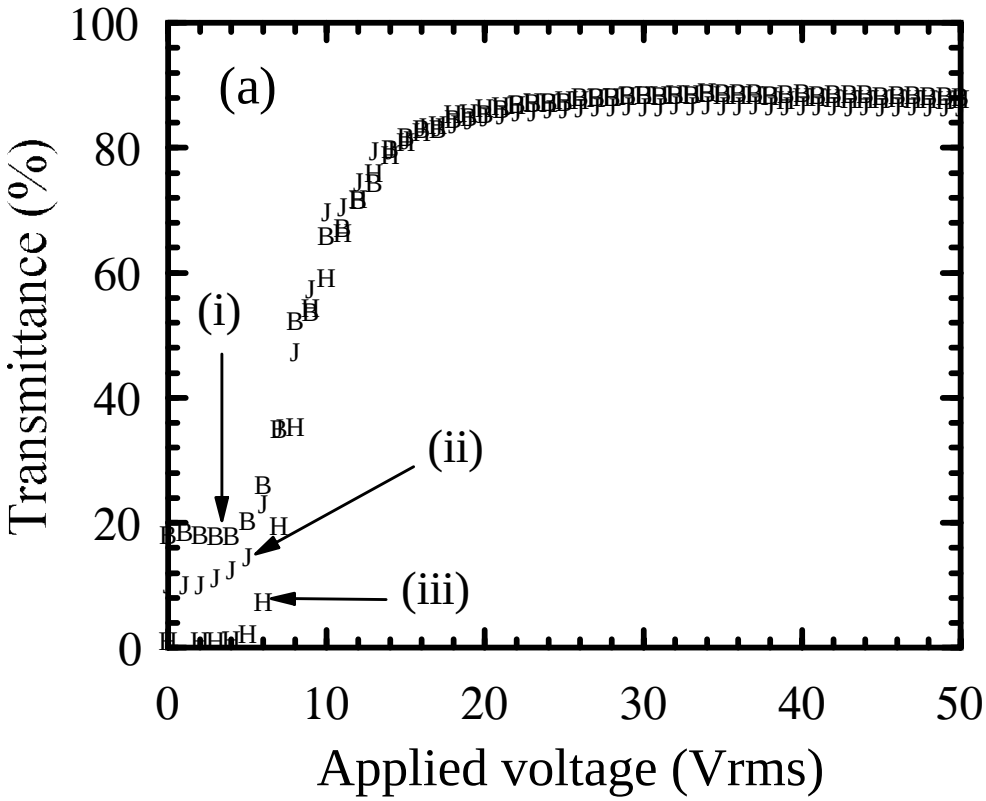

Fig. 4.4(a). The composite films formed from the water emulsion with added photocured polymer. The composite films consisted of 30 wt% of PVA205, 6 wt% of 9EG-A, 4 wt% of FA108, and 60 wt% of ZLI2061. Film thicknesses were (i) 5 μm, (ii) 8 μm and (iii) 11 μm.

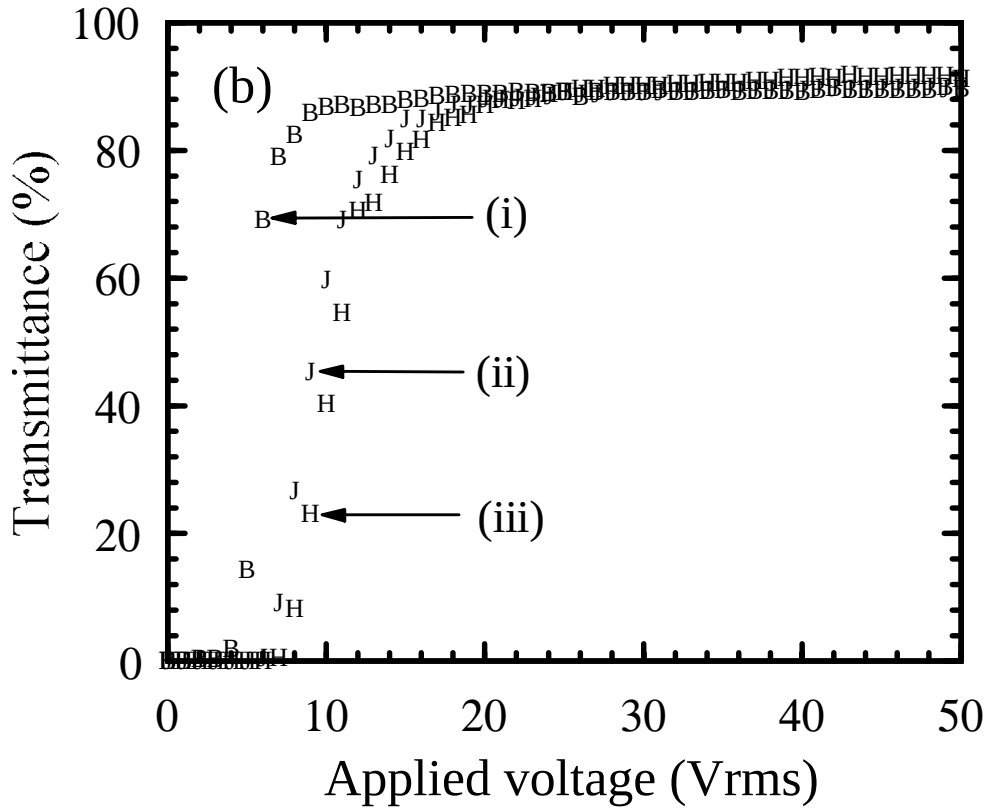

Fig. 4.4(b). The composite films formed from the WM-mixture with added photocured polymer. The composite films consisted of 30 wt% of PVA205, 6 wt% of 9EG-A, 4 wt% of FA108, and 60 wt% of ZLI2061. Film thicknesses were (i) 5 μm, (ii) 8 μm and (iii) 11 μm.

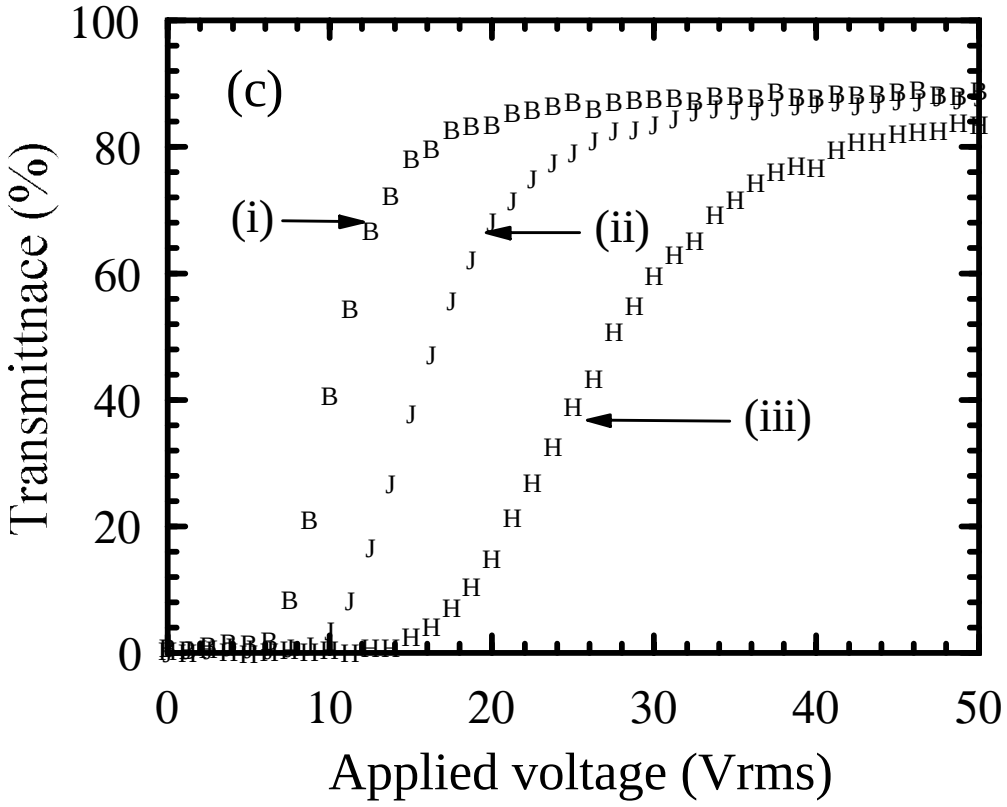

Fig. 4.4(c). The composite films formed from the WM-mixture without photocured polymer. The composite films consisted of 40 wt% and 60 wt% of ZLI2061. Film thicknesses were (i) 5 μm, (ii) 8 μm and (iii) 11 μm.

The V-T curves for composite films without the photocured polymer formed from the WM-mixture are also shown in Fig. 4.4(c). The driving voltages in the composite film were 18, 28 and 49 V_{rms} at the film thicknesses of 5, 8 and 11 μm, respectively. The driving voltage was considerably decreased upon addition of the photocured polymer. These results suggest the possibility that the photocured polymer formed an interface layer between the domains of PVA205 and ZLI2061 in the composite film formed from the WM-mixture, and reduced the anchoring strength in the composite film.

The hysteresis characteristic of the composite film was measured by varying a square output with 1 kHz between 0 and 8 V_{rms}. In order to determine the response time, the electric field (1 kHz, 6 V_{rms}) was turned on and off while monitoring the transmitted light intensity with a digitizing oscilloscope. Figures 4.5(a) and 4.5(b) show the hysteresis and electric-switching characteristics, respectively, in the composite film composed of 30 wt% of PVA205, 6 wt% of 9EG-A, 4 wt% of FA108, and 60 wt% of ZLI2061 and formed from the WM-mixture. The composite film exhibited the low driving voltage of 6 V_{rms}, low hysteresis of less than 0.2 V_{rms}, high contrast, and short response time of 11 ms. The improvements in the electrooptic characteristics were possibly caused by strong light scattering from deformed nematic droplets and the low anchoring energy at the interface between the polymer and the LC.

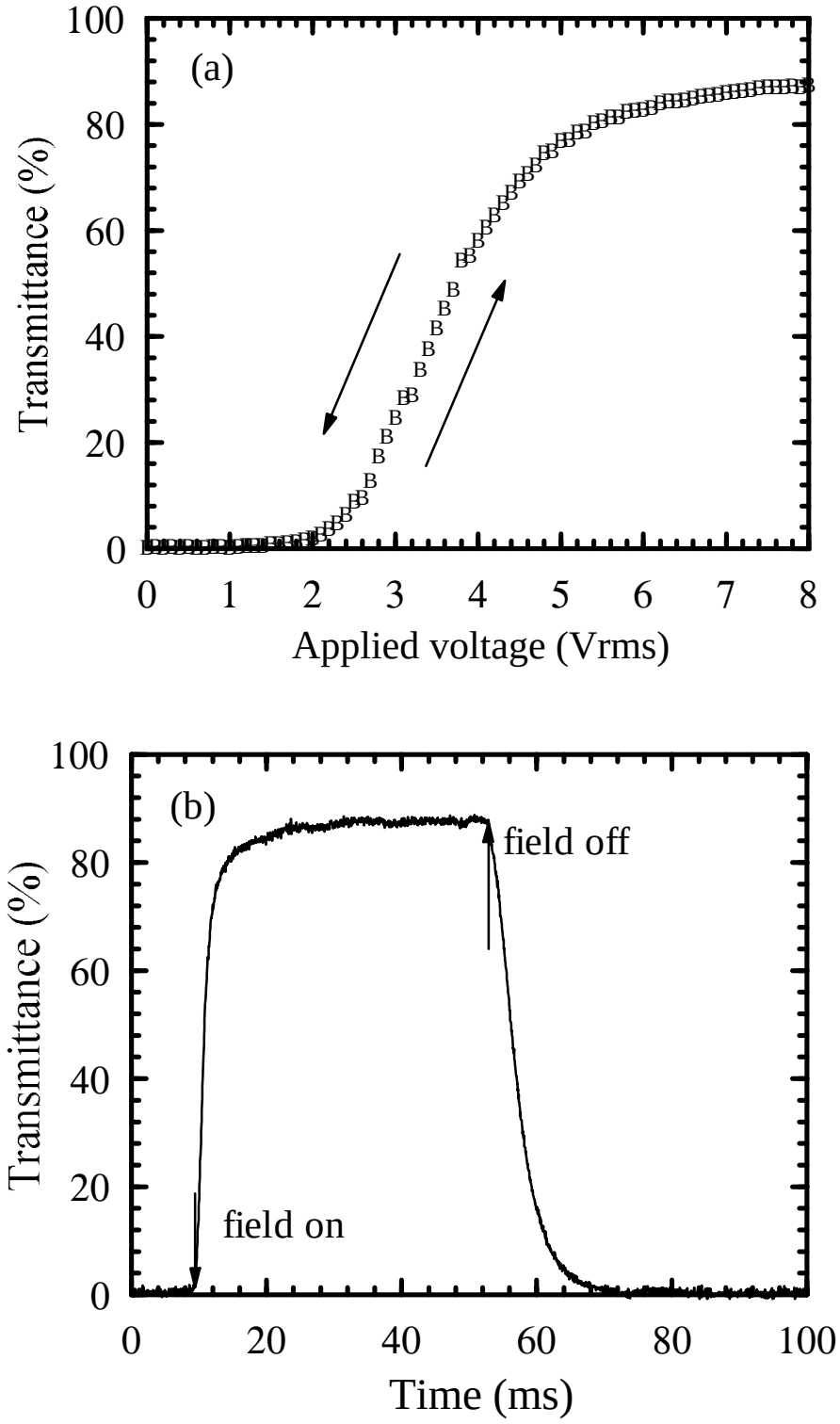

Fig. 4.5. The hysteresis and electric-switching characteristic of the composite film formed from the WM-mixture with added photocured polymer. The composite film consisted of 30 wt% of PVA205, 6 wt% of 9EG-A, 4 wt% of FA108, and 60 wt% of ZLI2061. Film thickness was 5 μm.

Conclusions

The electrooptical properties and morphologies of the composite films formed from the mixture of water with methanol (WM-mixture) were investigated. The droplets in the composite film formed from the emulsion including the WM-mixture, PVA205, and ZLI2061 were deformed and disordered compared with those in the film formed from the aqueous emulsion without methanol. The enhancement of the light scattering could be occurred from the deformed droplets since the light scattering resulted from not only the refractive index mismatching but also the inhomogeneous nematic director. The Hv- and Vv-scattering patterns occurred from the composite film formed from the water emulsion were similar to those occurred from the optically anisotropy spheres and disks in the polymer films. In contrast, those occurred from the composite film formed from the WM-mixture were similar to those occurred from the deformed and disordered crystals. The results were consistent with SEM observations. The electric-switching contrast of the composite film formed from the WM-mixture was high though the film thickness was thin (5 μm) since the light was intensively scattered by the deformed LC droplets. The driving voltage could be reduced by the thin films with high contrast by using the composite films with added photocured polymer.

The PVA/LC composite film having the low driving voltage of 6 V_{rms}, the low hysteresis less than 0.2 V_{rms}, the high contrast, and the fast response time of 11 ms was formed from the emulsion including the mixture of water with methanol, PVA205, 9EG-A, FA108, and ZLI2061. In conclusion, the superior performance was achieved because of the strong light scattering from deformed nematic droplets and the low

anchoring energy at the interface between the photocured polymer surrounding the nematic droplet and the LC.

References

1) S. Zumer and J. W. Doane: *Phys. Rev.* A **34** (1986) 3373.

2) P. S. Drzaic and A. M. Gonzales: *Mol. Cryst. Liq. Cryst.* **222** (1992) 11.

3) O. A. Aphonin, Yu. V. Panina, A. B. Pravdin, and D. A. Yakovlev: *Liq. Cryst.* **15** (1993) 395.

4) H. Ono and N. Kawatsuki: *Jpn. J. Appl. Phys.* **33** (1994) 6268.

5) R. J. Samuels: *J. Polym. Sci.* **9** (1971) 2165.

6) R. S. Stein and T. Hashimoto: *J. Polym. Sci.* **9** (1971) 517.

4.2. Control of Size of LC Droplets by Changing Saponification Rate of PVA

The relationship between the saponification rate of poly(vinyl alcohol) (PVA), and the electrooptical properties and morphology of PVA/liquid crystal (LC) composite films is investigated. Light transmission clazing and the LC droplet size have been varied by changing the saponification rate or the blend ratio of two kinds of PVA with different saponification rates because the refractive index and surface tension can be controlled by the saponification rate of PVA. The threshold voltage has been decreased with increasing saponification rate though the extrapolation length was decreased. It is suggested that the electrooptical properties are strongly dependent on the droplet size.

4.2.1. Introduction

In order to apply the composite film to the devices, it is important to control the morphology and optical property. Several studies on the light scattering properties and electrooptical properties of PVA/LC composite films have been performed.[1-5] However the detailed relationship between the physical characteristic of PVA matrix and the electrooptical properties has not yet been clarified.

The purpose of this section is to clarify the relationship between the electrooptical properties, morphology and saponification rate of PVA and the blend ratio of two kinds of PVA with different saponification rates.

4.2.2. Experimental

Materials

The saponification rate was defined as the degree of hydrosis in PVA. PVA samples with different saponification rates were supplied by Kuraray Co., Ltd., and their trade names and characters are summarized in Table 4.1. Nematic LC mixtures with positive dielectric anisotropy were obtained from Merk Japan Ltd. and the refractive indexes of these LC mixtures are summarized in Table 4.2. The glass substrate with an ITO electrode was obtained from Matsunami Glass Company.

Table 4.1. Characterization of PVA.

PVA trade name	105	205	405	505
Saponification rate (%)	99	88	81	73
Degree of polymerization	500	500	500	500

Table 4.2. Refractive index of nematic mixtures.

LC trade name	E7	ZLI4151-100	ZLI2061
n_e	1.7464	1.6942	1.676
n_o	1.5211	1.514	1.496

Sample preparation

PVA/LC composite films were prepared by an emulsification method. PVA was dissolved in distilled water at 23 ℃ to prepare a 15 wt% aqueous solution of PVA. The solution was heated up to 100 ℃ to dissolve PVA completely. The PVA blends were formed by mixing the different kinds of PVA aqueous solutions. After the solution was allowed to be at room temperature, LC was dispersed in the solution and stirred at 5000 rpm for 5 min on and off every 15 s with a small propeller blade to prepare an LC emulsion (water-in-oil type emulsion). This procedure produced a creamy white emulsion containing air, which was allowed to

rest for 20-24 h to degas. The concentration of ZLI2061 was controlled at 60 wt% in the composite film. The emulsion was then spin-coated onto an ITO-coated glass substrate at 1500 rpm for 90 s, forming a 12 ±1-μm-thick film. For the measurements of electrooptical properties, the resultant film sample was sandwiched with another ITO glass substrate. Transmittance, morphology, and electrooptical properties of the composite films were stable at room temperature and did not change for 1 year or longer. The characteristics of the PVA/LC composite films are summarized in Table 4.3. In the present study, the saponification rate of the PVA blend was defined by the following equation;

$$[S.R.] = \frac{m_a S_a + m_b S_b}{m_a + m_b}, \qquad (1)$$

where [*S.R.*] means saponification rate of the PVA blend, m_a and m_b are the weights of two kinds of PVA with different saponification rates, and S_a and S_b are the saponification rates.

Table 4.3. Components and wt% of composite films.

Sample	PVA content (w/w)[a)]	LC
sample 1	PVA105	ZLI2061
sample 2	PVA105	E7
sample 3	PVA105/PVA205 =75/25	ZLI2061
sample 4	PVA105/PVA205 =50/50	ZLI2061
sample 5	PVA105/PVA205 =50/50	E7
sample 6	PVA105/PVA205 =25/75	ZLI2061
sample 7	PVA205	ZLI2061
sample 8	PVA205	E7
sample 9	PVA205	ZLI4151-100
sample 10	PVA405	ZLI2061
sample 11	PVA505	ZLI2061

a) Weight ratio of PVA blend with different saponification rates.

4.2.3. Results and Discussion

Morphology of the PVA blend films

Films of the PVA blends consisting of two kinds of PVA with different saponification rates were prepared by spin-coating the PVA aqueous solution on the quartz substrate. Figure 4.6 shows the morphology of the films observed by a photo-microscope. PVAs with different saponification rates were phase separated. The domain size increased with increasing difference in the saponification rate, and the optical character was affected by the domain size. The films of the blends of PVA105/PVA205, PVA205/PVA405 and PVA405/PVA505 were transparent in the visible region since the domain size was sufficiently small compared with the wavelength of visible light, whereas the films of the blends of PVA105/PVA405, PVA205/PVA505 and PVA105/PVA505 scattered light slightly due to their large domain size and the refractive index mismatching between two kinds of PVA with different saponification rates.

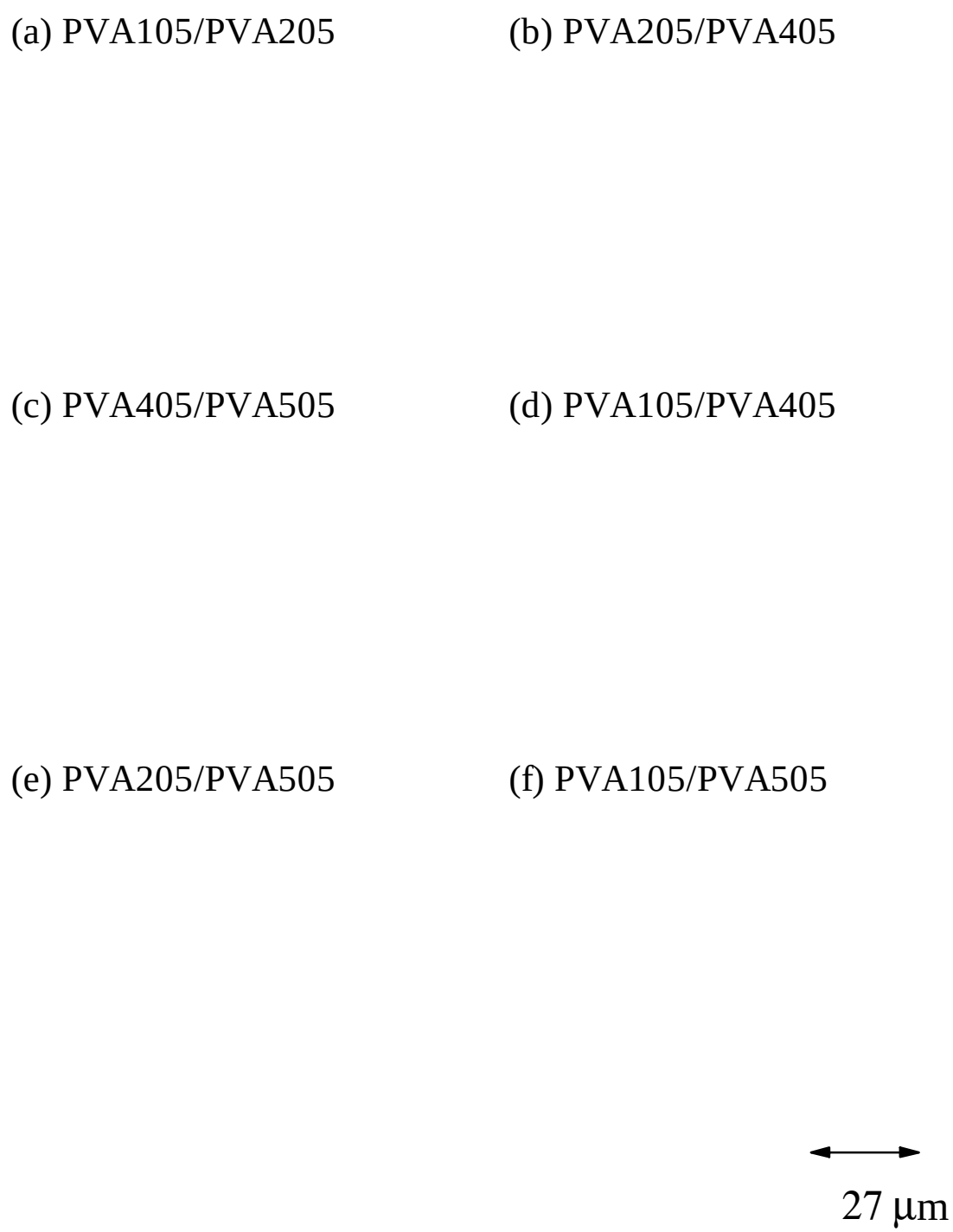

Fig. 4.6. Morphology of the PVA blend films. Films (a) to (c) show a small domain, while films (d) to (e) a large domain.

Refractive index of the PVA blend films

In order to determine the refractive index of the PVA or PVA blend film, the PVA film was prepared by spin-coating the PVA or PVA blend aqueous solutions on the quartz substrate. Then the films were dried at 80 ℃ for 24 h. The refractive index was measured by a prism coupling method using a He-Ne laser light source (632.8 nm). The saponification rate dependence of the refractive index of the PVA films is shown in Fig. 4.7. It was found that the refractive index of the PVA film could be varied continuously by changing the saponification rate or the blend ratio of two kinds of PVA with different saponification rates.

Surface tension of the aqueous solutions of PVA

The saponification rate dependence of the surface tension of 15 wt% of PVA aqueous solution are shown in Fig. 4.8. The surface tension of the PVA aqueous solution is varied continuously by changing the saponification rate or the blend ratio of two kinds of PVA with different saponification rates.

Anchoring strength at the interface between the PVA and the LC

The extrapolation length increased with increasing saponification rate of PVA, as shown in Fig. 4.9. This result led to the conclusion that the interaction at the interface between the PVA and the LC decreased with decreasing saponification rate.

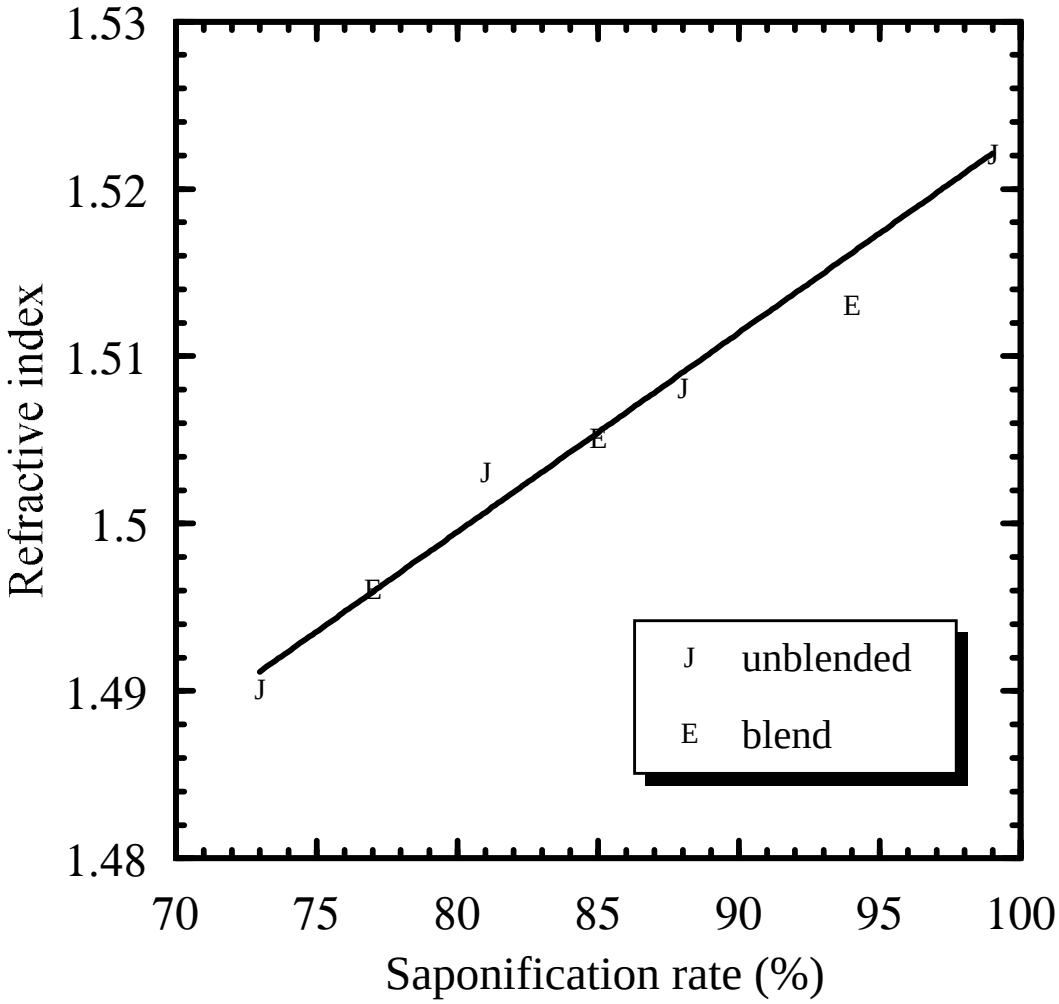

Fig. 4.7. Saponification rate dependence of refractive index of PVA.

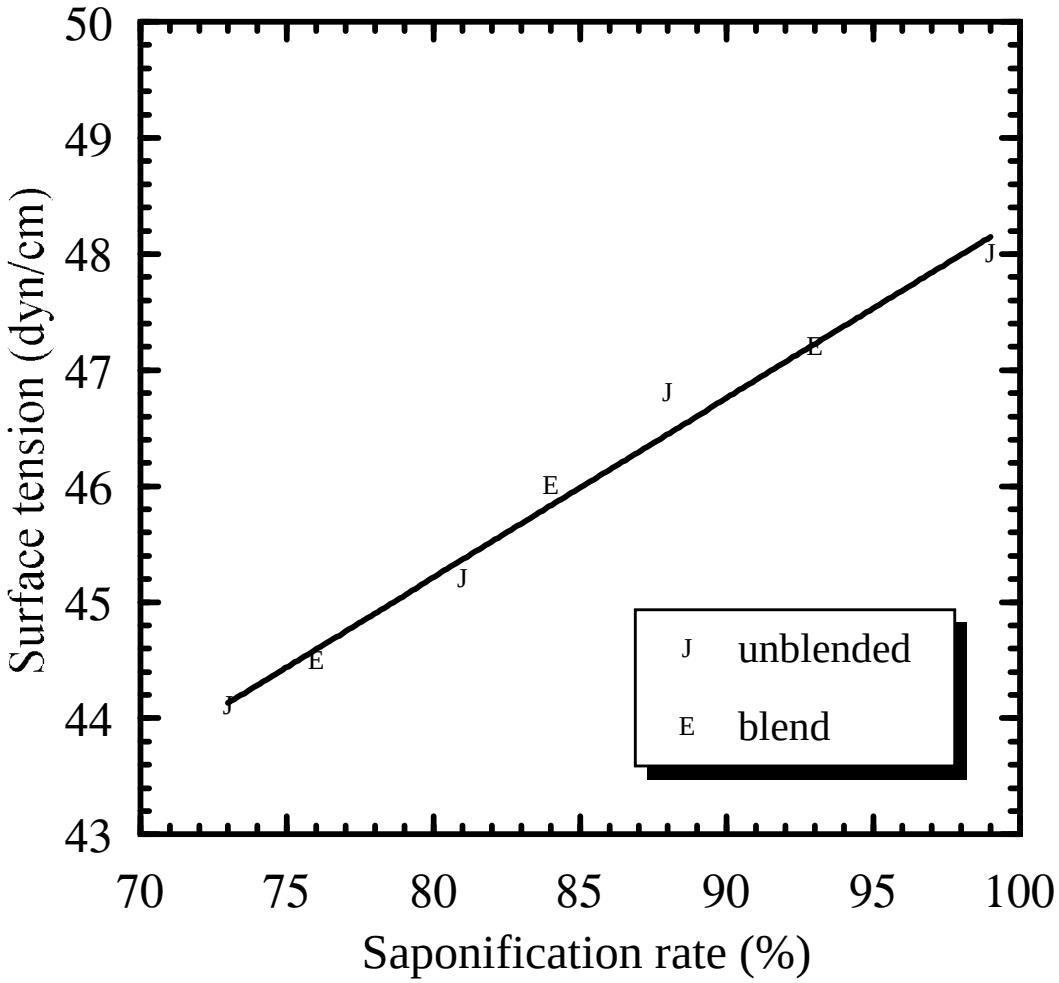

Fig. 4.8. Saponification rate dependence of surface tension of 15 wt% of PVA aqueous solutions.

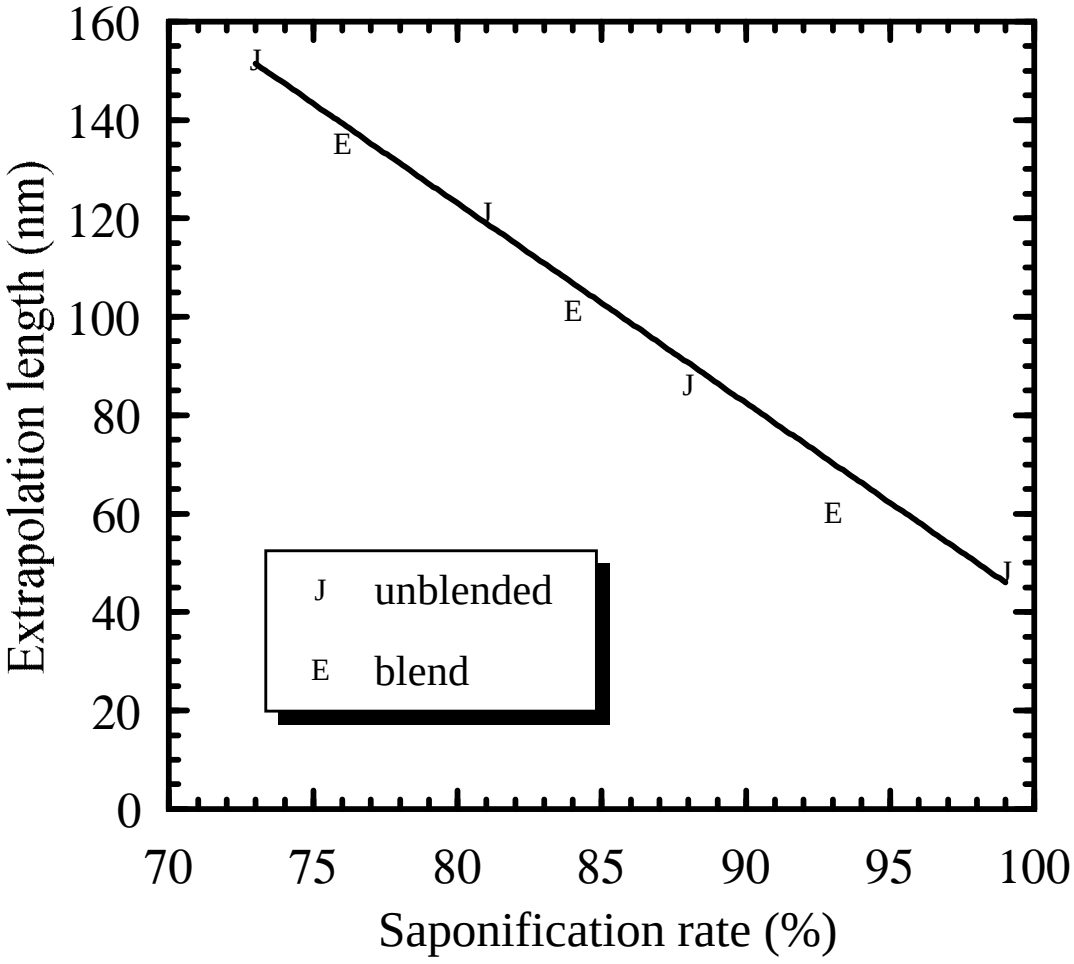

Fig. 4.9. Saponification rate dependence of extrapolation length at the interface between the PVA and ZLI2061.

Morphology of composite films

The morphology of the composite films was observed by a polarizing microscope. Fig. 4.10 shows photographs of sample 1, sample 4, sample 7, and sample 11, respectively. The LC domain size in the composite films increased with increasing saponification rate or increasing ratio of the high saponification rate in the PVA blend. The LC domain size was expected to be affected by the structure of the emulsion. The LC droplet size in the emulsion was affected by the difference between the surface tension of the LC and that of the PVA aqueous solution. The surface tension of the ZLI2061 was 30 dyn/cm and that of the PVA aqueous solution increased with increasing saponification rate of the PVA, as shown in Fig. 4.8. These results led to the conclusion that the LC domain size increased with increasing saponification rate because the difference between the surface tension of the LC and that of the PVA aqueous solution was increased. It was suggested that the LC domain size could be continuously varied by the saponification rate or the blend ratio of two kinds of PVA with different saponification rates since the surface tension of PVA aqueous solution was continuously varied.

(a) sample 1

(b) sample 4

(c) sample 7

(d) sample 11

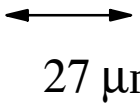

Fig. 4.10. Morphology of PVA/ZLI2061 composite films.

Transmittance of composite films in the ON-state

Light transmission clazing in the ON-state was observed by measuring the transmittance spectrum at operating voltage of 80 V_{rms}. Figure 4.11(a) shows the change in the transmittance spectrum achieved by changing the PVA matrix. The transmittance of the PVA/LC composite films in the ON-state increased with increasing saponification rate of the PVA matrix. The ordinary refractive index of E7 was 1.5211, as shown in Table 4.2. The refractive indexes of PVA105, a 50:50 blend of PVA105 and PVA205 and PVA205 were 1.520, 1.513 and 1.508, respectively, as shown in Fig. 4.7. Figure 4.11(b) shows the change in the transmittance spectrum achieved by changing the PVA matrix in the case of ZLI2061. The ordinary refractive index of ZLI2061 was 1.496, as shown in Table 4.2. The transmittance of the PVA/LC composite films in the ON-state decreased with increasing saponification rate of the PVA matrix. Figure 4.11(c) shows the change in the transmittance spectrum achieved by changing LC mixture. The matrix of the PVA/LC was fixed at PVA205 and the refractive index was 1.500. The transmittance of the PVA/LC composite films in the ON-state decreased with increasing index difference between the PVA and the LC in the ordinary state. The results suggest that the light scattering of the PVA/LC composite films results from the refractive index mismatching, and that the light transmission clazing in the ON-state can be controlled by the saponification rate of PVA.

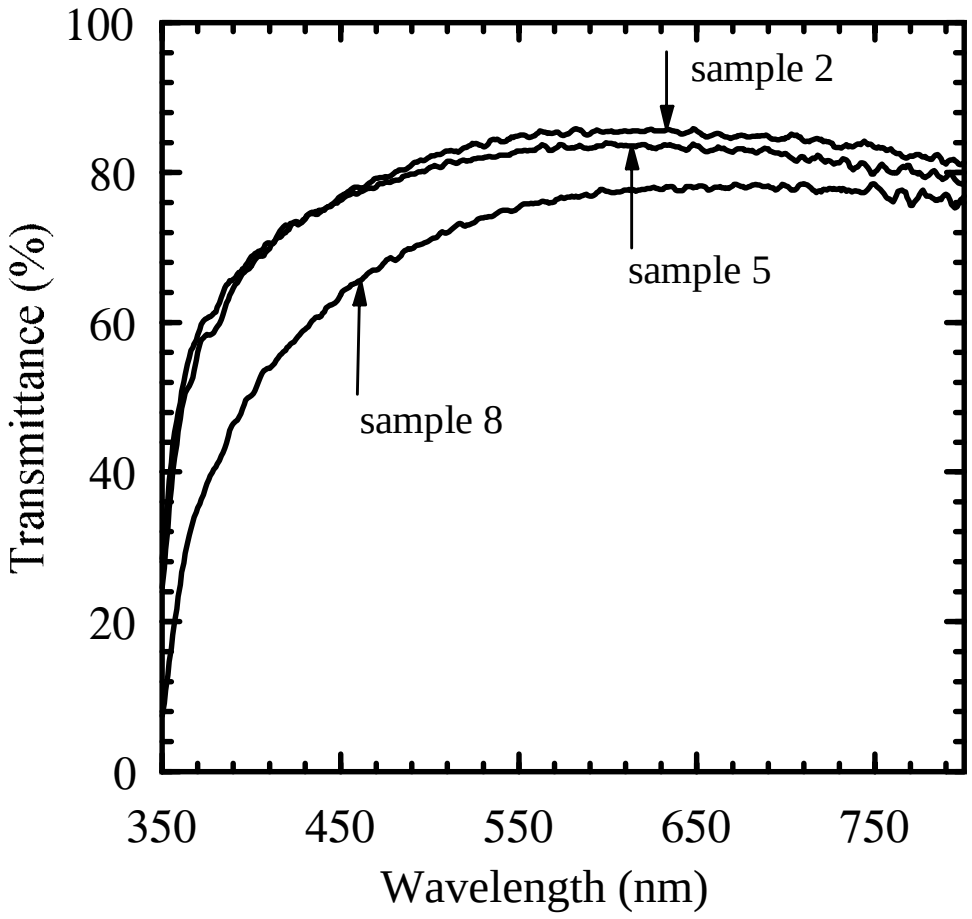

Fig. 4.11(a). Transmittance spectrum of PVA/LC composite films. Change of the transmittance by changing the PVA matrix. LC is fixed to E7.

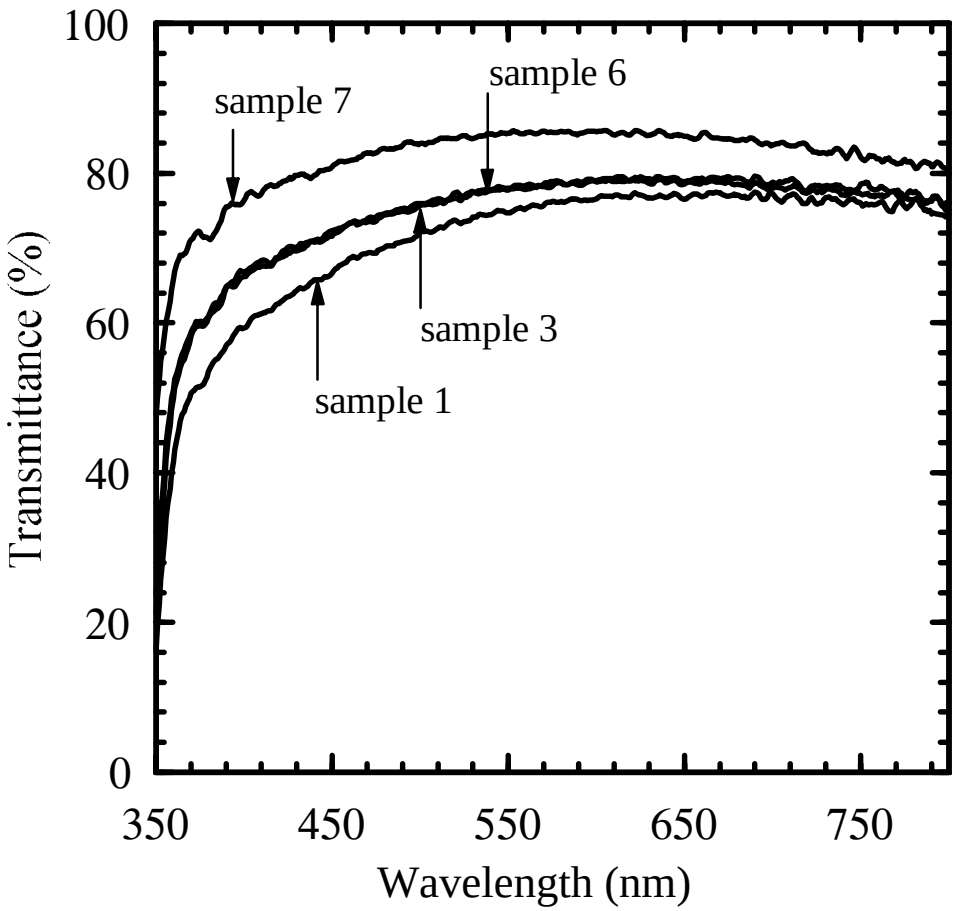

Fig. 4.11(b). Transmittance spectrum of PVA/LC composite films. Change of the transmittance by changing the PVA matrix. LC is fixed to ZLI2061.

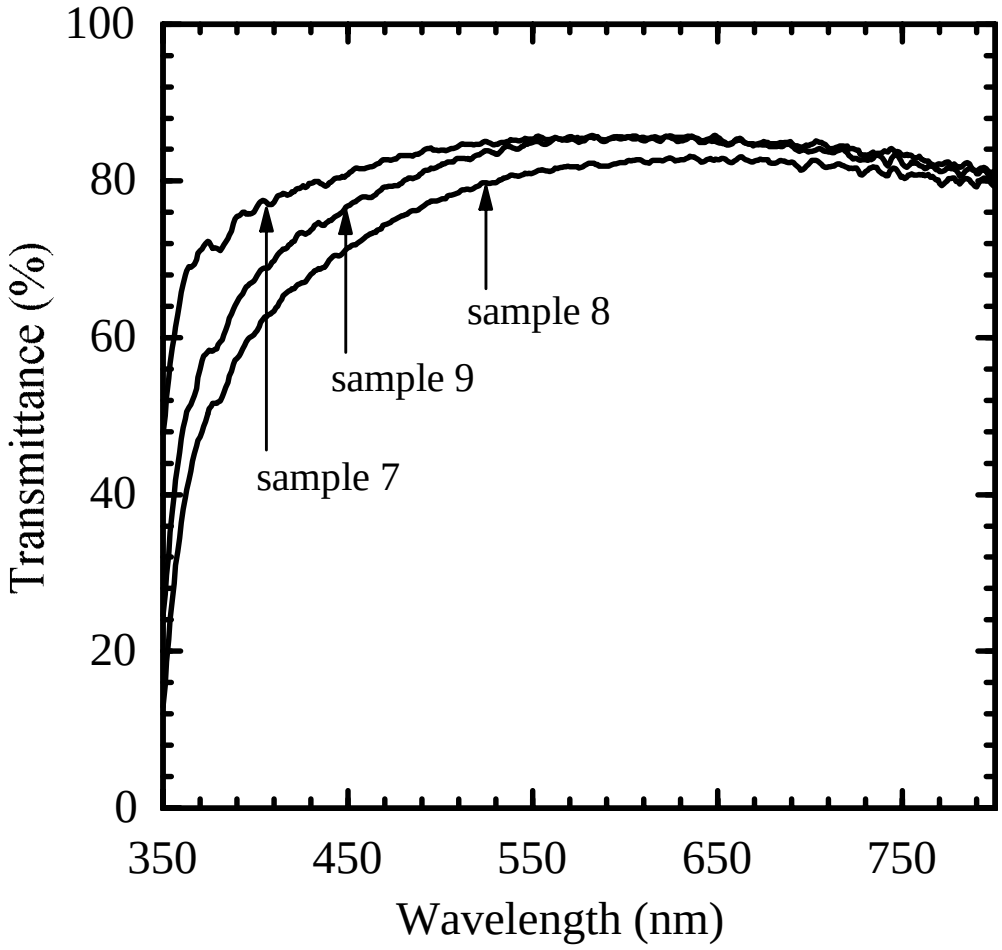

Fig. 4.11(c). Transmittance spectrum of PVA/LC composite films. Change of the transmittance by changing the kind of the LC mixture.

Electrooptical properties of composite films

The electrooptical property of the composite film was affected by the morphology (LC droplet size and shape) and the anchoring strength at the interface between the LC and the polymer. The threshold voltage (V_{th}) has been found to be dependent on the size of the LC droplets and should be a linear function of the reciprocal size of the droplets R according to eq. (2) :[6)]

$$V_{th} \cong \frac{d}{R}\left|\frac{K(l^2-1)}{\Delta\varepsilon}\right|^{1/2} \qquad (2)$$

where d is film thickness, R is droplet radius, K is effective elastic constant, $\Delta\varepsilon$ is dielectric anisotropy, and l is aspect ratio of elongated droplet. From eq. (2), V_{th} decreased with increase in droplet size. On the other hand, V_{th} was also affected by the anchoring strength at the interface between the LC and the polymer as described in the previous study.[7,8)] As shown in Fig. 3.12, V_{th} decreased with increasing saponification rate though the extrapolation length at the interface between the PVA and LC was increased. This result suggests that V_{th} was affected predominantly by the droplet size, and that a long extrapolation length such as that of fluorinated acrylate was needed in order to reduce V_{th}. The saturated transmittance decreased with increasing saponification rate because the refractive index mismatching between the PVA and LC was increased.

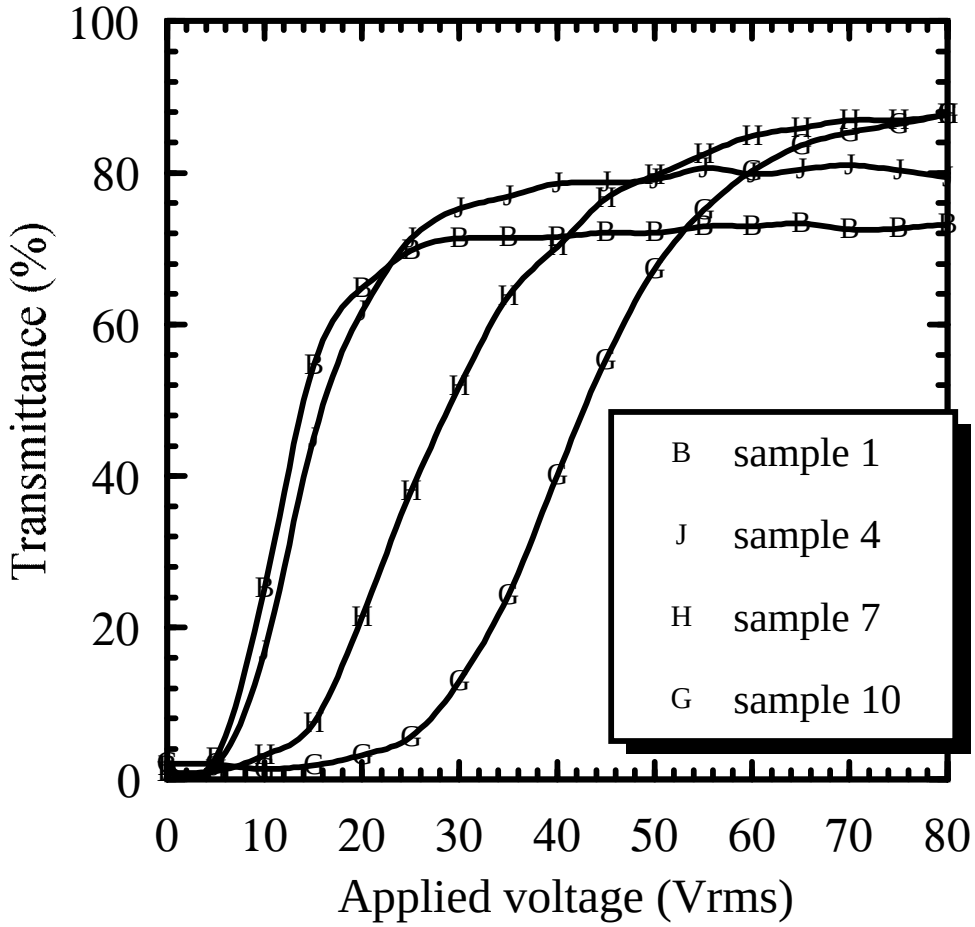

Fig. 4.12. Change of V-T curves by changing the PVA matrix.

Conclusions

The electrooptical properties and morphology of PVA/LC composite films were studied in terms of the saponification rate of PVA and blend ratio of two kinds of PVA with different saponification rates. The surface tension, refractive index, and extrapolation length could be varied continuously by changing the saponification rate or the blend ratio of two kinds of PVA with different saponification rates. The LC droplet size increased with increasing saponification rate and could be controlled by the blend ratio of two kinds of PVA with different saponification rates because the surface tension of PVA aqueous solution increased with increasing saponification rate. Light transmission clazing could be reduced by controlling the saponification rate or the blend ratio of two kinds of PVA with different saponification rates because the refractive index of PVA varied with the saponification rate or blend ratio and the refractive index mismatching between the PVA and LC was reduced. Threshold voltage decreased with increasing saponification rate though the extrapolation length was increased. It was suggested that the effect of change of LC droplet size was dominant, and that a long extrapolation length such as that of fluorinated acrylate was needed in order to reduce the threshold voltage.

References

1) P. S. Drzaic: *J. Appl. Phys.* **60** (1986) 2142.

2) P. S. Drzaic and A. M. Gonzales: *Mol. Cryst. Liq. Cryst.* **222** (1992) 11.

3) J. W. Doane, N. A. Vaz, B. G. Wu, and S Zumer: *Appl. Phys. Lett.* **48** (1986) 269.

4) G. M. Zhang, Z. H. Zhou, Z. Changxing, B. Wu, and J. W. Lin: *Proc. SPIE* **1815** (1992) 233.

5) B. G. Wu, J. H. Erdmann, and J. W. Doane: *Liq. Cryst.* **5** (1989) 1453.

6) P. S. Drzaic: *Liq. Cryst*. **3** (1988) 1543.

7) H. Ono and N. Kawatsuki: *Jpn. J. Appl. Phys*. **33** (1994) 6268.

8) H. Ono and N. Kawatsuki: *Jpn. J. Appl. Phys*. **33** (1994) L1778.

4.3. Control of Size of LC Droplets by Changing Block Character of PVA

A new fabrication method for poly(vinyl alcohol) (PVA)/liquid crystal (LC) composite film with controlled LC droplet size is presented by changing the dispersion state of hydroxyl groups in the PVA (block character). The LC droplet size can be controlled by the block character without changing the refractive index of the PVA matrix. The threshold voltage has been strongly dependent on the LC droplet size though the anchoring strength is dependent on the block character.

4.3.1. Introduction

In the present section, a new fabrication method for the PVA/LC composite film with controlled LC droplet size was presented by changing the dispersion state of hydroxyl groups in the PVA (block character).

The block character shows the distribution of the hydrolysis (OH) and residual acetate (OAc) and is defined by the following formulas.[1)]

$$\eta = (\mathrm{OH},\mathrm{OAc}) / 2(\mathrm{OH})(\mathrm{OAc})$$

where (OH, OAc) is ^{13}C-NMR intensity from the following chemical structure,

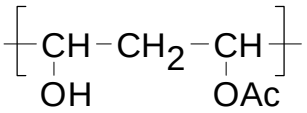

(OH) shows the saponification rate, and (OAc) is the residual acetate. The block character is a convenient guide for characterizing a sequence distribution ; it takes $0 \leqq \eta < 1$ for blockier distributions, $\eta = 1$ for a completely random case and the randomness was increased with decreasing the block character. It is expected that the morphology of PVA/LC composite is changed since the surface tension of PVA is changed by changing the block character.

4.3.2. Experimental

PVA with different block characters was supplied by Kuraray Co., Ltd. The trade name and the characteristics of PVA are summarized in Table 4.4.

Table 4.4. Characterization of PVA.

PVA trade name	217	217E	217EE
Saponification rate (%)	88	88	88
Degree of polymerization	1700	1700	1700
Block Character	0.508	0.494	0.477

PVA was dissolved in distilled water at 23 ℃ to prepare a 10 wt% solution. The solution was heated up to 90 ℃ to dissolve PVA completely, and left at room temperature. Nematic LC mixture with positive dielectric anisotropy (ZLI2061, Merck Japan Ltd.) was dispersed in the solution and stirred at 5000 rpm for 5 min on and off every 15 s with a propeller blade to prepare a LC emulsion. This procedure produced a creamy white emulsion containing air, which was allowed to rest for 20-24 h to degas. The concentration of ZLI2061 was controlled at 60 wt% in the composite film. The emulsion was then spin-coated onto an ITO-coated glass substrate (Matsunami Glass Company) at 1500 rpm for 90 s at 23 ℃,

forming a 12-μm-thick film. For the measurements of electrooptical properties, the resultant film sample was sandwiched with another ITO glass substrate.

4.3.3. Results and Discussion

Figure 4.13 shows the applied voltage dependence of transmittance of the composite films with different block character. The threshold voltage was increased with decreasing block character of PVA. The saturated transmittance of the composite films was 83 % (nearly equal to the transmittance of an ITO-coated glass substrate) and was scarcely changed by the block character.

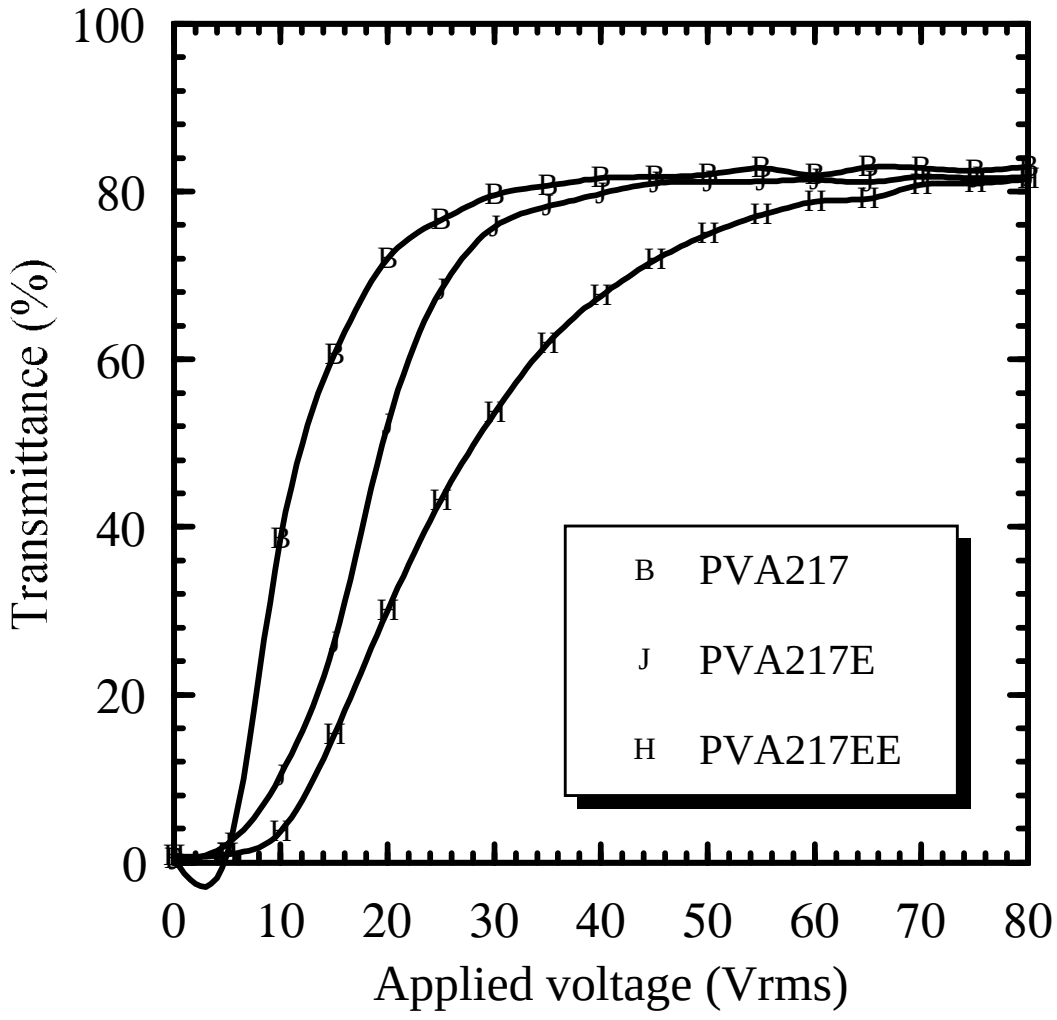

Fig. 4.13. Transmittance vs applied voltage curves for a PVA/LC composite films.

It is well known that the electrooptical properties of the composite films are affected by the morphology. The morphology of the composite films was observed by a polarization microscope. Figure 4.14(a), 4.14(b) and 4.14(c) show the photographs of PVA217/ZLI2061, PVA/217E/ZLI2061 and PVA217EE/ZLI2061 composite films, respectively. The LC domain size in the composite films was decreased with increasing block character. The LC domain size was expected to be affected to be affected by the structure of the emulsion. Surface tensions of the LC and PVA aqueous solution were determined from the contact angle (θ). The contact angle measurements were carried out on the Teflon sheet surface at 23 ℃ with a Kyowa contact angle meter. The value of $\cos\theta$ against surface tensions (Zisman plots) of a Teflon sheet was plotted by measuring the contact angles of *n*-heptane, *n*-hexane, water, ethyleneglycol, and diethyleneglycol, whose surface tension was well known. The surface tension of a test liquid could be determined from Zisman plots by measuring the contact angle of the liquid on the Teflon sheet surface. Surface tensions of 10 wt% of PVA aqueous solutions are shown in Fig. 4.15. The surface tension of PVA aqueous solution was increased with increasing block character. The surface tension of ZLI2061 was 30 dyn/cm. The result suggests that the LC droplet size was increased because the difference in surface tension between the LC and PVA aqueous solution was increased with increasing block character.

(a) PVA217/ZLI2061

(b) PVA217E/ZLI2061

(c) PVA217EE/ZLI2061

Fig. 4.14. Polarized microscope observation of the PVA/LC composite films.

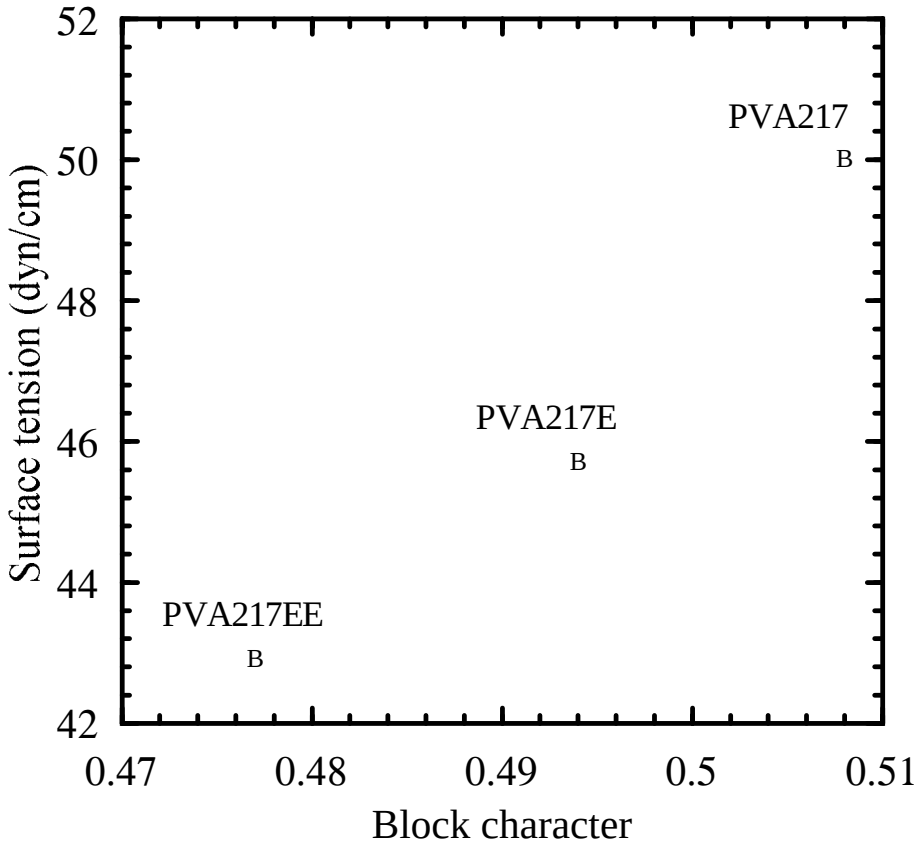

Fig. 4.15. Surface tension of 10 wt% of PVA aqueous solutions.

The threshold voltage (V_{th}) has been found to be dependent on the size of the LC droplets and should be a linear function of the reciprocal of the size of the droplets *R* according to eq. (1):

$$V_{th} \cong \frac{d}{R}\left|\frac{K(l^2-1)}{\Delta\varepsilon}\right|^{1/2} \qquad (1)$$

where *d* is film thickness, *R* is droplet radius, *K* is effective elastic constant, Δε is dielectric anisotropy, and *l* is aspect ratio of elongated droplet. From eq. (1), threshold voltage was decreased with the rise in droplet size. It was suggested that the threshold voltage of the composite films was dependent on the LC droplet size, as shown in Fig. 4.14.

On the other hand, the threshold voltage decreased with the decreasing the anchoring strength at the interface between the polymer and the LC as shown in the previous work.[2)] The extrapolation length, inversely proportional to the anchoring strength at the interface between the LC and the PVA with different block characters, was measured by the method of Yokoyama and van Sprang[3)] and the experimental setup was described in the previous work. A Freedericksz cell consisting of a pair of 30 mm × 30 mm glass substrates coated with ITO and PVA was used as a model for the composition of the polymer matrix in the PVA/LC composite film. PVA was dissolved in water and spin-coated on the ITO-coated glass substrates, and the PVA films were annealed at 80 ℃ for 20 h. The PVA films were rubbed with a silk cloth. Sufficiently thick sandwich-type cells were prepared by using a 50-μm-thick polyester spacer and were filled with ZLI2061. The extrapolation length was decreased with decreasing block character of PVA, as shown in Fig. 4.16. The threshold

voltage decreased with increasing extrapolation length in the previous study but the threshold voltage was increased though the extrapolation length was increased. The result suggests that the threshold voltage was strongly dependent on the droplet size, and that a long threshold voltage such as that of fluorinated acrylate[2)] was needed to reduce the threshold voltage.

It is well known that the saturated transmittance of the composite film was dependent on the mismatching between the ordinary refractive index of the LC and refractive index of the polymer. In order to determine the refractive index of PVA with different block characters, the PVA film was prepared by spin-coating the PVA aqueous solutions on the quartz substrate. Then the films were dried at 80 ℃ for 24 h. The refractive index was measured by a prism coupling method using a He-Ne laser light source (632.8 nm). The block character dependence of the refractive index of the PVA films is shown in Fig. 4.17. It was found that the refractive index of the PVA film was scarcely changed by changing the block character. The result suggests that the saturated transmittance was not changed because the refractive index of PVA was scarcely changed by the block character of PVA.

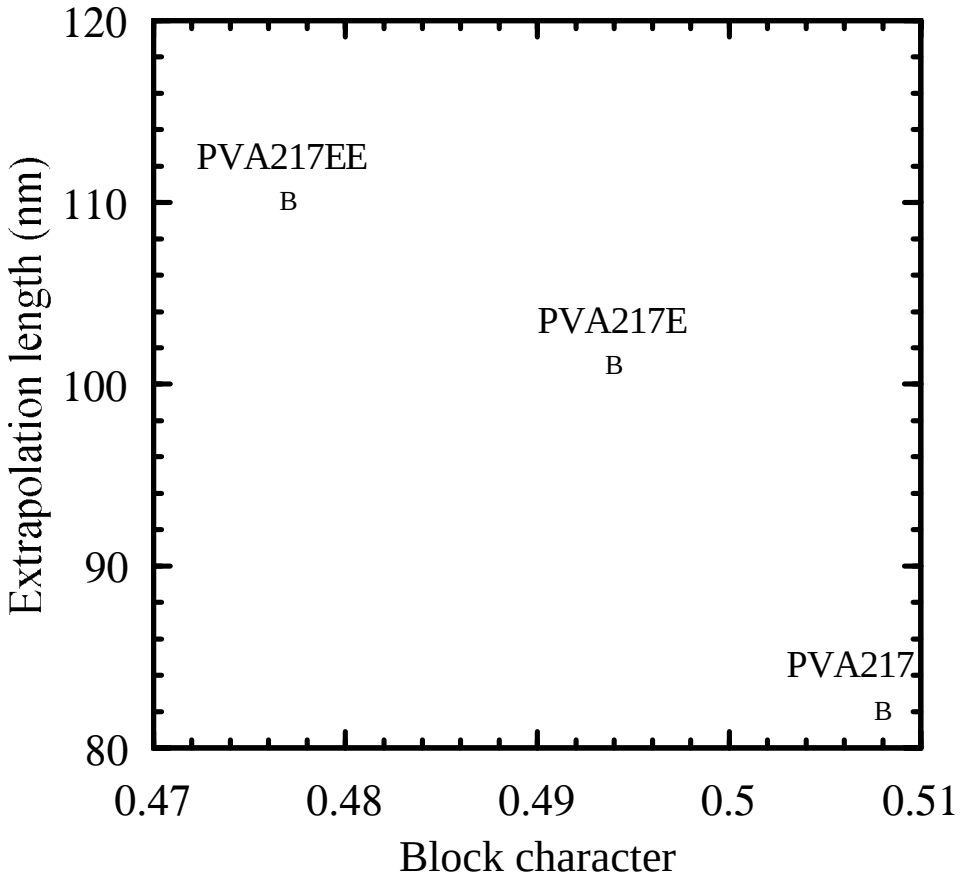

Fig. 4.16. Extrapolation length at the interface between the PVA and LC.

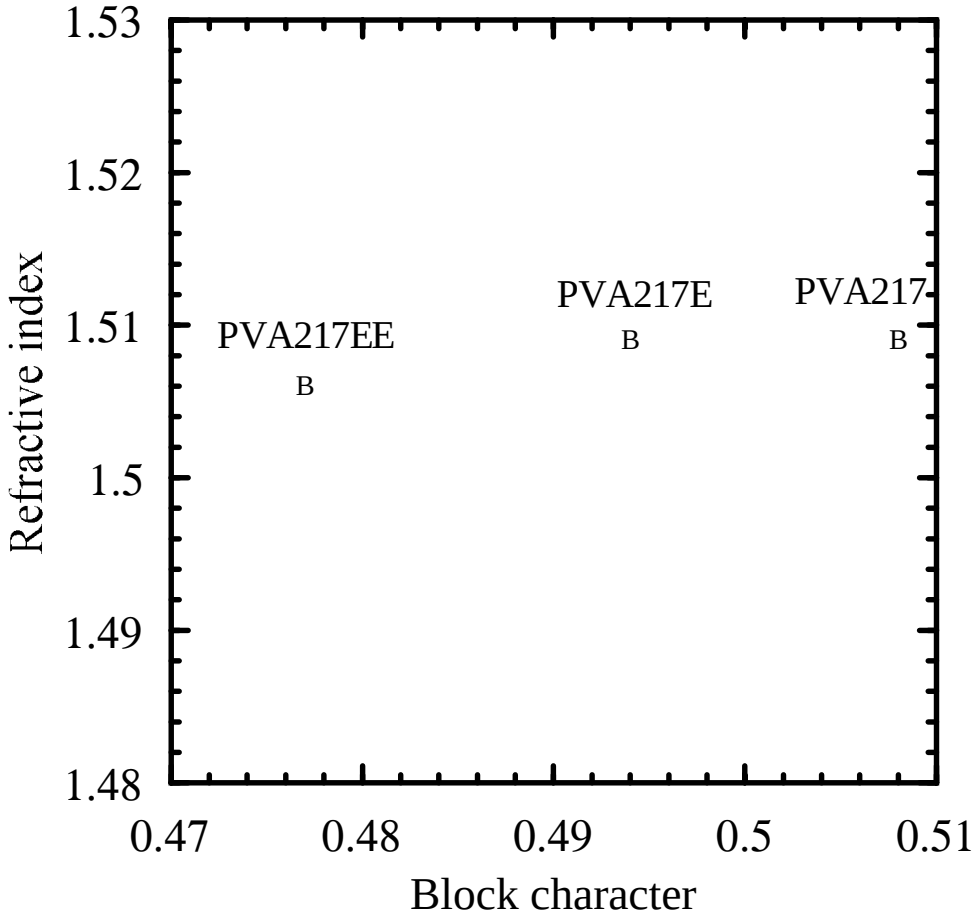

Fig. 4.17. Refractive index of the PVA.

Conclusions

The LC droplet size of PVA/LC composite film could be controlled without changing the light transmission clazing by the block character of PVA. The LC droplet size was changed because the surface tension of the PVA aqueous solution was dependent on the block character of PVA. The light transmittance clazing in the field-on state was not changed by the block character, and the refractive index of PVA was independent of the block character.

References

1) T. Moritani and Y. Fujiwara: *Macromolecules* **10** (1977) 532.
2) H. Ono and N. Kawatsuki: *Jpn. J. Appl. Phys.* **33** (1994) 6637.
3) H. Yokoyama and H. A. Van Sprang: *J. Appl. Phys.* **57** (1985) 4520.

Summary

A new type of polymer/liquid crystal (LC) composite film was presented in the present thesis. The composite film was formed by casting the poly(vinyl alcohol) (PVA)/LC emulsion with added mixture of two kinds of photocurable monomers with different solubility in LC followed by photocuring, resulting in low driving voltage, low hysteresis and rapid response time. It was found that photocurable mixture polymerized at the interface and reduced the anchoring strength at the interface between the PVA and the LC. In order to enhance the light scattering in the OFF-state and obtain the low driving voltage and high contrast by forming a thin composite film, a novel PVA/LC composite film bearing deformed and disordered nematic droplets was also presented. The composite film was formed from the mixture of water with methanol (WM-mixture). The polymer/LC composite film formed from the emulsion composed of a WM-mixture, PVA, LC, and a photocrosslinkable mixture of nonaoxyethylendiacrylate (9EG-A) with perfluotooctylethylacrylate (FA108) showed electrooptical properties as follows: the driving voltage was less than 6 V_{rms}, hysteresis less than 0.2 V_{rms}, and response time 11 ms. This data is superior to that of the traditional NCAP cell possessing the electrooptical properties of the driving voltage 56 V_{rms}, hysteresis 14 V_{rms}, and response time 500 ms.

Acknowledgments

The work described in this thesis has been carried out at Central Research Laboratories, Kuraray Co., Ltd. during 1989-1991 and 1993-1995 and at Department of Physics, Faculty of Science, University of Tokyo during 1992-1993 under the direction of Professor Takayoshi Kobayashi. This thesis is concerned with new type of the polymer/liquid crystal composite films for the minute display without polarizers.

The author wishes to express his sincere gratitude to Professor Takayoshi Kobayashi and Dr. Kazuhiko Misawa for valuable suggestions and hearty encouragements.

The author wishes to express his grateful acknowledgment to his coworker, Dr. Nobuhiro Kawatsuki for valuable suggestions and hearty encouragements. The author's grateful acknowledgment is due to Professor Yoshio Nishida for his precious comments and suggestions for this thesis.

The author wishes to show his deep gratitude to Dr. Masao Uetsuki for their hearty encouragements and his precious comments and suggestions for this thesis. The author wishes to show his deep gratitude to Dr. Shiro Nagata for his useful discussions in this work.

Finally, the author wishes to thank to his wife and family, Chieko Ono, Emiko Ono and Ko-hei Ono for their constant encouragements and supports.

Hiroshi Ono

1995 *February*

Appendix I Characteristics of Liquid Crystal (ZLI2061)

(1) Main component of ZLI2061

cyanophenylcyclohexane

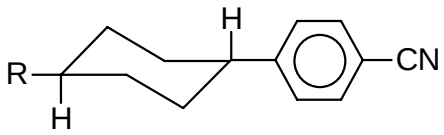

cyanoester

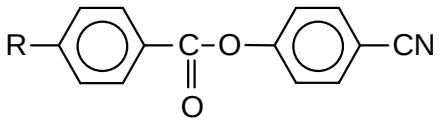

R: Alkyl group

(2) Physical characteristics of ZLI2061

Clearing point[°C]	Viscosity[mm^2s^{-1}]	Δn	n_e	$\varepsilon_{\parallel}$	$\varepsilon_{\perp}$
91	41				+0.18
1.676	5.50	23.8			

Appendix II List of Abbreviations

9EG-A	Nonaoxyethylenediacrylate
AIBN	2,2'-Azobis-(2-methylpropionitrile)
BAF	Mixture of BzA with FA108
BMF	Mixture of BzMA with FA108
BzA	Benzylacrylate
BzMA	Benzylmethacrylate
DMPA	Dimethoxyphenylacetophenone
EGF	Mixture of 9EG-A with FA108
FA108	Perfluorooctylethylacrylate
FMA	Perfluorooctylethylmethacrylate
ITO	Indium tin oxide
LC	Liquid crystal
M-film	PMMA/BzMA/FA108/LC composite film
NCAP	Nematic curvilinear aligned phase
P-film	Conventional PMMA/LC composite film
PB-film	Poly-BzMA-co-FMA/LC composite film
PLP-cell	PVA/LC/photocured polymer cell
PMMA	Polymethylmethacrylate
PPIPS	Photopolymerization-induced phase separation
PVA	Poly(vinyl alcohol)
SEM	Scanning electron microscopy
SIPS	Solvent-induced phase separation
T-cell	Traditional PVA/LC cell
TFT	Thin film transistor
WM-mixture	Water and methanol mixture

Appendix III List of Publications

1. New fabrication method for highly oriented *J* aggregates dispersed in polymer films.
   K. Misawa, H. Ono, K. Minoshima and T. Kobayashi
   Appl. Phys. Lett. **63** (1993) 577.

2. Giant static dipole moment change on electronic excitation in highly oriented J-aggregates.
   K. Misawa, H. Ono, K. Minoshima and T. Kobayashi
   Chem. Phys. Lett. **220** (1994) 251.

3. Electrooptical properties of poly(vinyl alcohol)/liquid crystal composite films with added photocured polymers. 2.1.

   H. Ono and N. Kawatsuki
   Jpn. J. Appl. Phys. **33** (1994) 6268.

4. New model of excitonic bands and molecular arrangement of highly-oriented J-aggregates in polymer films prepared by a novel method.
   K. Misawa, H. Ono, K. Minoshima and T. Kobayashi
   J. Luminescence **60 & 61** (1994) 812.

5. Poly(vinyl alcohol)/liquid crystal composite films with low driving voltage. 4.1.
   H. Ono and N. Kawatsuki

   Jpn. J. Appl. Phys. **33** (1994) L1778.

6. Effects of anchoring strength in poly(vinyl alcohol)/liquid crystal composite films with interface layers. 2.2.
   H. Ono and N. Kawatsuki
   Jpn. J. Appl. Phys. **33** (1994) 6637.

7. New fabrication method for poly(vinyl alcohol)/ liquid crystal composite films with controlled droplet size. 4.3.
H. Ono and N. Kawatsuki
Jpn. J. Appl. Phys. **34** (1995) L54.

8. Synthesis of poly-(benzylmethacrylate-co-perfluoroocthyl methacrylate) and electrooptical properties of the resultant polymer/liquid crystal composite films. 3.1.
N. Kawatsuki and H. Ono
J. Appl. Polym. Sci. **55** (1995) 911.

9. Effects of saponification rate on electrooptical properties and morphology of poly(vinyl alcohol)/liquid crystal composite films. 4.2.
H. Ono and N. Kawatsuki
Jpn. J. Appl. Phys. **34** (1995), in press .

10. Improvement of electrooptical properties of poly(vinyl alcohol)/liquid crystal composite films by controlling surface interaction and morphology.
H. Ono and N. Kawatsuki
Ko-bunshi Ronbunsyu., **52** (1995), in press.

11. Electro-optical properties of polymer/liquid crystal composite films fabricated from two-steps phase separation method. 3.2.
N. Kawatsuki and H. Ono
Submitted to Chem. Lett.

12. Complex electro-optic constants of dye-doped polymer films determined by a Mach-Zehnder interferometer.
H. Ono, K. Misawa, K. Minoshima, A. Ueki and T. Kobayashi
J. Appl. Phys., in press.